

BANYAN. XIII. A FIRST LOOK AT NEARBY YOUNG ASSOCIATIONS WITH *GAIA* DATA RELEASE 2

JONATHAN GAGNÉ^{1,2} AND JACQUELINE K. FAHERTY³

¹*Carnegie Institution of Washington DTM, 5241 Broad Branch Road NW, Washington, DC 20015, USA*

²*NASA Sagan Fellow*

³*Department of Astrophysics, American Museum of Natural History, Central Park West at 79th St., New York, NY 10024, USA*

(Received 2018 May 7; Revised 2018 May 26)

Submitted to ApJ

ABSTRACT

In this paper we examine the nearest 100 pc entries in the data release 2 of *Gaia* to identify previously unrecognized candidate members in young associations. We analyze 695 952 stars with the BANYAN Σ Bayesian classification software and discover 898 new high-likelihood candidate members that span a wide range in properties, from spectral types B9 to L2, including 104 co-moving systems, 111 brown dwarfs and 31 new bona fide members. Our sample is mostly composed of highly active M dwarfs and will be crucial to examine the low-mass end of the initial mass function of young associations. Our sample includes new candidate members near the Galactic plane where previous surveys suffered from a high rate of contamination. This paper represents the first step towards a full reassessment of young associations in the Solar neighborhood with the second data release of the *Gaia* mission.

Keywords: methods: data analysis — stars: kinematics and dynamics — proper motions

1. INTRODUCTION

The recent Data Release 2 of the *Gaia* mission (*Gaia* DR2 hereafter; [Gaia Collaboration et al. 2018](#); [Lindegren et al. 2018](#))¹ on 2018 April 25 presented a catalog of ~ 1.3 billion trigonometric distances to stars in the Milky Way, a more than 600-fold improvement over the number of sources in the Tycho–*Gaia* Astrometric Solution ([Gaia Collaboration et al. 2016](#)) that came out less than a year ago, and a more than 10 000-fold improvement over that of the Hipparcos mission ([Perryman et al. 1997](#)), which shaped our understanding of the Solar neighborhood for the past few decades. *Gaia* DR2 revolutionizes the quantity and quality of stellar kinematics data that are immediately available, and it will have a profound impact on our understanding of Galactic kinematics, among many other things.

In this paper, we examine the 27 nearest known young associations within 150 pc of the Sun (e.g., the AB Do-

radus and β Pictoris moving groups, the TW Hya and Hyades associations; [Zuckerman & Song 2004](#); [Torres et al. 2008](#)). These associations and their global properties are listed in Table 1, and are described in more detail in [Gagné et al. \(2018\)](#). A detailed analysis of their properties and known members based on *Gaia* DR2 will be the subject of separate papers. The ages of these associations span a few Myr to almost a Gyr, and they thus provide a window into the star-formation history of the Solar neighborhood as well as important astrophysical laboratories to understand how the properties of stars, substellar objects and exoplanets evolve with time. Previous searches for new low-mass members in these young associations (e.g., [Rodriguez et al. 2011](#); [Shkolnik et al. 2012](#); [Malo et al. 2013](#); [Kraus et al. 2014](#); [Shkolnik et al. 2017](#)) identified only a fraction of the mid-to-late M dwarfs because of their faintness and the need to obtain follow-up trigonometric parallaxes and radial velocities for a large number of objects (the initial mass function peaks around \sim M3). *Gaia* DR2 now opens the door to a search down to the substellar domain (spectral type \sim L2) with an unprecedented efficiency, as the immediate availability of trigonometric parallaxes makes it possible to cut down the number of

jgagne@carnegiescience.edu

¹ See also [Luri et al. \(2018\)](#), [Mignard et al. \(2018\)](#), [Babusiaux et al. \(2018\)](#), [Sartoretti et al. \(2018\)](#), [Soubiran et al. \(2018\)](#), [Copper et al. \(2018\)](#), [Evans et al. \(2018\)](#), [Hambly et al. \(2018\)](#), and [Riello et al. \(2018\)](#) for relevant calibration.

contaminants (mostly unrelated background field stars) by an order of magnitude (e.g., see Gagné et al. 2018).

Table 1. Nearby young associations considered here.

Group	$\langle \varpi \rangle^a$	$\langle \nu \rangle^b$	S_{spa}^c	S_{kin}^d	Age	Ref.
Name	(pc)	(km s $^{-1}$)	(pc)	(km s $^{-1}$)	(Myr)	
118TAU	100 ± 10	14 ± 2	3.4	2.1	~ 10	1
ABDMG	30^{+20}_{-10}	10^{+10}_{-20}	19.0	1.4	149^{+51}_{-19}	2
β PMG	30^{+20}_{-10}	10 ± 10	14.8	1.4	24 ± 3	2
CAR	60 ± 20	20 ± 2	11.8	0.8	45^{+11}_{-7}	2
CARN	30 ± 20	15^{+7}_{-10}	14.0	2.1	~ 200	3
CBER	85^{+4}_{-5}	-0.1 ± 0.8	3.6	0.5	562^{+98}_{-84}	4
COL	50 ± 20	21^{+3}_{-8}	15.8	0.9	42^{+6}_{-4}	2
EPSC	102 ± 4	14 ± 3	2.8	1.8	$3.7^{+4.6}_{-1.4}$	5
HYA	42 ± 7	39^{+3}_{-4}	4.5	1.2	750 ± 100	6
LCC	110 ± 10	14 ± 5	11.6	2.2	15 ± 3	7
OCT	130^{+30}_{-20}	8^{+8}_{-9}	22.4	1.3	35 ± 5	8
PL8	130 ± 10	22 ± 2	5.0	1.1	~ 60	9
TAU	120 ± 10	16 ± 3	10.7	3.6	$1-2$	10
THA	46^{+8}_{-6}	9^{+5}_{-6}	9.1	0.8	45 ± 4	2
THOR	96 ± 2	19 ± 3	3.9	2.1	22^{+4}_{-3}	2
TWA	60 ± 10	10 ± 3	6.6	1.5	10 ± 3	2
UCL	130 ± 20	5 ± 5	17.4	2.5	16 ± 2	7
UMA	$25.4^{+0.8}_{-0.7}$	-12 ± 3	1.2	1.3	414 ± 23	11
USCO	130 ± 20	-5 ± 4	9.9	2.8	10 ± 3	7
XFOR	100 ± 6	19 ± 2	2.6	1.3	~ 500	12

^aPeak of distance distribution and $\pm 1\sigma$ range.

^bPeak of radial velocity distribution and $\pm 1\sigma$ range.

^cCharacteristic spatial scale in XYZ space.

^dCharacteristic kinematic scale in UVW space.

NOTE—The full names of young associations are: 118 Tau (118TAU), AB Doradus (ABDMG), β Pictoris (β PMG), Carina (CAR), Carina-Near (CARN), Coma Berenices (CBER), Columba (COL), ϵ Chamaeleontis (EPSC), the Hyades cluster (HYA), Lower Centaurus Crux (LCC), Octans (OCT), Platais 8 (PL8), the Tucana-Horologium association (THA), 32 Orionis (THOR), TW Hya (TWA), Upper Centaurus Lupus (UCL), the core of the Ursa Major cluster (UMA), Upper Scorpions (USCO), Taurus (TAU) and χ^1 For (XFOR).

References—(1) Mamajek 2016; (2) Bell et al. 2015; (3) Zuckerman et al. 2006; (4) Silaj & Landstreet 2014; (5) Murphy et al. 2013; (6) Brandt & Huang 2015; (7) Pecaut & Mamajek 2016; (8) Murphy & Lawson 2015; (9) Platais et al. 1998; (10) Kenyon & Hartmann 1995; (11) Jones et al. 2015; (12) Pöhnl & Paunzen 2010.

In this work, we use the 100 pc sample of *Gaia* DR2 to recover 898 new candidate members (mostly mid-M dwarfs) that were never identified as such in the literature. In Section 2, we describe the sample selection based on the nearest 100 pc entries of *Gaia* DR2 and the BANYAN Σ Bayesian classifier, and we describe our further validation of the targets as well as our literature search in Section 3. The general properties of the resulting set of new candidate members are described in Section 4, along with those of the co-moving systems that we identified. We conclude in Section 5.

2. SAMPLE SELECTION

We selected all *Gaia* DR2 sources within 100 pc of the Sun with a parallax measurement at least three times as large as its measurement error so as to identify new candidate members in young associations based on robust parallax measurements. We used a generous criterion on the parallax quality to avoid rejecting faint candidate members that may correspond to young brown dwarfs. This sample was downloaded from the *Gaia* DR2 archive² with the following SQL query:

```
PARALLAX > 10 AND PARALLAX/PARALLAX_ERROR >= 3,
```

which returned 695 952 entries. All entries were analyzed with the BANYAN Σ Bayesian classification algorithm (Gagné et al. 2018) to identify those for which the proper motion and trigonometric parallax are consistent with membership in a known young association. BANYAN Σ uses spatial and kinematic models of the 27 young associations within 150 pc as well as field stars within 300 pc to derive membership probabilities in each young association based on the sky position, proper motion, radial velocity and trigonometric distances of the targets using Bayesian inference. Radial velocities and trigonometric distances are optional, and BANYAN Σ can calculate probabilities in their absence by taking a marginalization integral of the membership probability density over all possible values. BANYAN Σ is computationally efficient and achieves a more accurate classification performance than previous tools in the literature in part because it is based on an analytical solution of the marginalization integrals (see Gagné et al. 2018 for more detail).

We found all 3,510 entries with a total young association Bayesian membership probably above 90% that are separated by less than 5 km s^{-1} from their best-matching young association in UVW space (727 of which have a *Gaia* DR2 radial velocity measurement). In the absence of a radial velocity measurement, BANYAN Σ provides

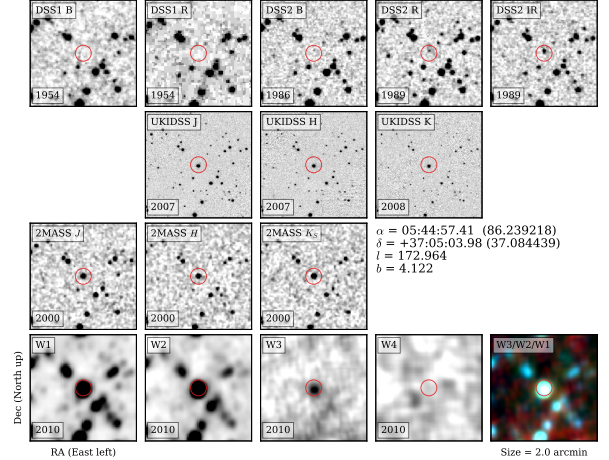


Figure 1. Finder chart for 2MASS J05445741+3705039, a new Galactic plane \sim L1 candidate member of the AB-DMG. The red circle displays its expected position at epoch 2000 based on the *Gaia* astrometric solution. Its large proper motion ($\mu_\alpha \cos \delta = 6.6 \pm 0.9 \text{ mas yr}^{-1}$, $\mu_\delta = -230.8 \pm 0.8 \text{ mas yr}^{-1}$) can clearly be seen from the 1989 DSS2 infrared image and the \sim 2007 UKIDSS images, and its non-detection at bluer wavelengths is consistent with its estimated spectral type. See Section 3 for more detail.

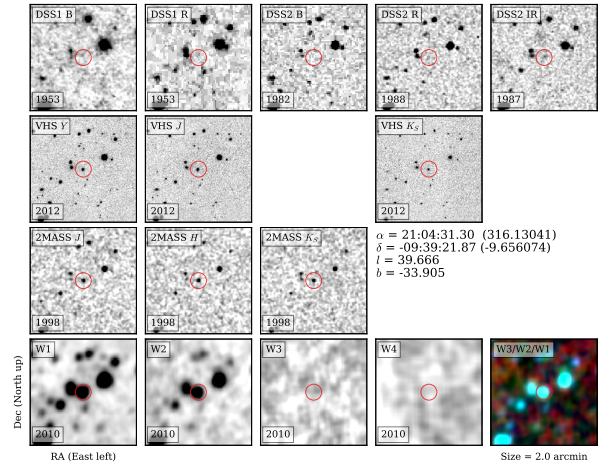


Figure 2. Finder chart for 2MASS J21043128-0939217, a new \sim L3 candidate member of the β PMG. The red circle displays its expected position at epoch 2000 based on the *Gaia* astrometric solution. Its proper motion can be seen from the marginal detection in the 1989 DSS2 infrared image as well as the slightly off-center sources in the VHS and *WISE* images, and is consistent with the *Gaia* proper motion ($\mu_\alpha \cos \delta = 59 \pm 3 \text{ mas yr}^{-1}$, $\mu_\delta = -58 \pm 2 \text{ mas yr}^{-1}$). Its non-detection at optical wavelengths is also consistent with its estimated spectral type. See Section 3 for more detail.

² <https://archives.esac.esa.int/gaia>

the optimal value that would minimize the distance between a target and its most probable young association in spatial-kinematic $XYZUVW$ space. The 90% probability threshold is associated with a recovery rate of only 50% of the bona fide members (Gagné et al. 2018), and was selected as a first pass to identify only the most unambiguous members of young associations in *Gaia* DR2 while minimizing the rate of contamination from random field interlopers.

3. LITERATURE SEARCH AND TARGET VALIDATION

Gagné et al. (2018) compiled a list of candidate or bona fide members of young associations. Before our sample was analyzed in more detail, we cross-matched it with this list and removed from our sample the 1399 that were found in both lists. The known young brown dwarfs will be discussed in J. K. Faherty et al. (in preparation), and the known stellar members will be discussed in J. Gagné et al. (in preparation) along with an update of the spatial-kinematic models of the young associations and the field used in BANYAN Σ . We also ignored 12 K-type stars that will be discussed by M. Chalifour, A. Binks, J. Kastner et al. (in preparation).

Several parallax solutions near the Galactic plane in *Gaia* DR2 suffer from cross-matching confusion, especially for faint targets (Lindegren et al. 2018; see also Faherty et al. 2018). In order to assess which *Gaia* entries corresponded to physical objects, we built finder charts with all available data from the Digitized Sky Survey, SDSS (Alam et al. 2015), 2MASS (Skrutskie et al. 2006), WISE (Wright et al. 2010), Pan-STARRS (Chambers et al. 2016), VHS (McMahon et al. 2013) and UKIDSS (Lawrence et al. 2007) with the `finder_charts.py` Python package (Gagné et al. 2018)³. We visually examined the 2195 charts to confirm the non-zero proper motion of the targets and to verify that their colors were consistent with their absolute *Gaia* G -band magnitudes (e.g., see Figures 1 and 2). This step allowed us to remove 504 contaminants that corresponded to unphysical entries in the *Gaia* catalog. Their distribution in relative G -band magnitude versus Galactic latitude is displayed in Figure 3 compared to the full input sample, which demonstrates that most of the unphysical *Gaia* DR2 parallax solutions are caused by cross-match confusion of faint objects near the Galactic plane. Most of them can also be rejected from an inspection of the `ASTROMETRIC_SIGMA5D_MAX`

and `VISIBILITY_PERIODS_USED` flags in the *Gaia* DR2 catalog, which respectively correspond to the maximal measurement error of all astrometric solution parameters (in mas), and to the number of epochs that were used in the solution (see Figure 4). However, a simple rejection filter based on these criteria would also inevitably reject some good solutions.

A total of 250/261 initial entries with *Gaia* DR2 parallax measurements in the range 3–8 times larger than the measurement error were rejected by our visual inspection of the finder charts. A large fraction of low-precision parallaxes thus corresponded to unphysical *Gaia* DR2 entries, but we keep the remaining 11 low-precision entries because they likely correspond to valid late-M or early-L candidate members.

Our literature search revealed that 36 of our new candidate members without a *Gaia* DR2 radial velocity have such measurements in the literature, 6 of which rejected the membership hypothesis.

There are four high-probability candidate members of β PMG and ABDMG in our sample that appear in the literature as candidates of the more distant PLE and HYA associations and the TAU and Sco-Cen star-forming regions. These objects were rejected from our sample as a consequence of this, but we provide below a short discussion of their membership.

Both 2MASS J17513421–4854558 (\approx M1) and 2MASS J17194204–4615275 (M2; Galicher et al. 2016) were identified as young candidate members of USCO with Li absorption (290 mÅ and 520 mÅ respectively) by Song et al. (2012). However, their *Gaia* DR2 trigonometric distances (66.5 ± 1.2 pc and 53.0 ± 0.2 pc respectively) preclude membership in USCO, and strongly favors membership in the β PMG. In both cases, radial velocity measurements are still needed to confirm their membership, but the *Gaia* DR2 parallax measurements safely reject membership in USCO.

2MASS J04203904+2355502 was identified as a L1 candidate member of the TAU star-forming region by Luhman (2006), but he noted that its weak spectroscopic signatures of low surface gravity were indicative of an age between that of TAU and field brown dwarfs. Its trigonometric distance from *Gaia* DR2 (38.7 ± 1.3 pc) makes it a candidate member of the ABDMG in the foreground of TAU. A radial velocity measurement is still needed to fully confirm its membership in the ABDMG.

2MASS J04254357+1616214 was identified by (Bouvier et al. 2008) as a low-probability candidate member of the HYA, however its nearby distance (67.0 ± 0.3 pc) makes it a candidate member of the β PMG instead. The same is true of 2MASS J04341301+1510569 (van Altena

³ Available at https://github.com/jgagneastro/finder_charts and at <http://www.astro.umontreal.ca/~gagne/finderchart.php> as a web tool.

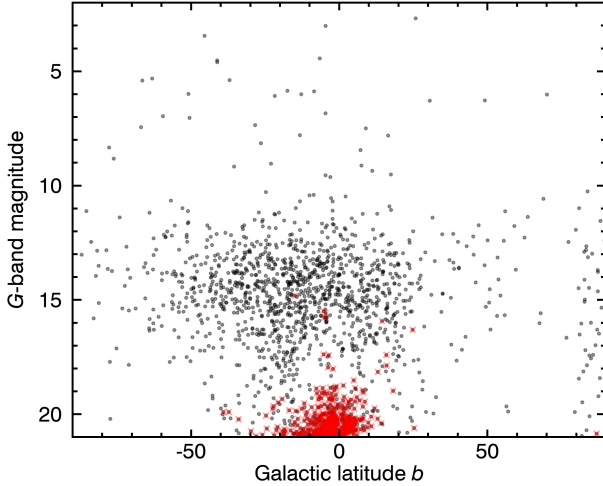


Figure 3. Relative *Gaia* G -band magnitude versus Galactic latitude for the full sample (black circles) and unphysical objects rejected by the finder charts examination (red crosses). Some *Gaia* DR2 parallax solutions correspond to unphysical objects, and are mainly caused by cross-match confusion of faint objects near the Galactic plane. See Section 3 for more detail.

1966), but its distance (49.1 ± 0.2 pc) makes it a viable candidate member of the ABDMG.

We used *Gaia* absolute G -band magnitude versus $G - G_{RP}$ color-magnitude diagrams to further reject any candidates not consistent with the known young members and candidate members or their respective young associations. The list of members compiled by Gagné et al. (2018) were compared to our candidates one group at a time (e.g., see Figure 5, and any candidates significantly fainter than the young sequences were rejected from our sample. This step rejected an additional 327 candidates, most of them in the ABDMG (114), β PMG (79) and COL (37). This is consistent with the determination of Gagné et al. (2018) that these associations are the most subject to contamination by unrelated field interlopers in kinematic-based searches, mostly because of their proximity (i.e., their members cover a larger fraction of the sky).

4. DISCUSSION

Our sample of new candidate members is the first step towards filling a gap in the current census of low-mass stars in young associations. Until now, obtaining trigonometric parallax measurements for a large number of low-mass stars has prevented completing the census of young associations especially in the M spectral class, which are fainter and much more numerous than the more massive members. Previous works have been successful at identifying a large fraction of the early M-type

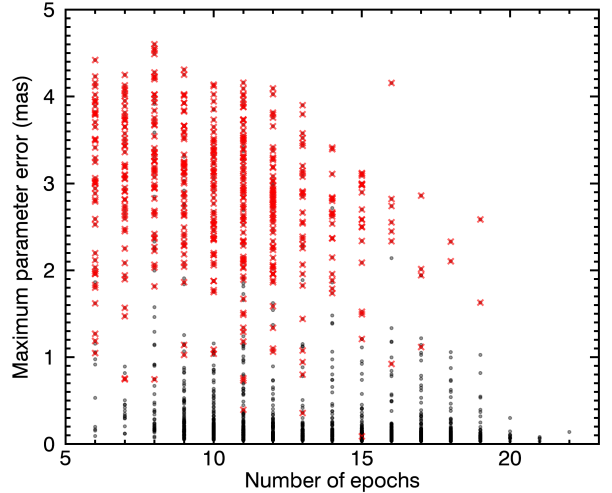


Figure 4. Maximum measurement error on all parameters of the *Gaia* DR2 astrometric solution (`ASTROMETRIC_SIGMA5D_MAX`) versus the number of visibility windows used in the solution (`VISIBILITY_PERIODS_USED`), for the full sample (black circles) and those rejected as unphysical entries by a visual examination of the finder charts (red crosses). As expected, entries with less epochs and larger error bars are more prone to correspond to unphysical objects, but a simple rejection criterion based on these parameters would also reject some good solutions. See Section 3 for more detail.

members (e.g., Shkolnik et al. 2012; Malo et al. 2013, 2014a; Kraus et al. 2014; Shkolnik et al. 2017; Gagné et al. 2018b), but there remains a dearth of late-M type members. In Figure 6, we show a color-magnitude diagram of the current census of bona fide members (Gagné et al. 2018), compared with the sample discussed here. This figure demonstrates how *Gaia* DR2 is particularly powerful at completing the faint, low-mass end of the color-magnitude diagram.

An advantage of *Gaia* DR2-based searches is that trigonometric distances make it possible to cover the Galactic plane with significantly less contamination than searches based on only proper motion. In Figure 7, we show the distribution in sky positions of the new candidate members identified here. This figure demonstrates how our search is not biased away from the Galactic plane like most previous all-sky searches (e.g., Gagné et al. 2015a). Confirming membership still requires a spectroscopic follow-up to assess their youth and measure their radial velocities. In this section, we estimate the basic properties of the new candidates uncovered here in order to guide future telescope observations.

4.1. Photometric Spectral Type Estimates

In this section, we build an absolute G -band magnitude versus spectral type sequence in order to estimate

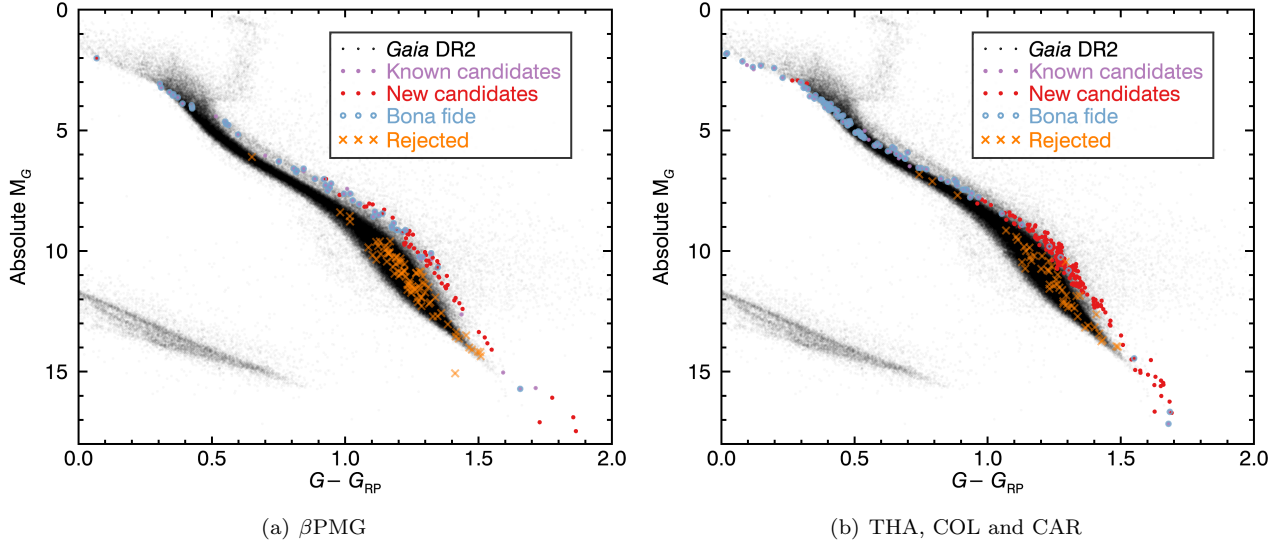


Figure 5. Color-magnitude diagrams of known bona fide members (blue circles) and candidate members (filled purple circles) of young associations of similar ages (Gagné et al. 2018) compared to the new candidate members identified in this work (filled red circles). All candidates too faint to be consistent with their respective association (orange crosses) were rejected from our sample. See Section 3 for more detail.

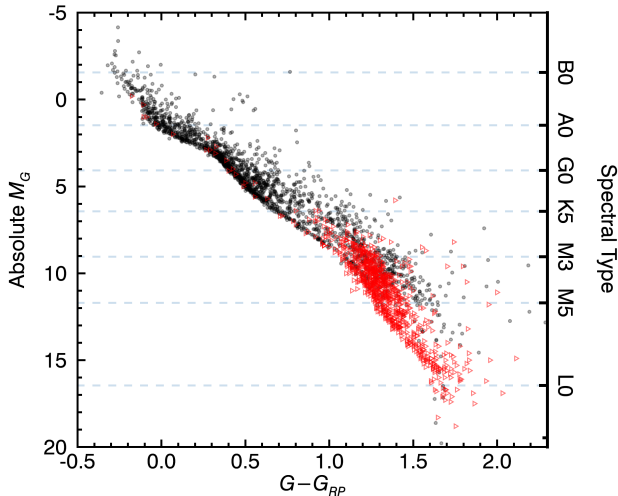


Figure 6. *Gaia* DR2 color-magnitude diagram of known bona fide members in young associations (black unfilled circles) compiled in Gagné et al. (2018). We choose $G - G_{RP}$ as a comparison color because photometric quality in *Gaia* DR2 remains good down to the substellar regime. New candidate members identified in this work are displayed as red unfilled circles. These data include pre-main sequence as well as main-sequence objects, depending on their masses and ages, which explains the large scatter especially at low masses (red colors). Some of the slightly older and more massive objects have also started to depart from the main sequence. See Section 4 for more detail.

the spectral types of the new young association candidates discovered here. We preferentially include young stars and brown dwarfs with ages $\sim 5\text{--}200$ Myr which are more representative of our sample, but we do not

build separate sequences at different ages because only approximate spectral types will be calculated.

We cross-matched the lists of bona fide members of young associations compiled by Gagné et al. (2018) with *Gaia* DR2 to build the bulk of the sequence across the stellar domain. Because the current list of bona fide members is incomplete for spectral types later than \approx K0, we added the lists of candidate members compiled by Gagné et al. (2018b) and Gagné et al. (2018a), which cover spectral types down to \approx M5, and the known young brown dwarfs compiled by Faherty et al. (2016) and Gagné et al. (2015b). The resulting list of young objects contains a small number of objects in the ranges of spectral types M6–M9 and L5–T0, and we therefore completed these spectral ranges with the compilations of Hawley et al. (2002); Cruz et al. (2007); West et al. (2008) and Smart et al. (2017). These data likely do not represent the full spread in absolute *G*-band magnitudes that are due to young ages, but they remain useful to estimate spectral type.

We calculated the median absolute G -band magnitude and the corresponding standard deviation for each spectral type in the range B5–L9 with bins of 0.5 sub-types using the compilation described above. A 3σ outlier rejection step was then applied, and the median and standard deviation across the full sequence was recalculated. The resulting sequence is displayed in Figure 8, and was used to estimate the spectral types of the new candidates identified here unless they already had a measured spectral type in the literature. The average standard deviation around the resulting sequence

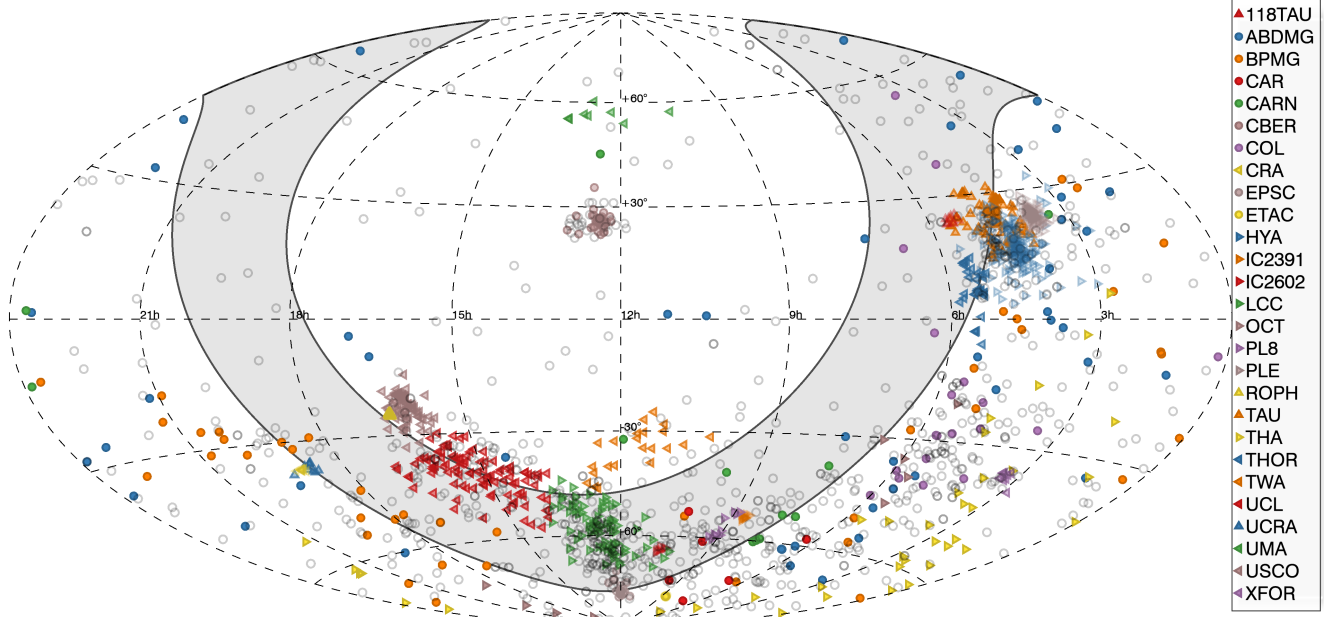


Figure 7. Sky position of known bona fide members in young associations (colored symbols, see legend for individual association names) compared with new candidate members uncovered here (black unfilled circles). The Galactic plane (Galactic latitudes $\pm 15^\circ$) is marked with a thick black line and a gray shaded region. The distribution of newly identified young associations generally tracks that of known members, and several new candidates were uncovered near the Galactic plane where previous searches were incomplete. See Section 4 for more detail.

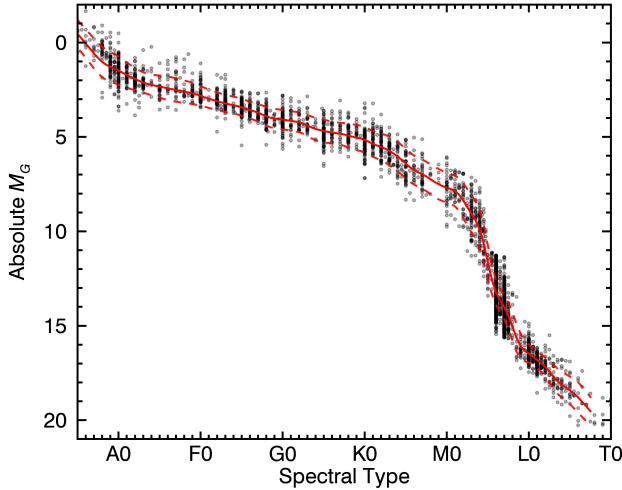


Figure 8. Absolute *Gaia* G -band magnitude as a function of spectral type for various young and field objects (black circles). The median sequence is displayed as a solid red line and its standard deviation as dashed red lines. This median sequence was used to estimate the spectral types of new candidate members uncovered here, based on their absolute G -band magnitudes. Section 4.1 for more detail.

is ≈ 0.6 mag, which corresponds to a spectral type uncertainty of 3–5 subtypes, depending on spectral class. The resulting spectral type estimates are listed in Table 3 with our compilation of new candidate members.

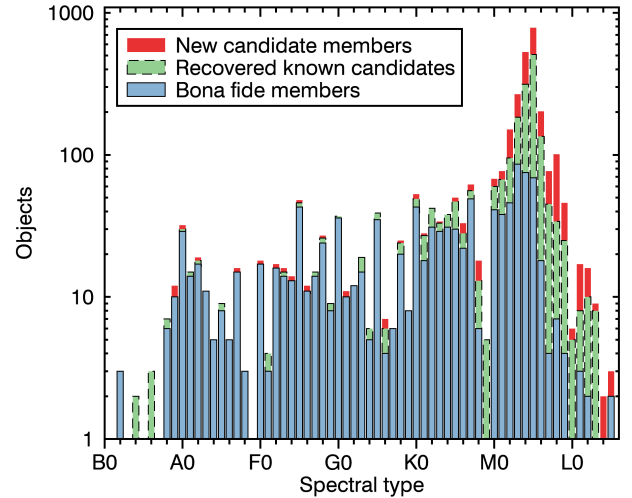


Figure 9. Spectral type histogram of known bona fide members of young associations (blue solid line), recovered known candidate members (green dashed lines), and new candidate members identified in this work (red bars without outline). The contribution of this work is most important in the range of spectral types K7–L2. See Section 4.1 for more detail.

We compare the distribution of estimated spectral types in the current sample with the known members and candidate members of young associations in Figure 9.

4.2. Chromospheric Activity

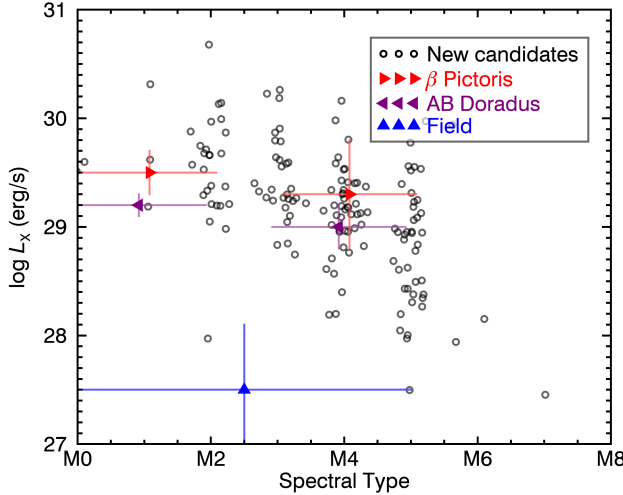


Figure 10. X-ray luminosity of our sample of new candidates (black unfilled circles) compared to the different samples of Malo et al. (2014a). Artificial noise with a standard deviation of 0.15 subtypes was added to our candidates for visibility. Most of the new candidates identified here have an X-ray luminosity consistent with the age of ABDMG or younger, as expected. See Section 4.2 for more detail.

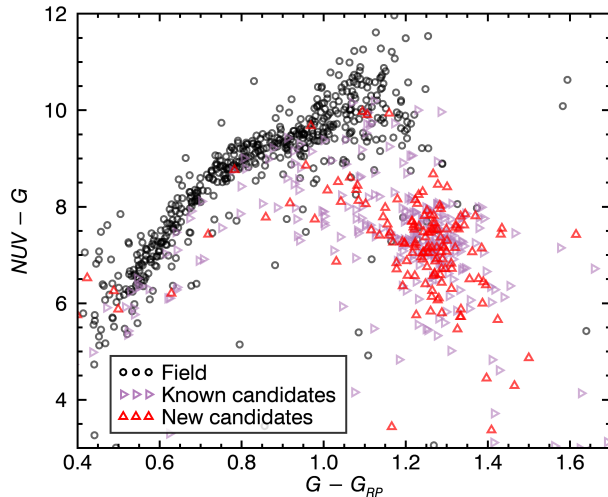


Figure 11. *Galex* $NUV - G$ color versus *Gaia* $G - R$ color for our sample of new candidates (red upward triangles) compared to known candidates and bona fide members recovered in our sample (rightward purple triangles) and field objects (black circles). Our sample mostly consists of highly active mid-M dwarfs, as would be expected at given the young ages of the associations considered here. See Section 4.2 for more detail.

One of the well known signs of youth for early- and mid-type M dwarfs is their chromospheric activity compared (e.g., Shkolnik et al. 2011; Rodriguez et al. 2011; Malo et al. 2014a; Schmidt et al. 2015). Signatures of high chromospheric activity include overluminosity at

X-ray and ultraviolet wavelengths, as well as strong H α emission (e.g., West et al. 2008; Schmidt et al. 2015) and a high rate of flares (e.g., Schmidt et al. 2007; Davenport et al. 2012). While assessing the latter two characteristics in our sample will require follow-up at the telescope in spectroscopy and imaging, the X-ray and ultraviolet properties of several new candidates presented here can already be obtained from the *ROSAT* all-sky survey (Boller et al. 2016) and the *GALEX* catalog (Martin et al. 2005).

We cross-matched our sample of candidates with the second *ROSAT* all-sky catalog to obtain their X-ray luminosity and compare them with the young and field samples of early- to mid-M dwarfs of Malo et al. (2014a). We used the *Gaia* DR2 proper motions and positions to project back positions to epoch 1994.5 and used a cross-match radius of $30''$, yielding 194 matches⁴. The resulting X-ray luminosities are compared with the field objects, and the ABDMG and β PMG candidate members of Malo et al. (2014a) in Figure 10. Most of our candidates demonstrate a clear X-ray over-luminosity compared to the field sample of Malo et al. (2014a), and are consistent with ages younger than ~ 200 Myr, which is expected based on the ages of the young associations considered here (see Table 1).

A similar cross-match was performed with the data release 5 of *GALEX* (at epoch 2007.5 and a cross-match radius of $10''$) and yielded 180 matches. The $NUV - G$ *GALEX*–*Gaia* color of our sample versus its $G - R$ *Gaia* color (which traces spectral type) are compared to a sample of field stars and recovered known candidates or bona fide members in Figure 11. Most of the new candidate members identified here have unusually blue $NUV - G$ colors compared to field stars, which is a signature of high chromospheric activity.

4.3. Co-Moving Systems

We searched the *Gaia* DR2 catalog for co-moving systems by examining a $2'$ radius around each source in our sample of new candidate members. We searched for objects with proper motions within 10 mas yr^{-1} and a trigonometric parallax within 5 mas of each other. We chose these very conservative limits to identify only the most likely co-moving systems while minimizing contamination from chance alignments. Deriving false-contamination probabilities at larger spatial or kinematic separations will require a careful examination of

⁴ $30''$ corresponds to the astrometric precision of *ROSAT* due to its large point-spread function. Contamination by background X-ray bright galaxies is expected to be very small given their small density on the sky (e.g., see Böhringer et al. 2004).

chance alignments within the members of a young association (e.g., see Gagné et al. 2017).

Our conservative criteria identified 104 co-moving systems, 82 of which are co-moving with an object outside of our sample. Sixteen of the latter cases are new companions to known bona fide or candidate members of young associations. In 40 cases, we identified a co-moving system that had a radial velocity measurement in the literature. Including this measurement in BANYAN Σ allowed us to reject 12 candidate members from our sample and strengthen the membership of 28 others. All co-moving systems identified here are listed in Table 4.

Table 2. New likely L-type candidates identified in this work.

Spectral Type ^a	Assoc.	R.A. ^b (hh:mm:ss.sss)	Decl. ^b (dd:mm:ss.ss)
(L0)	ABDMG	01:38:47.53	-34:52:32.8
(L1)	HYA	04:33:56.71	+05:37:23.7
(L1)	HYA	04:45:43.83	+12:46:31.2
(L2)	ABDMG	05:08:16.60	-14:13:49.6
(L2)	CARN	05:19:28.80	-45:06:38.1
(L1)	ABDMG	05:44:57.42	+37:05:00.5
(L1)	COL	06:16:56.25	-25:43:55.9
(L5)	CARN	07:23:52.61	-33:09:43.0
(L1)	CAR	09:18:56.29	-61:01:18.7
L2	CARN	09:28:39.53	-16:03:12.4
(L2)	CARN	09:42:32.37	-25:51:37.6
(L1)	CARN	11:50:42.86	-29:14:48.9
L4	CARN	12:13:02.96	-04:32:44.3
(L2)	BPMG	18:10:35.72	-55:13:45.0
(L1)	BPMG	18:26:46.80	-46:02:24.5
(L1)	ABDMG	18:40:59.39	-09:59:17.5
(L3)	BPMG	21:04:31.36	-09:39:22.7
(L1)	ABDMG	21:13:41.87	+35:07:39.6
(L2)	ABDMG	23:54:12.69	+22:08:21.2

^aSpectral types between parentheses were estimated from the absolute *Gaia* G -band magnitude.

^bJ2000 position at epoch 2015 from the *Gaia* DR2 catalog.

4.4. Isochrone Ages

We compared the absolute *Gaia* G -band magnitudes versus $G - R$ color of our new mid to late M-type candidates ($G - G_{RP} > 1.3$ mag) with those of the MIST solar-metallicity tracks v1.1 (Choi et al. 2016). We used

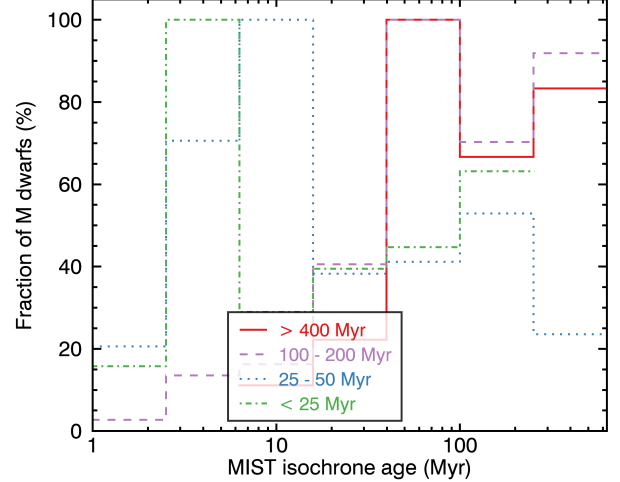


Figure 12. Distribution of MIST isochrone ages for new M-type candidate members in young associations of different age ranges. These age estimates ignore the effects of magnetic fields and are therefore expected to be systematically too low, but the relative differences in age distribution between candidates in associations of different ages can already be seen clearly. See Section 4.4 for more detail.

the Bayesian method described by Gagné et al. (2018b) to verify if we find relative differences in the distribution of isochrone ages in our candidate members of associations with different ages. The resulting isochrone age distributions for our targets are displayed in Figure 12. We note that the MIST isochrone age estimations ignore the contribution of magnetic fields. This is known to produce ages that are systematically too young compared to other age-dating methods such as the lithium depletion boundary for M dwarfs (Malo et al. 2014b). However, we can clearly see a correlation between the distributions of isochrone ages and the expected ages of the candidates based on their respective young associations. These new M dwarf candidates will be valuable to better understand the distribution of magnetic field strength versus age after a detailed spectroscopic follow-up is completed.

4.5. Brown Dwarfs

We used the bolometric luminosity versus spectral type relations of Faherty et al. (2016) combined with the Saumon & Marley (2008) evolutionary tracks to obtain a rough estimate of the spectral types that correspond to the substellar regime at the age of each young association considered here. We used these estimates to identify a total of 111 objects in our sample that are new brown dwarf candidate members in young associations with spectral types later than M6–L2, depending on the age of the young association they likely belong to.

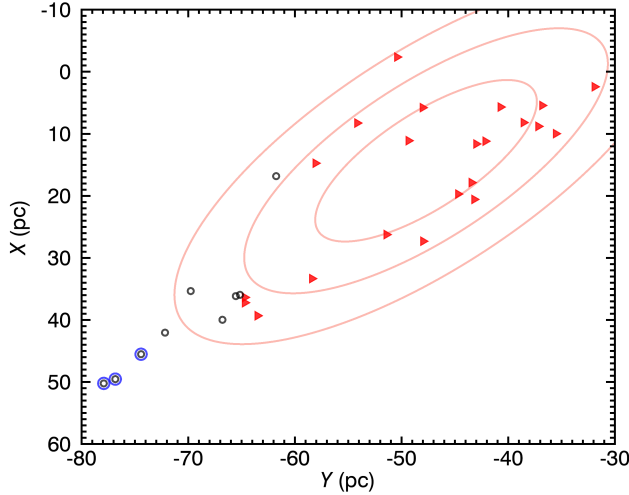


Figure 13. Galactic positions X and Y of known TWA members (rightward red triangles) compared to new candidates identified in this work (black unfilled circles). The new candidates identified here form an extension of the TWA distribution to slightly larger distances. Three of the new TWA candidates have a non-negligible membership probability in LCC (marked with larger blue unfilled circles) and may form a bridge between the two associations. The 1, 2 and 3σ contours of the BANYAN Σ spatial model of TWA are shown with thick orange lines. See Section 4.6 for more detail.

Obtaining near-infrared spectra yield gravity-sensitive spectroscopic indices (e.g., Allers & Liu 2013), and will provide valuable data for interpreting atmospheres similar to those of gaseous giant planets (e.g., Marois et al. 2008; Rameau et al. 2013). Ultimately this sample will place constraints on the very low-mass end of the initial mass function (e.g., Gagné et al. 2015b). There are 19 brown dwarfs in our sample with estimated spectral types in the L class. Their parallax measurements are 7–90 times larger than the measurement errors, with a median of 25. They are listed in Table 2.

4.6. Tentative Indications of Spatial Extension

It can be expected that the current census of the nearby young associations is biased toward nearby distances, because our knowledge of their spatial distribution is still based on members bright enough to have been detected by the Hipparcos mission (Perryman et al. 1997). Recent discoveries (Bowler et al. 2017; Desrochers et al. 2018) suggested for example that the ABDMG might be larger than previously thought, and its very similar kinematics and age to the more distant Pleiades association (e.g., see Luhman et al. 2005; Soderblom et al. 2014; Gagné et al. 2018) raises the question of whether the two associations may be related. In its default setting, BANYAN Σ compares the XYZ Galactic positions of objects to a fixed spatial model

density of young associations, and is therefore not designed to uncover such spatial extensions of known associations. Our search did not identify candidate members of ABDMG at larger distances, but this could be entirely caused by our bias in recovering new candidate members that are located spatially near those already known. Future work will be needed to explore this possibility. BANYAN Σ has the option to consider only UVW space velocities in its search for new candidate members, but in this case it will be important to confirm the youth of the candidate members because searches based on UVW only will suffer significant contamination from random field interlopers.

Our survey has however identified a possible extension of the TWA to slightly larger distances (see Figure 13) that may bridge it to the LCC region of the Sco-Cen star-formation complex. Searches for new candidate members in TWA have been known to be contaminated by the LCC region of the Sco-Cen star-formation complex (e.g., see Gagné et al. 2017), however BANYAN Σ now includes a model of LCC. We uncovered 5 candidates at the far end of TWA that have a zero LCC membership probability, and 4 slightly more distant candidates that are most likely TWA candidates but have non-negligible membership probabilities in LCC. Determining the ages of these stars seemingly bridging the two associations may allow us to understand whether they are simply contaminants or whether TWA and LCC are related.

Our sample of new candidates in CAR and COL also show slightly different spatial distributions than the currently known bona fide members (see Figure 14). Confirming the radial velocities and youth of the new candidates will be required to determine whether the spatial models of BANYAN Σ will need to be refined, and to test whether the spatial distribution of the lower-mass members are distinct from those of the more massive members. The distributions of new candidate members closely followed that of known bona fide members for all other associations and spatial-kinematic projections.

4.7. New Bona Fide Members

There are 17 B9–G8 stars in our sample that have full kinematics and were not previously recognized as candidate members of young associations in the literature. We calculated MIST isochrone ages for them (see Section 4.4 for more detail) and report them in Table 5 as new bona fide members of their respective young associations. All of them have ages consistent with their young association, except for iot Cen (7_{-2}^{+2} Myr) which is much too young to belong in CARN. The ages of the F-type stars in Table 5 cannot be constrained with isochrones,

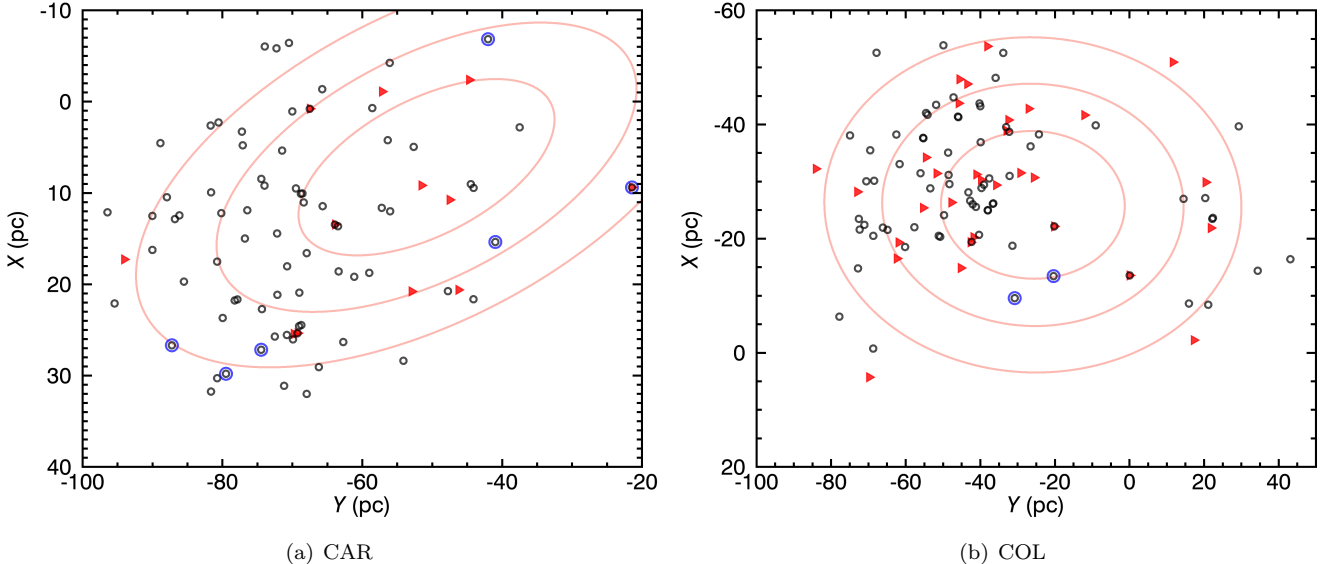


Figure 14. Galactic positions X , Y and Z of known members in CAR and COL (rightward red triangles) compared to new candidates identified in this work (black unfilled circles). The 1, 2 and 3σ contours of the BANYAN Σ spatial models of the respective groups are shown with thick orange lines. The candidates with a non-negligible membership probability in more than one young association are marked with larger blue unfilled circles. The new candidate members identified in this survey show slightly different spatial distributions than the known members. This could be caused by non-uniform contamination, a bias in the inferred distribution caused by the small number of known bona fide members, or a mass dependency on the spatial distribution of members. The distance limit of 100 pc that we imposed on our sample did not affect these nearby objects. See Section 4.6 for more detail.

and it will be difficult to pose any age constraints for these stars. In addition to these, there are 15 stars in our sample that are co-moving with a known bona fide member (see Section 4.3). Those are also reported in Table 5.

5. CONCLUSIONS

We used the BANYAN Σ algorithm with the nearest 100 pc entries in the *Gaia* DR2 to identify 898 new candidate members with spectral types in the range B9–L2 in the 27 nearest young associations from an initial sample of 3158 candidates (1411 were already known in the literature, 504 *Gaia* DR2 entries were rejected from a visual examination of finder charts, and 18 were rejected with a literature radial velocity measurement). 104 of these objects are co-moving systems, and will serve as important benchmarks for the calibration of atmosphere and evolutionary models. Spectroscopic follow-up of these targets to obtain radial velocities and signatures of youth such as lithium absorption will be needed to confirm their membership. Our search identified mostly mid-M candidate members, which contribute most importantly to the initial mass function. The ongoing TESS mission (Ricker et al. 2015) will uncover exoplanet companions to several of these nearby M dwarfs with the transit method. Identifying age-calibrated stars among the TESS sample in 27 distinct populations with ages in

the range ~ 2 –750 Myr will provide crucial information on the fundamental parameters of these future exoplanet discoveries, and will inform how the structure of planetary systems evolve with time.

We thank the anonymous referee for thoughtful comments that improved the quality of this work. We thank Ricky L. Smart and Joel Kastner for useful comments. This research made use of: the SIMBAD database and VizieR catalog access tool, operated at the Centre de Données astronomiques de Strasbourg, France (Ochsenbein et al. 2000); data products from the Two Micron All Sky Survey (2MASS; Skrutskie et al. 2006), which is a joint project of the University of Massachusetts and the Infrared Processing and Analysis Center (IPAC)/California Institute of Technology (Caltech), funded by the National Aeronautics and Space Administration (NASA) and the National Science Foundation (Skrutskie et al. 2006); data products from the *Wide-field Infrared Survey Explorer* (*WISE*; and Wright et al. 2010), which is a joint project of the University of California, Los Angeles, and the Jet Propulsion Laboratory (JPL)/Caltech, funded by NASA. The Digitized Sky Surveys were produced at the Space Telescope Science Institute under U.S. Government grant NAG W-2166. The images of these surveys are based on photographic data obtained using the Oschin Schmidt

Telescope on Palomar Mountain and the UK Schmidt Telescope. The plates were processed into the present compressed digital form with the permission of these institutions. The Second Palomar Observatory Sky Survey (POSS-II) was made by the California Institute of Technology with funds from the National Science Foundation, the National Geographic Society, the Sloan Foundation, the Samuel Oschin Foundation, and the Eastman Kodak Corporation. The Oschin Schmidt Telescope is operated by the California Institute of Technology and Palomar Observatory. This work presents

results from the European Space Agency (ESA) space mission Gaia. Gaia data are being processed by the Gaia Data Processing and Analysis Consortium (DPAC). Funding for the DPAC is provided by national institutions, in particular the institutions participating in the Gaia MultiLateral Agreement (MLA). The Gaia mission website is <https://www.cosmos.esa.int/gaia>. The Gaia archive website is <https://archives.esac.esa.int/gaia>. This research was started at the NYC Gaia DR2 Workshop at the Center for Computational Astrophysics of the Flatiron Institute in 2018 April.

Table 3. New candidates identified in this work.

Name	Spectral Type ^a	Assoc. ABDMG	R.A. ^b (hh:mm:ss.sss)	Decl. ^b (dd:mm:ss.ss)	$\mu_\alpha \cos \delta$ (mas yr ⁻¹)	μ_δ (mas yr ⁻¹)	Parallax (mas)	Rad. Vel. (km s ⁻¹)	Ambiguous Assoc. ^c	Ref. ^d
J0644-4137	(M4)	ABDMG	06:44:54.065	-41:37:27.38	-5.17 ± 0.07	-20.89 ± 0.07	20.37 ± 0.04	-,-
J0646+1015	(M6)	ABDMG	06:46:05.803	+10:15:37.96	-19.38 ± 0.38	-98.25 ± 0.44	16.95 ± 0.14	-,-
J0650-3203	(M5)	ABDMG	06:50:27.278	-32:03:19.11	-26.22 ± 0.08	-54.64 ± 0.09	31.70 ± 0.05	-,-
J0700-4447	(M6)	ABDMG	07:00:34.277	-44:47:13.56	-43.50 ± 0.25	-14.42 ± 0.25	45.22 ± 0.13	-,-
J0703-4152	(M9)	ABDMG	07:03:02.270	-41:52:22.68	-11.7 ± 1.2	-20.2 ± 2.5	20.72 ± 0.86	-,-
J0703-6110	(M8)	ABDMG	07:03:23.851	-61:10:03.23	-11.27 ± 0.68	26.39 ± 0.63	15.94 ± 0.32	-,-
J0703-1723	(M4)	ABDMG	07:03:38.676	-17:23:39.06	-39.40 ± 0.17	-77.74 ± 0.14	24.67 ± 0.10	-,-
J0703-5505	(M8)	ABDMG	07:03:59.359	-55:05:58.52	-27.22 ± 0.44	11.64 ± 0.42	19.83 ± 0.19	-,-
J0716+0817	(M6)	ABDMG	07:16:06.314	+08:17:24.19	-36.67 ± 0.83	-151.22 ± 0.79	27.18 ± 0.49	-,-
J0724-4052	(M4)	ABDMG	07:24:34.961	-40:52:12.98	-53.46 ± 0.08	-26.27 ± 0.08	24.01 ± 0.04	-,-
J0727-5320	(M7)	ABDMG	07:27:25.752	-53:20:32.24	-32.78 ± 0.24	-2.87 ± 0.22	22.47 ± 0.10	-,-
J0741-4630	(M4)	ABDMG	07:41:49.814	-46:30:17.04	-28.97 ± 0.09	-5.21 ± 0.09	15.88 ± 0.05	-,-
J0757-2226	(M5)	ABDMG	07:57:05.117	-22:26:43.83	-34.95 ± 0.11	-71.91 ± 0.18	23.04 ± 0.10	-,-
J0801-5034	(M5)	ABDMG	08:01:25.118	-50:34:26.64	-47.97 ± 0.36	-7.98 ± 0.31	29.40 ± 0.18	-,-
J0827-5152	(M6)	ABDMG	08:27:36.408	-51:52:52.67	-54.75 ± 0.15	0.81 ± 0.15	20.76 ± 0.08	-,-
J0831+1025	M9V	ABDMG	08:31:55.920	+10:25:39.10	-64.86 ± 0.58	-171.81 ± 0.44	31.56 ± 0.30	1,-
J0836-4838	(M6)	ABDMG	08:36:36.106	-48:38:11.23	-104.82 ± 0.29	-18.24 ± 0.22	35.94 ± 0.12	-,-
J0836-4838	(M6)	ABDMG	08:36:36.139	-48:38:10.10	-91.35 ± 0.41	-12.74 ± 0.42	36.60 ± 0.21	-,-
J0840-5753	(M7)	ABDMG	08:40:35.686	-57:53:58.80	-72.64 ± 0.18	13.98 ± 0.21	25.96 ± 0.09	-,-
J0916-5440	(M5)	ABDMG	09:16:19.306	-54:40:44.64	-57.80 ± 0.10	0.08 ± 0.10	17.09 ± 0.05	-,-
J0922-5917	(M8)	ABDMG	09:22:36.002	-59:17:27.33	-78.79 ± 0.33	5.03 ± 0.25	23.08 ± 0.15	-,-
J0947+0224	M8.2V	ABDMG	09:47:44.669	+02:24:30.38	-107.31 ± 0.40	-162.45 ± 0.43	29.85 ± 0.25	2,-
J0100+5055	M5.5e	ABDMG	01:00:44.577	+50:55:43.28	116.16 ± 0.18	-89.13 ± 0.15	25.28 ± 0.11	3,-
J0101-7250	(M9)	ABDMG	01:01:17.145	-72:50:49.25	74.5 ± 3.0	-7.2 ± 1.8	18.6 ± 1.0	-,-
J0103+6105	(M2)	ABDMG	01:03:03.752	+61:05:47.87	86.67 ± 0.04	-63.96 ± 0.05	18.70 ± 0.03	-17.1 ± 0.3	...	-,4
J1019+4822	(M5)	ABDMG	10:19:17.198	+48:22:24.94	-104.15 ± 0.08	-112.25 ± 0.09	23.37 ± 0.10	-,-
J1016-1417	(M4)	ABDMG	01:06:25.510	-14:17:28.82	101.82 ± 0.11	-98.76 ± 0.08	22.02 ± 0.05	8.0 ± 0.6	...	-,5
J1057+4142	(M3)	ABDMG	10:57:14.628	+41:42:52.93	-103.51 ± 0.07	-116.11 ± 0.08	23.55 ± 0.07	-13 ± 5	...	-,5
J1111-5316	(M6)	ABDMG	11:11:57.142	-53:16:56.80	-92.44 ± 0.15	-37.71 ± 0.16	21.12 ± 0.11	-,-
J1116-8027	(M5)	ABDMG	11:16:56.426	-80:27:51.67	-140.15 ± 0.10	34.11 ± 0.10	35.40 ± 0.05	...	ABDMG(88);CAR(7)	-,-
J1121-6534	(M5)	ABDMG	11:21:08.594	-65:34:10.49	-78.5 ± 1.1	-13.35 ± 0.95	18.30 ± 0.67	...	ABDMG(89);BPMG(11)	-,-
J1121-7427	(M5)	ABDMG	11:21:59.825	-74:27:48.45	-65.61 ± 0.10	-4.00 ± 0.09	15.82 ± 0.05	-,-
J1134-7330	(M4)	ABDMG	11:34:54.787	-73:30:34.84	-176.39 ± 0.09	-18.97 ± 0.07	34.86 ± 0.05	-,-
J1147-3017	G6V	ABDMG	11:47:15.490	-30:17:14.97	-266.12 ± 0.04	-228.01 ± 0.03	56.37 ± 0.03	14.0 ± 0.1	...	6,4
J1212-5214	(M6)	ABDMG	12:12:01.150	-52:14:30.21	-112.79 ± 0.13	-94.59 ± 0.10	27.82 ± 0.10	-,-
J1232-6856	M8	ABDMG	12:32:17.126	-68:56:02.25	-216.04 ± 0.21	-100.04 ± 0.16	47.42 ± 0.12	7,-
J0122+5452	(M5)	ABDMG	01:22:43.945	+54:52:53.39	92.41 ± 0.14	-83.70 ± 0.11	20.27 ± 0.08	-,-

Table 3 continued

Table 3 (*continued*)

Name	Spectral	Assoc.	R.A. ^b	Decl. ^b	$\mu_\alpha \cos \delta$	μ_δ	Parallax	Rad. Vel.	Ambiguous	Ref. ^d
	Type ^a		(hh:mm:ss.sss)	(dd:mm:ss.ss)	(mas yr ⁻¹)	(mas yr ⁻¹)	(mas)	(km s ⁻¹)	Assoc. ^c	
J0122-2556	(M6)	ABDMG	01:22:51.607	-25:56:19.14	127.66 ± 0.18	-110.03 ± 0.12	28.77 ± 0.09	-,-
J1334-6314	(M5)	ABDMG	13:34:17.237	-63:14:26.96	-99.27 ± 0.06	-80.76 ± 0.07	23.13 ± 0.05	-,-
J1336-8002	(M9)	ABDMG	13:36:53.496	-80:02:06.55	-81.42 ± 0.70	-38.72 ± 0.45	19.55 ± 0.33	-,-
J1344-6134	(M6)	ABDMG	13:44:48.024	-61:34:24.10	-89.55 ± 0.12	-90.06 ± 0.14	20.31 ± 0.11	-,-
J0127-5717	(M3)	ABDMG	01:27:12.309	-57:17:37.17	95.97 ± 0.05	-36.43 ± 0.04	21.82 ± 0.03	20 ± 1	...	-,4
J1415-7743	(M4)	ABDMG	14:15:41.498	-77:43:06.56	-66.18 ± 0.07	-61.65 ± 0.07	17.28 ± 0.04	-,-
J1415-7742	(M4)	ABDMG	14:15:42.072	-77:42:46.73	-66.01 ± 0.06	-63.29 ± 0.06	17.14 ± 0.04	-,-
J1432-0314	(M8)	ABDMG	14:32:36.564	-03:14:10.99	-154.14 ± 0.26	-225.45 ± 0.20	44.60 ± 0.13	-,-
J0128+3318	(M8)	ABDMG	01:28:39.294	+33:18:08.01	77.35 ± 0.54	-99.45 ± 0.49	18.94 ± 0.30	-,-
J1441-4357	(M5)	ABDMG	14:41:07.109	-43:57:01.40	-131.50 ± 0.40	-201.81 ± 0.26	33.62 ± 0.18	-,-
J1441-4357	(M5)	ABDMG	14:41:07.502	-43:57:01.67	-120.85 ± 0.26	-190.40 ± 0.18	34.71 ± 0.15	-,-
J1452-2816	(M5)	ABDMG	14:52:11.102	-28:16:43.89	-71.94 ± 0.10	-121.46 ± 0.09	21.40 ± 0.06	-,-
J1455-8131	(M6)	ABDMG	14:55:16.253	-81:31:26.50	-91.38 ± 0.19	-69.64 ± 0.21	23.82 ± 0.13	-,-
J1459-4210	(M5)	ABDMG	14:59:57.293	-42:10:11.49	-107.50 ± 0.15	-188.46 ± 0.12	32.82 ± 0.08	-,-
J1516-0037	(M5)	ABDMG	15:16:55.651	-00:37:14.65	-116.74 ± 0.15	-191.97 ± 0.17	37.72 ± 0.10	-,-
J1518-4509	(M5)	ABDMG	15:18:46.872	-45:09:52.61	-55.87 ± 0.14	-104.53 ± 0.12	18.51 ± 0.08	-,-
J1529+4646	M4.5V	ABDMG	15:29:02.774	+46:46:23.53	-118.71 ± 0.94	-32.6 ± 1.3	45.62 ± 0.56	8,-
J1532-7021	(M4)	ABDMG	15:32:15.881	-70:21:04.39	-50.78 ± 0.05	-88.57 ± 0.07	19.28 ± 0.04	-,-
J1557+2748	(M5)	ABDMG	15:57:08.472	+27:48:59.50	-66.73 ± 0.06	-76.52 ± 0.07	27.22 ± 0.04	-,-
J0138-3452	(L0)	ABDMG	01:38:47.534	-34:52:32.75	75.42 ± 0.80	-52.39 ± 0.65	18.76 ± 0.74	-,-
J0139+7342	K5V	ABDMG	01:39:46.332	+73:42:30.61	159.98 ± 0.22	-111.11 ± 0.21	37.13 ± 0.13	-23 ± 2	...	9.4
J0139+2611	(M4)	ABDMG	01:39:58.869	+26:11:00.80	138.98 ± 0.26	-146.21 ± 0.12	31.02 ± 0.08	-10 ± 10	...	-,5
J1606-7200	(M4)	ABDMG	16:06:07.018	-72:00:47.62	-43.69 ± 0.04	-80.90 ± 0.05	17.04 ± 0.03	-,-
J1609-3431	(M6)	ABDMG	16:09:46.080	-34:31:10.40	-86.17 ± 0.23	-225.49 ± 0.13	36.35 ± 0.12	-,-
J1631+3243	(M7)	ABDMG	16:31:02.105	+32:43:24.61	-48.23 ± 0.13	-53.94 ± 0.15	25.66 ± 0.08	-,-
J1636-4041	(M4)	ABDMG	16:36:57.473	-40:41:13.30	-72.86 ± 0.14	-283.07 ± 0.09	44.72 ± 0.07	-,-
J1637-7348	(M6)	ABDMG	16:37:52.810	-73:48:32.61	-30.74 ± 0.13	-89.92 ± 0.20	17.94 ± 0.10	-,-
J1638-4232	(M5)	ABDMG	16:38:07.963	-42:32:14.99	-37.25 ± 0.17	-158.88 ± 0.11	25.13 ± 0.10	-,-
J0144+5332	(M5)	ABDMG	01:44:25.883	+53:32:55.47	133.09 ± 0.10	-139.38 ± 0.10	30.99 ± 0.06	-,-
J0145+7118	(M6)	ABDMG	01:45:58.460	+71:18:25.07	74.06 ± 0.16	-67.79 ± 0.17	17.98 ± 0.12	-,-
J1729-5547	(M7)	ABDMG	17:29:44.676	-55:47:57.60	-26.09 ± 0.18	-161.79 ± 0.19	26.41 ± 0.13	-,-
J1738+6114	M4	ABDMG	17:38:40.870	+61:14:00.02	-16.88 ± 0.08	46.84 ± 0.09	30.96 ± 0.04	10,-
J1739-5321	(M9)	ABDMG	17:39:57.967	-53:21:43.74	-4.60 ± 0.81	-141.36 ± 0.97	20.66 ± 0.68	-,-
J1747-5221	(M4)	ABDMG	17:47:03.530	-52:21:23.59	-10.19 ± 0.09	-119.48 ± 0.08	19.22 ± 0.06	-,-
J1755-2301	(M7)	ABDMG	17:55:06.775	-23:01:07.48	-11.93 ± 0.41	-158.86 ± 0.36	24.93 ± 0.27	-,-
J0148-4831	(M5)	ABDMG	01:48:47.900	-48:31:16.38	110.54 ± 0.06	-53.67 ± 0.06	25.62 ± 0.04	21.5 ± 0.2	...	-,-
J1815+0237	(M5)	ABDMG	18:15:49.990	+02:37:22.85	8.96 ± 0.13	-140.40 ± 0.14	28.22 ± 0.08	-,-
J1816-5534	(M5)	ABDMG	18:16:12.379	-55:34:57.21	-3.63 ± 0.07	-113.95 ± 0.07	18.75 ± 0.05	-,-
J1825-6237	(M5)	ABDMG	18:25:22.056	-62:37:50.06	-3.74 ± 0.11	-100.16 ± 0.13	16.72 ± 0.12	-,-

Table 3 continued

Table 3 (*continued*)

Name	Spectral	Assoc.	R.A. ^b	Decl. ^b	$\mu_\alpha \cos \delta$	μ_δ	Parallax	Rad. Vel.	Ambiguous	Ref. ^d
	Type ^a		(hh:mm:ss.sss)	(dd:mm:ss.ss)	(mas yr ⁻¹)	(mas yr ⁻¹)	(mas)	(km s ⁻¹)	Assoc. ^c	
J1829-7726	(M7)	ABDMG	18:29:29.887	-77:26:44.05	-5.54 ± 0.20	-95.43 ± 0.24	18.08 ± 0.13	-,-
J0153+1917	A2IV	ABDMG	01:53:31.897	+19:17:36.37	78.11 ± 0.72	-97.50 ± 0.62	19.98 ± 0.35	-1 ± 2	...	11,12
J0153+1917	A0V	ABDMG	01:53:31.904	+19:17:43.77	77.85 ± 0.91	-106.97 ± 0.73	18.88 ± 0.42	4 ± 2	...	13,12
J1840-0959	(L1)	ABDMG	18:40:59.386	-09:59:17.47	23.90 ± 0.98	-245.19 ± 0.89	40.57 ± 0.55	-,-
J1911-4739	(M5)	ABDMG	19:11:04.147	-47:39:17.43	49.04 ± 0.49	-201.17 ± 0.50	30.96 ± 0.28	-,-
J1912+4931	(M4)	ABDMG	19:12:52.706	+49:31:15.23	22.64 ± 0.27	-4.66 ± 0.31	30.42 ± 0.14	-,-
J1918-6910	(M5)	ABDMG	19:18:48.816	-69:10:22.45	14.96 ± 0.07	-92.23 ± 0.09	16.16 ± 0.06	-,-
J1925+0938	M8/9V	ABDMG	19:25:30.998	+09:38:19.56	83.79 ± 0.47	-240.82 ± 0.40	59.43 ± 0.29	-21 ± 4	...	14,14
J1930-6630	(M5)	ABDMG	19:30:33.653	-66:30:30.28	19.22 ± 0.06	-104.74 ± 0.09	18.26 ± 0.06	-,-
J1947+3346	(M6)	ABDMG	19:47:23.563	+33:46:27.54	73.35 ± 0.18	-74.22 ± 0.19	40.82 ± 0.10	-,-
J1952+2356	(M7)	ABDMG	19:52:01.692	+23:56:03.65	62.80 ± 0.14	-97.40 ± 0.14	33.88 ± 0.10	-,-
J1955-1548	(M8)	ABDMG	19:55:24.826	-15:48:39.97	49.09 ± 0.62	-178.27 ± 0.44	29.38 ± 0.27	-,-
J0014+4758	(M6)	ABDMG	00:14:18.395	+47:58:06.35	104.54 ± 0.12	-79.57 ± 0.07	22.13 ± 0.09	-,-
J0015-5041	(M5)	ABDMG	00:15:33.864	-50:41:30.76	107.74 ± 0.08	-79.00 ± 0.09	24.02 ± 0.07	-,-
J2004-2342	M4.5	ABDMG	20:04:30.922	-23:42:07.52	119.10 ± 0.19	-338.92 ± 0.10	55.00 ± 0.12	-7 ± 1	...	15,16
J2040-0119	(M5)	ABDMG	20:40:47.683	-01:19:20.95	70.41 ± 0.09	-121.25 ± 0.06	25.65 ± 0.06	-,-
J2050+2253	K0	ABDMG	20:50:27.946	+22:53:02.15	74.98 ± 0.07	-71.01 ± 0.06	25.56 ± 0.05	17,-
J2105+0425	(M3)	ABDMG	21:05:56.510	+04:25:38.07	124.19 ± 0.10	-175.65 ± 0.10	37.01 ± 0.08	-,-
J2113+3507	(L1)	ABDMG	21:13:41.866	+35:07:39.57	110.44 ± 0.48	-77.11 ± 0.61	32.17 ± 0.36	-,-
J2146-2515	(M5)	ABDMG	21:46:05.731	-25:15:39.76	86.21 ± 0.10	-139.69 ± 0.10	24.93 ± 0.07	-,-
J2158-7048	(M5)	ABDMG	21:58:47.556	-70:48:38.73	69.64 ± 0.05	-84.49 ± 0.07	20.02 ± 0.04	-,-
J2158-4705	(M2)	ABDMG	21:58:53.527	-47:05:56.15	94.38 ± 0.20	-120.71 ± 0.32	24.53 ± 0.16	11.8 ± 0.5	...	-,4
J0213+1803	M4.5	ABDMG	02:13:00.902	+18:03:42.22	129.08 ± 0.15	-211.74 ± 0.14	36.98 ± 0.08	18,-
J0213+3851	(M5)	ABDMG	02:13:04.889	+38:51:48.08	64.86 ± 0.12	-105.67 ± 0.16	18.63 ± 0.06	-,-
J2206+4734	(M4)	ABDMG	22:06:05.726	+47:34:02.99	97.19 ± 0.06	-58.49 ± 0.06	27.08 ± 0.04	-,-
J2208+7005	(M5)	ABDMG	22:08:06.845	+70:05:21.90	114.13 ± 0.07	9.50 ± 0.07	27.72 ± 0.04	-,-
J2224-1020	(M5)	ABDMG	22:24:44.794	-10:20:28.14	74.55 ± 0.16	-100.31 ± 0.14	19.92 ± 0.08	-,-
J2225+6905	(M4)	ABDMG	22:25:42.646	+69:05:29.94	118.05 ± 0.05	-1.52 ± 0.04	27.71 ± 0.02	-,-
J0216+1858	(M5)	ABDMG	02:16:43.791	+18:58:02.13	71.89 ± 0.20	-107.08 ± 0.17	18.76 ± 0.12	-,-
J0217+5604	(M5)	ABDMG	02:17:08.624	+56:04:06.10	86.75 ± 0.17	-92.72 ± 0.20	20.91 ± 0.09	-,-
J2244+1754	(M3)	ABDMG	22:44:41.405	+17:54:16.02	82.11 ± 0.16	-80.73 ± 0.09	20.76 ± 0.07	-13 ± 1	...	-,4
J2244+1754	K0IV-V	ABDMG	22:44:41.635	+17:54:17.02	82.70 ± 0.30	-81.84 ± 0.20	20.11 ± 0.11	-13.0 ± 0.5	...	19,4
J2255+2847	(M4)	ABDMG	22:55:34.495	+28:47:29.26	97.17 ± 0.11	-77.62 ± 0.10	24.03 ± 0.07	-,-
J2318-4049	F4V	ABDMG	23:18:10.058	-40:49:29.60	126.92 ± 0.13	-122.58 ± 0.14	29.32 ± 0.11	15.1 ± 0.3	...	6,4
J2319-4748	(M4)	ABDMG	23:19:29.460	-47:48:12.00	98.49 ± 0.06	-91.52 ± 0.09	22.29 ± 0.08	-,-
J2334+2739	(M4)	ABDMG	23:34:27.425	+27:39:41.88	94.38 ± 0.10	-75.82 ± 0.07	20.38 ± 0.07	-,-
J2335+5656	(M5)	ABDMG	23:35:42.612	+56:56:03.56	86.92 ± 0.12	-40.37 ± 0.09	18.61 ± 0.08	-,-
J2348-2807	K1V	ABDMG	23:48:50.609	-28:07:17.30	96.65 ± 0.08	-105.23 ± 0.08	22.61 ± 0.05	6.9 ± 0.2	...	20,4
J2354+2208	(L2)	ABDMG	23:54:12.686	+22:08:21.20	104.9 ± 1.7	-89.14 ± 0.76	23.3 ± 1.0	-,-

Table 3 continued

Table 3 (*continued*)

Name	Spectral	Assoc.	R.A. ^b	Decl. ^b	$\mu_\alpha \cos \delta$	μ_δ	Parallax	Rad. Vel.	Ambiguous	Ref. ^d
	Type ^a		(hh:mm:ss.sss)	(dd:mm:ss.ss)	(mas yr ⁻¹)	(mas yr ⁻¹)	(mas)	(km s ⁻¹)	Assoc. ^c	
J0225-1432	(M5)	ABDMG	02:25:50.829	-14:32:33.87	94.80 ± 0.11	-103.37 ± 0.11	24.30 ± 0.07	-,-
J0226+5010	(M8)	ABDMG	02:26:03.242	+50:10:30.28	60.50 ± 0.77	-82.24 ± 0.52	16.01 ± 0.39	-,-
J0238+1637	(M6)	ABDMG	02:38:32.591	+16:37:07.84	66.92 ± 0.23	-97.39 ± 0.19	18.52 ± 0.15	-,-
J0247+2508	(M5)	ABDMG	02:47:38.764	+25:08:54.34	55.68 ± 0.15	-97.29 ± 0.14	16.88 ± 0.10	-,-
J0247-6808	(M6)	ABDMG	02:47:53.871	-68:08:06.31	67.21 ± 0.25	9.13 ± 0.20	17.13 ± 0.11	...	ABDMG(88);CAR(11)	-,-
J0249-6228	(M5)	ABDMG	02:49:13.034	-62:28:10.50	66.83 ± 0.08	1.36 ± 0.07	17.44 ± 0.04	-,-
J0256+3830	(M7)	ABDMG	02:56:03.283	+38:30:58.02	59.41 ± 0.49	-98.83 ± 0.39	16.79 ± 0.28	-,-
J0303-1119	(M5)	ABDMG	03:03:49.475	-11:19:42.71	74.31 ± 0.11	-105.77 ± 0.11	23.70 ± 0.09	-,-
J0310-2341	M3.5	ABDMG	03:10:03.159	-23:41:32.95	98.81 ± 0.11	-140.64 ± 0.12	37.96 ± 0.06	21,-
J0317+1557	(M5)	ABDMG	03:17:53.517	+15:57:27.21	49.34 ± 0.21	-96.31 ± 0.17	16.58 ± 0.11	-,-
J0021+4304	(M5)	ABDMG	00:21:47.103	+43:04:20.32	93.01 ± 0.13	-67.79 ± 0.06	20.09 ± 0.11	-,-
J0321+1406	(M4)	ABDMG	03:21:41.526	+14:06:03.41	56.27 ± 0.31	-92.56 ± 0.21	16.89 ± 0.14	-,-
J0324+5813	(M6)	ABDMG	03:24:40.134	+58:13:24.59	48.59 ± 0.16	-106.87 ± 0.19	17.81 ± 0.12	-,-
J0329-3812	(M5)	ABDMG	03:29:50.378	-38:12:01.07	93.86 ± 0.06	-64.42 ± 0.09	28.85 ± 0.04	-,-
J0331-2117	(M5)	ABDMG	03:31:14.840	-21:17:28.20	85.20 ± 0.09	-94.46 ± 0.09	26.33 ± 0.06	-,-
J0331-1525	(M0)	ABDMG	03:31:47.091	-15:25:39.24	58.09 ± 0.08	-86.55 ± 0.09	20.79 ± 0.06	21.8 ± 0.5	...	-,4
J0332-0339	(M6)	ABDMG	03:32:13.743	-03:39:41.51	54.85 ± 0.29	-100.31 ± 0.32	19.73 ± 0.16	-,-
J0340+5114	(M5)	ABDMG	03:40:20.437	+51:14:18.15	52.88 ± 0.13	-110.76 ± 0.11	18.09 ± 0.07	-,-
J0345+2733	(M7)	ABDMG	03:45:52.818	+27:33:24.60	41.76 ± 0.42	-116.99 ± 0.26	17.86 ± 0.31	-,-
J0346-6246	(M5)	ABDMG	03:46:25.083	-62:46:23.25	53.74 ± 0.08	18.48 ± 0.08	18.17 ± 0.04	-,-
J0346-6246	(M5)	ABDMG	03:46:29.412	-62:46:11.77	53.00 ± 0.11	17.74 ± 0.11	18.14 ± 0.06	-,-
J0346-3906	(M4)	ABDMG	03:46:38.059	-39:06:40.03	63.00 ± 0.06	-44.55 ± 0.08	22.73 ± 0.04	-,-
J0347+3406	(M9)	ABDMG	03:47:54.093	+34:06:46.98	38.4 ± 1.6	-95.96 ± 0.96	15.50 ± 0.84	-,-
J0350-0353	(M2)	ABDMG	03:50:39.672	-03:53:55.93	57.41 ± 0.07	-85.01 ± 0.06	18.70 ± 0.04	15 ± 3	...	-,4
J0350-6949	(M5)	ABDMG	03:50:43.609	-69:49:28.65	47.25 ± 0.08	27.83 ± 0.09	16.08 ± 0.05	...	ABDMG(68);COL(32)	-,-
J0355+2918	(M8)	ABDMG	03:55:06.953	+29:18:41.63	51.05 ± 0.65	-107.85 ± 0.37	17.54 ± 0.33	-,-
J0355-2041	(M5)	ABDMG	03:55:51.948	-20:41:10.78	73.66 ± 0.09	-81.79 ± 0.09	23.99 ± 0.07	-,-
J0024-2522	(M3)	ABDMG	00:24:32.140	-25:22:54.51	106.93 ± 0.08	-100.24 ± 0.07	23.24 ± 0.05	-,-
J0024-4053	(M6)	ABDMG	00:24:46.259	-40:53:33.98	84.15 ± 0.12	-62.75 ± 0.13	18.08 ± 0.10	...	ABDMG(95);CAR(5)	-,-
J0025-0957	M3.0V	ABDMG	00:25:51.106	-09:57:42.36	124.17 ± 0.15	-157.13 ± 0.09	30.73 ± 0.07	15,-
J0400-2609	(M5)	ABDMG	04:00:26.196	-26:09:34.45	66.92 ± 0.07	-66.44 ± 0.08	24.85 ± 0.05	-,-
J0406-2149	(M5)	ABDMG	04:06:13.930	-21:49:37.61	55.25 ± 0.06	-71.07 ± 0.07	21.46 ± 0.06	-,-
J0417-2419	(M3)	ABDMG	04:17:37.081	-24:19:49.88	47.76 ± 0.05	-103.81 ± 0.07	31.15 ± 0.04	27.0 ± 0.6	...	-,4
J0420-4001	(M5)	ABDMG	04:20:37.411	-40:01:59.61	48.37 ± 0.08	-33.86 ± 0.13	20.63 ± 0.05	-,-
J0422-0611	(M4)	ABDMG	04:22:25.450	-06:11:42.28	44.34 ± 0.36	-79.60 ± 0.27	17.35 ± 0.24	-,-
J0423+3349	(M5)	ABDMG	04:23:26.236	+33:49:08.44	29.08 ± 0.25	-133.64 ± 0.16	19.80 ± 0.11	-,-
J0423-4308	(M4)	ABDMG	04:23:57.766	-43:08:59.53	37.11 ± 0.05	-32.23 ± 0.08	25.25 ± 0.04	31 ± 4	...	-,4
J0424-4308	(M3)	ABDMG	04:24:01.237	-43:08:05.88	35.90 ± 0.04	-33.36 ± 0.06	25.27 ± 0.03	32 ± 1	...	-,4
J0427+4852	(M5)	ABDMG	04:27:00.742	+48:52:49.25	59.25 ± 0.91	-206.61 ± 0.64	30.09 ± 0.45	-,-

Table 3 continued

Table 3 (*continued*)

Name	Spectral	Assoc.	R.A. ^b	Decl. ^b	$\mu_\alpha \cos \delta$	μ_δ	Parallax	Rad. Vel.	Ambiguous	Ref. ^d
	Type ^a		(hh:mm:ss.sss)	(dd:mm:ss.ss)	(mas yr ⁻¹)	(mas yr ⁻¹)	(mas)	(km s ⁻¹)	Assoc. ^c	
J0429-5802	(M5)	ABDMG	04:29:16.189	-58:02:41.13	39.45 ± 0.11	18.70 ± 0.13	18.72 ± 0.05	-, -
J0433-0330	(M4)	ABDMG	04:33:22.495	-03:30:14.16	25.89 ± 0.10	-87.82 ± 0.06	17.24 ± 0.05	-, -
J0433-4212	(M9)	ABDMG	04:33:49.865	-42:12:40.96	57.31 ± 0.72	-29.56 ± 0.79	23.22 ± 0.36	-, -
J0436-6001	(M6)	ABDMG	04:36:44.206	-60:01:01.03	36.87 ± 0.17	19.62 ± 0.24	16.58 ± 0.09	-, -
J0440-5841	(M4)	ABDMG	04:40:14.681	-58:41:03.19	29.52 ± 0.09	16.76 ± 0.10	15.21 ± 0.05	-, -
J0441-1523	(M4)	ABDMG	04:41:42.940	-15:23:16.20	45.23 ± 0.06	-77.86 ± 0.05	20.07 ± 0.05	-, -
J0442-2613	(M4)	ABDMG	04:42:28.889	-26:13:46.88	33.61 ± 0.06	-69.91 ± 0.08	23.11 ± 0.04	-, -
J0443+3740	(M4)	ABDMG	04:43:16.040	+37:40:58.09	24.69 ± 0.11	-99.27 ± 0.06	15.05 ± 0.05	-, -
J0447+0331	(M5)	ABDMG	04:47:00.774	+03:31:40.90	28.71 ± 0.16	-77.32 ± 0.11	15.29 ± 0.09	-, -
J0448-0422	(M5)	ABDMG	04:48:48.605	-04:22:14.11	28.45 ± 0.11	-104.49 ± 0.09	21.39 ± 0.07	-, -
J0449-5741	(M5)	ABDMG	04:49:44.700	-57:41:19.01	32.87 ± 0.09	15.44 ± 0.13	16.39 ± 0.05	-, -
J0449+2341	M0Ve	ABDMG	04:49:56.511	+23:41:00.16	23.08 ± 0.12	-161.22 ± 0.08	24.55 ± 0.06	9 ± 2	...	22, 4
J0452+5922	(M6)	ABDMG	04:52:42.120	+59:22:10.39	46.43 ± 0.14	-183.69 ± 0.12	28.99 ± 0.10	-, -
J0453-2222	(M5)	ABDMG	04:53:57.433	-22:22:17.28	23.97 ± 0.08	-46.40 ± 0.10	15.10 ± 0.07	-, -
J0455-6051	(M5)	ABDMG	04:55:36.011	-60:51:42.15	15.42 ± 0.09	31.04 ± 0.09	22.49 ± 0.05	-, -
J0455-3347	(M4)	ABDMG	04:55:38.614	-33:47:54.63	22.75 ± 0.07	-48.88 ± 0.09	22.46 ± 0.05	-, -
J0456-3936	(M5)	ABDMG	04:56:49.901	-39:36:12.88	21.45 ± 0.08	-35.28 ± 0.09	22.62 ± 0.05	-, -
J0458+5606	(M8)	ABDMG	04:58:00.482	+56:06:59.82	39.19 ± 0.31	-149.01 ± 0.27	24.67 ± 0.21	-, -
J0500-2311	(M4)	ABDMG	05:00:08.932	-23:11:36.46	23.86 ± 0.07	-48.73 ± 0.08	15.70 ± 0.05	-, -
J0501-2932	(M4)	ABDMG	05:01:33.768	-29:32:00.27	20.67 ± 0.14	-50.99 ± 0.18	19.64 ± 0.08	-, -
J0503-2423	(M5)	ABDMG	05:03:49.884	-24:23:07.93	25.98 ± 0.08	-40.17 ± 0.10	17.04 ± 0.06	26 ± 5	...	-, 5
J0504+4024	(M5)	ABDMG	05:04:41.454	+40:24:00.79	15.93 ± 0.18	-116.73 ± 0.14	16.42 ± 0.09	8 ± 6	...	-, 5
J0508-1413	(L2)	ABDMG	05:08:16.602	-14:13:49.57	18.5 ± 1.0	-98.0 ± 1.1	23.77 ± 0.67	-, -
J0508+4956	(M7)	ABDMG	05:08:38.362	+49:56:29.48	14.17 ± 0.55	-178.26 ± 0.47	26.95 ± 0.35	-, -
J0517-6634	(M6)	ABDMG	05:17:49.020	-66:34:51.81	22.84 ± 0.14	37.40 ± 0.16	20.10 ± 0.08	-, -
J0526+1003	(M5)	ABDMG	05:26:23.623	+10:03:38.25	35.88 ± 0.18	-207.38 ± 0.14	37.68 ± 0.12	-, -
J0528-3327	(M3)	ABDMG	05:28:42.348	-33:27:00.08	15.73 ± 0.32	-29.46 ± 0.37	16.50 ± 0.19	-, -
J0529-1908	G8V	ABDMG	05:29:03.287	-19:08:35.89	8.46 ± 0.06	-79.75 ± 0.08	20.99 ± 0.05	26.3 ± 0.2	...	23, 4
J0530-6705	(M5)	ABDMG	05:30:49.765	-67:05:54.47	19.22 ± 0.08	45.60 ± 0.08	19.59 ± 0.04	-, -
J0532-2020	(M5)	ABDMG	05:32:34.088	-20:20:19.37	9.09 ± 0.19	-75.11 ± 0.28	22.84 ± 0.17	-, -
J0535-7053	(M5)	ABDMG	05:35:00.955	-70:53:51.37	16.83 ± 0.08	56.43 ± 0.11	19.32 ± 0.05	-, -
J0542-1535	(M5)	ABDMG	05:42:30.126	-15:35:02.00	5.28 ± 0.23	-92.18 ± 0.27	24.55 ± 0.09	-, -
J0542-1535	(M5)	ABDMG	05:42:30.178	-15:35:02.14	8.10 ± 0.72	-91.83 ± 0.77	26.98 ± 0.50	-, -
J0544+3705	(L1)	ABDMG	05:44:57.421	+37:05:00.52	6.64 ± 0.93	-230.80 ± 0.78	34.06 ± 0.55	-, -
J0545+2350	(K6)	ABDMG	05:45:06.670	+23:50:08.94	3.72 ± 0.09	-113.34 ± 0.07	16.81 ± 0.05	-, -
J0545+2350	(M3)	ABDMG	05:45:06.899	+23:50:09.73	2.94 ± 0.10	-111.73 ± 0.08	16.73 ± 0.05	-, -
J0545-1630	(M5)	ABDMG	05:45:35.068	-16:30:34.23	15.38 ± 0.14	-59.25 ± 0.15	17.42 ± 0.09	-, -
J0545-1630	(M5)	ABDMG	05:45:35.095	-16:30:36.77	14.07 ± 0.08	-59.88 ± 0.08	17.44 ± 0.05	-, -
J0545+6638	(M4)	ABDMG	05:45:45.441	+66:38:28.13	20.97 ± 0.05	-145.30 ± 0.07	23.85 ± 0.05	-, -

Table 3 continued

Table 3 (*continued*)

Name	Spectral	Assoc.	R.A. ^b	Decl. ^b	$\mu_\alpha \cos \delta$	μ_δ	Parallax	Rad. Vel.	Ambiguous	Ref. ^d
	Type ^a		(hh:mm:ss.sss)	(dd:mm:ss.ss)	(mas yr ⁻¹)	(mas yr ⁻¹)	(mas)	(km s ⁻¹)	Assoc. ^c	
J0545+6638	(M4)	ABDMG	05:45:46.897	+66:38:20.99	23.92 ± 0.05	-148.69 ± 0.07	23.89 ± 0.06	-, -
J0548-2255	(M5)	ABDMG	05:48:30.870	-22:55:34.89	6.07 ± 0.06	-45.17 ± 0.09	16.86 ± 0.05	-, -
J0553+2458	(M5)	ABDMG	05:53:44.410	+24:58:48.73	14.51 ± 0.15	-170.84 ± 0.12	25.01 ± 0.10	-, -
J0556-2822	(M8)	ABDMG	05:56:18.078	-28:22:04.02	-1.17 ± 0.37	-34.63 ± 0.46	16.18 ± 0.27	-, -
J0600+2310	(M5)	ABDMG	06:00:28.171	+23:10:27.97	10.13 ± 0.10	-114.09 ± 0.09	18.26 ± 0.06	-, -
J0602-1355	(M5)	ABDMG	06:02:21.074	-13:55:17.47	-5.70 ± 0.35	-91.18 ± 0.34	21.35 ± 0.18	-, -
J0602-1356	(M6)	ABDMG	06:02:25.913	-13:56:39.99	-8.15 ± 0.22	-83.79 ± 0.23	22.25 ± 0.11	-, -
J0614-3419	(M5)	ABDMG	06:14:16.342	-34:19:25.29	6.99 ± 0.08	-29.10 ± 0.07	17.37 ± 0.04	-, -
J0618-5645	(M7)	ABDMG	06:18:12.219	-56:45:59.13	2.34 ± 0.19	23.49 ± 0.20	18.02 ± 0.09	-, -
J0624-6948	(M5)	ABDMG	06:24:02.151	-69:48:10.93	-0.05 ± 0.11	46.23 ± 0.13	17.02 ± 0.07	-, -
J0626+4852	(M5)	ABDMG	06:26:23.039	+48:52:53.46	-28.69 ± 0.14	-172.19 ± 0.15	24.49 ± 0.08	-, -
J0628-0026	(M6)	ABDMG	06:28:30.463	-00:26:51.76	-9.96 ± 0.25	-113.12 ± 0.27	23.04 ± 0.16	-, -
J0630-7643	M6.0	ABDMG	06:30:46.675	-76:43:01.11	-12.63 ± 0.16	447.54 ± 0.31	112.68 ± 0.11	24, -
J0635-5737	(M2)	ABDMG	06:35:22.234	-57:37:34.35	-17.49 ± 0.06	53.22 ± 0.06	42.77 ± 0.03	31.2 ± 0.5	...	-, 4
J0635-5737	(M5)	ABDMG	06:35:22.392	-57:37:33.52	-40.93 ± 0.77	49.8 ± 1.2	44.08 ± 0.36	30.9 ± 0.9	...	-, 25
J0638-8402	(M4)	ABDMG	06:38:10.516	-84:02:44.20	-1.90 ± 0.05	61.66 ± 0.09	16.06 ± 0.04	-, -
J0706-4943	(M7)	β PMG	07:06:37.462	-49:43:23.66	-32.93 ± 0.46	35.30 ± 0.37	22.91 ± 0.21	-, -
J0046+1909	(M6)	β PMG	00:46:06.185	+19:09:43.28	94.10 ± 0.84	-57.53 ± 0.47	23.77 ± 0.48	-, -
J0050+0702	(M7)	β PMG	00:50:52.379	+07:02:54.46	80.52 ± 0.53	-40.75 ± 0.26	20.59 ± 0.32	...	BPMG(81);THA(19)	-, -
J1442-6458	A7V	β PMG	14:42:29.950	-64:58:34.12	-190.47 ± 0.49	-232.61 ± 0.63	62.94 ± 0.43	6.2 ± 0.2	...	6, 26
J1612-4556	(M4)	β PMG	16:12:05.110	-45:56:25.90	-33.66 ± 0.24	-104.40 ± 0.18	22.79 ± 0.11	-, -
J1644-6747	(M5)	β PMG	16:44:30.281	-67:47:37.25	-26.67 ± 0.08	-97.31 ± 0.13	23.68 ± 0.08	-, -
J1657-5343	(M5)	β PMG	16:57:21.408	-53:43:29.18	-16.20 ± 0.16	-85.70 ± 0.14	19.82 ± 0.14	1.4 ± 0.2	...	-, 5
J1702-6734	(M4)	β PMG	17:02:09.319	-67:34:46.27	-20.27 ± 0.04	-99.48 ± 0.06	24.22 ± 0.04	-, -
J1702-6734	(M5)	β PMG	17:02:09.818	-67:34:33.84	-20.46 ± 0.05	-99.24 ± 0.08	24.18 ± 0.05	-, -
J1702-4522	(M2)	β PMG	17:02:40.126	-45:22:00.86	-20.11 ± 0.09	-137.69 ± 0.07	31.27 ± 0.06	-3.2 ± 0.4	...	-, 4
J1709-5235	(M3)	β PMG	17:09:29.453	-52:35:20.89	-10.21 ± 0.13	-65.62 ± 0.13	16.24 ± 0.09	-, -
J1738-4700	(M5)	β PMG	17:38:04.234	-47:00:53.40	-3.10 ± 0.12	-49.01 ± 0.10	11.63 ± 0.08	-, -
J1744-5315	(M3)	β PMG	17:44:42.566	-53:15:48.41	-0.96 ± 0.11	-82.75 ± 0.09	18.74 ± 0.07	-, -
J1748-5306	(M2)	β PMG	17:48:33.744	-53:06:12.72	-1.93 ± 0.09	-56.13 ± 0.07	12.97 ± 0.05	-0 ± 2	...	-, 5
J1749-4005	(M4)	β PMG	17:49:43.591	-40:05:36.22	-2.47 ± 0.11	-76.47 ± 0.09	19.50 ± 0.06	-, -
J1803-3412	(M5)	β PMG	18:03:05.309	-34:12:32.82	2.59 ± 0.14	-71.64 ± 0.12	19.40 ± 0.08	-, -
J1804-3018	(M2)	β PMG	18:04:16.186	-30:18:28.97	3.33 ± 0.10	-64.97 ± 0.08	18.16 ± 0.05	-8 ± 2	...	-, 4
J1805-5704	(M2)	β PMG	18:05:54.924	-57:04:31.88	0.86 ± 0.08	-73.03 ± 0.08	17.76 ± 0.06	-, -
J1809-7613	(M5)	β PMG	18:09:06.965	-76:13:26.23	6.86 ± 0.09	-150.17 ± 0.11	36.60 ± 0.06	-, -
J1809-5430	(M4)	β PMG	18:09:29.717	-54:30:54.95	4.28 ± 0.11	-107.93 ± 0.11	25.76 ± 0.08	-, -
J1810-5513	(L2)	β PMG	18:10:35.724	-55:13:45.00	4.3 ± 1.6	-90.8 ± 1.5	21.2 ± 1.0	-, -
J1815-3201	(M5)	β PMG	18:15:00.898	-32:01:56.61	4.29 ± 0.21	-52.35 ± 0.17	13.72 ± 0.13	-, -
J1816-5844	(M3)	β PMG	18:16:12.408	-58:44:07.83	14.24 ± 0.08	-146.37 ± 0.08	32.95 ± 0.07	-, -

Table 3 continued

Table 3 (*continued*)

Name	Spectral	Assoc.	R.A. ^b	Decl. ^b	$\mu_\alpha \cos \delta$	μ_δ	Parallax	Rad. Vel.	Ambiguous	Ref. ^d
	Type ^a		(hh:mm:ss.sss)	(dd:mm:ss.ss)	(mas yr ⁻¹)	(mas yr ⁻¹)	(mas)	(km s ⁻¹)	Assoc. ^c	
J1826-4602	(L1)	β PMG	18:26:46.805	-46:02:24.49	7.6 ± 3.6	-57.6 ± 3.2	16.0 ± 2.2	-,-
J1828-4421	(M2)	β PMG	18:28:16.517	-44:21:48.55	5.04 ± 0.08	-51.23 ± 0.07	12.31 ± 0.04	-,-
J1828-4457	(K7)	β PMG	18:28:35.246	-44:57:28.84	4.85 ± 0.06	-49.28 ± 0.05	11.98 ± 0.03	-,-
J1830-3238	(M5)	β PMG	18:30:13.188	-32:38:22.62	6.81 ± 0.15	-52.75 ± 0.13	14.01 ± 0.08	-,-
J0152+0833	(M3)	β PMG	01:52:57.452	+08:33:25.00	90.4 ± 1.6	-59.2 ± 1.7	23.24 ± 0.95	-,-
J1843-4058	(M2)	β PMG	18:43:05.990	-40:58:05.93	12.02 ± 0.09	-71.74 ± 0.08	17.00 ± 0.06	-,-
J1847-2808	(M5)	β PMG	18:47:13.524	-28:08:56.81	14.20 ± 0.20	-60.92 ± 0.16	16.80 ± 0.13	-,-
J1854-2621	(M4)	β PMG	18:54:09.233	-26:21:40.10	11.67 ± 0.13	-48.46 ± 0.12	13.75 ± 0.08	-,-
J1910-2830	(M3)	β PMG	19:10:00.077	-28:30:54.64	14.75 ± 0.10	-49.70 ± 0.09	14.14 ± 0.07	-,-
J1915-2847	(M4)	β PMG	19:15:00.811	-28:47:59.46	16.73 ± 0.91	-49.17 ± 0.84	14.10 ± 0.52	-,-
J1916-2707	(M4)	β PMG	19:16:29.623	-27:07:07.56	17.43 ± 0.11	-50.53 ± 0.10	14.60 ± 0.08	-,-
J1918-5002	(M6)	β PMG	19:18:18.096	-50:02:21.65	25.18 ± 0.26	-86.25 ± 0.21	21.91 ± 0.17	-,-
J1920-5111	(M5)	β PMG	19:20:34.937	-51:11:23.43	21.94 ± 0.14	-75.84 ± 0.12	19.45 ± 0.10	-,-
J1924-3204	(M5)	β PMG	19:24:59.364	-32:04:31.70	19.82 ± 0.16	-50.09 ± 0.16	14.65 ± 0.11	-,-
J1926-5331	(M3)	β PMG	19:26:00.794	-53:31:28.23	26.86 ± 0.10	-81.42 ± 0.08	20.82 ± 0.07	-,-
J1927-5401	(M5)	β PMG	19:27:47.220	-54:01:43.10	27.70 ± 0.16	-81.53 ± 0.10	20.85 ± 0.12	-,-
J1930-2939	(M3)	β PMG	19:30:03.986	-29:39:33.38	23.83 ± 0.14	-59.15 ± 0.12	16.60 ± 0.09	-,-
J1934-3009	(M5)	β PMG	19:34:11.470	-30:09:25.72	21.02 ± 0.22	-51.84 ± 0.18	14.61 ± 0.15	-,-
J1948-2720	(M2)	β PMG	19:48:16.548	-27:20:32.77	25.41 ± 0.11	-53.28 ± 0.06	15.42 ± 0.06	-6 ± 1	...	-,4
J1948-2720	(M6)	β PMG	19:48:17.076	-27:20:34.33	24.88 ± 0.28	-52.80 ± 0.17	15.03 ± 0.17	-6 ± 1	...	-,5
J2008-2545	(M4)	β PMG	20:08:37.891	-25:45:26.63	35.07 ± 0.15	-59.30 ± 0.08	17.64 ± 0.09	-,-
J2008-3519	(M4)	β PMG	20:08:53.717	-35:19:49.26	49.75 ± 0.13	-83.35 ± 0.09	22.22 ± 0.09	-5 ± 3	...	-,25
J2008-3519	(M4)	β PMG	20:08:53.772	-35:19:50.38	38.37 ± 0.12	-75.72 ± 0.09	22.43 ± 0.08	-5 ± 3	...	-,25
J2010-3844	(M5)	β PMG	20:10:50.597	-38:44:33.30	52.66 ± 0.35	-113.92 ± 0.16	29.02 ± 0.17	-,-
J2019-4404	(M9)	β PMG	20:19:09.838	-44:04:32.99	41.09 ± 0.79	-68.83 ± 0.70	20.51 ± 0.56	-,-
J2104-0939	(L3)	β PMG	21:04:31.358	-09:39:22.73	59.0 ± 3.2	-57.8 ± 1.9	21.2 ± 2.0	-,-
J2120-1645	(M4)	β PMG	21:20:07.870	-16:45:48.70	59.88 ± 0.13	-58.13 ± 0.11	20.68 ± 0.09	-,-
J2231-0633	F8V	β PMG	22:31:18.480	-06:33:20.24	145.6 ± 1.8	-75.7 ± 1.6	39.19 ± 0.62	-8 ± 4	...	27,4
J0216+3043	(M4)	β PMG	02:16:02.598	+30:43:56.27	86.23 ± 0.12	-73.05 ± 0.11	25.12 ± 0.06	-,-
J0244+1057	M5Ve	β PMG	02:44:22.804	+10:57:34.20	73.85 ± 0.18	-58.41 ± 0.15	21.32 ± 0.09	28,-
J0251+2227	M4	β PMG	02:51:54.221	+22:27:28.22	109.02 ± 0.11	-111.36 ± 0.09	36.92 ± 0.07	21,-
J0357+2445	M2	β PMG	03:57:33.970	+24:45:09.92	34.56 ± 0.08	-46.49 ± 0.06	14.54 ± 0.06	13 ± 1	...	29,4
J0405+0544	M4e	β PMG	04:05:38.938	+05:44:40.38	47.9 ± 2.0	-53.2 ± 2.0	27.2 ± 1.2	30,-
J0405+0531	(M4)	β PMG	04:05:53.456	+05:31:24.58	34.98 ± 0.17	-35.67 ± 0.11	15.95 ± 0.09	-,-
J0424+3613	(M5)	β PMG	04:24:24.452	+36:13:18.43	33.86 ± 0.25	-83.95 ± 0.18	21.50 ± 0.13	-,-
J0425+1852	(M5)	β PMG	04:25:48.976	+18:52:46.71	30.68 ± 0.33	-59.48 ± 0.26	20.25 ± 0.20	-,-
J0451+1622	(M5)	β PMG	04:51:07.314	+16:22:48.15	23.36 ± 0.23	-45.61 ± 0.10	15.26 ± 0.11	-,-
J0515+1954	(M5)	β PMG	05:15:14.931	+19:54:30.64	13.37 ± 0.75	-68.10 ± 0.57	20.59 ± 0.38	-,-
J0537-4240	(M5)	β PMG	05:37:47.576	-42:40:30.55	11.62 ± 0.12	35.04 ± 0.11	33.34 ± 0.06	-,-

Table 3 continued

Table 3 (*continued*)

Name	Spectral	Assoc.	R.A. ^b	Decl. ^b	$\mu_\alpha \cos \delta$	μ_δ	Parallax	Rad. Vel.	Ambiguous	Ref. ^d
	Type ^a		(hh:mm:ss.sss)	(dd:mm:ss.ss)	(mas yr ⁻¹)	(mas yr ⁻¹)	(mas)	(km s ⁻¹)	Assoc. ^c	
J1215+5239	M4.0V	UMA	12:15:39.542	+52:39:08.74	103.28 ± 0.29	0.99 ± 0.32	39.40 ± 0.21	31,--
J0700-4729	(M4)	CARN	07:00:35.657	-47:29:18.39	-10.08 ± 0.05	79.47 ± 0.06	17.68 ± 0.03	--,--
J0045-1823	(M5)	CARN	00:45:09.278	-18:23:10.64	165.73 ± 0.13	9.27 ± 0.09	25.48 ± 0.08	--,--
J0723-3309	(L5)	CARN	07:23:52.610	-33:09:43.03	-43.5 ± 3.0	99.4 ± 2.6	29.6 ± 3.4	--,--
J0744-4855	(M6)	CARN	07:44:37.841	-48:55:05.33	-26.85 ± 0.20	54.27 ± 0.20	15.69 ± 0.10	--,--
J0746-5841	(M5)	CARN	07:46:41.798	-58:41:00.00	-56.21 ± 0.08	155.33 ± 0.09	30.28 ± 0.04	--,--
J0749-0317	M3.5V	CARN	07:49:50.626	-03:17:20.36	-139.60 ± 0.14	-37.61 ± 0.10	58.78 ± 0.09	8,--
J0757-5348	(M5)	CARN	07:57:29.683	-53:48:00.71	-18.24 ± 0.11	47.50 ± 0.10	11.85 ± 0.05	--,--
J0757-5344	(M4)	CARN	07:57:31.313	-53:44:26.33	-18.63 ± 0.11	47.48 ± 0.10	11.82 ± 0.05	--,--
J0757-4551	(M5)	CARN	07:57:40.349	-45:51:24.85	-76.78 ± 0.15	117.32 ± 0.13	29.08 ± 0.07	--,--
J0802-4816	(M4)	CARN	08:02:21.365	-48:16:48.44	-45.67 ± 0.06	90.31 ± 0.06	21.30 ± 0.03	--,--
J0804-6243	(M5)	CARN	08:04:18.360	-62:43:30.38	-77.73 ± 0.09	173.91 ± 0.10	33.14 ± 0.05	--,--
J0818-4806	(M4)	CARN	08:18:46.078	-48:06:15.34	-75.80 ± 0.10	117.41 ± 0.09	28.35 ± 0.06	--,--
J0820-6247	(M4)	CARN	08:20:58.954	-62:47:47.62	-70.00 ± 0.06	144.90 ± 0.06	26.40 ± 0.03	--,--
J0833-4214	(M5)	CARN	08:33:56.842	-42:14:44.07	-55.93 ± 0.12	52.56 ± 0.13	16.89 ± 0.08	--,--
J0053-3459	(M5)	CARN	00:53:48.512	-34:59:32.78	164.44 ± 0.09	4.89 ± 0.06	27.50 ± 0.06	--,--
J0847-5919	(M4)	CARN	08:47:21.958	-59:19:22.70	-50.19 ± 0.05	80.12 ± 0.05	17.23 ± 0.03	--,--
J0847-7201	(M7)	CARN	08:47:37.558	-72:01:09.25	-79.00 ± 0.20	126.01 ± 0.25	22.84 ± 0.12	--,--
J0851-6301	(M6)	CARN	08:51:34.202	-63:01:06.28	-60.97 ± 0.81	88.31 ± 0.77	18.61 ± 0.42	--,--
J0858-2714	(M4)	CARN	08:58:29.045	-27:14:21.44	-157.98 ± 0.07	72.69 ± 0.07	41.51 ± 0.05	24 ± 2	...	-,25
J0906-3548	(M8)	CARN	09:06:42.007	-35:48:20.56	-143.22 ± 0.15	68.74 ± 0.20	31.95 ± 0.13	--,--
J0914-0035	(M5)	CARN	09:14:44.398	-00:35:47.21	-132.77 ± 0.35	-21.32 ± 0.31	27.62 ± 0.25	--,--
J0915-4638	(M5)	CARN	09:15:07.637	-46:38:22.15	-70.58 ± 0.53	53.19 ± 0.46	18.10 ± 0.30	--,--
J0920-6216	(M5)	CARN	09:20:13.452	-62:16:17.90	-120.54 ± 0.13	125.71 ± 0.12	29.13 ± 0.06	--,--
J0928-1603	L2	CARN	09:28:39.528	-16:03:12.38	-162.5 ± 2.0	26.6 ± 1.9	32.31 ± 0.90	32,--
J0937-5733	(M4)	CARN	09:37:57.274	-57:33:56.38	-102.12 ± 0.07	78.18 ± 0.06	26.23 ± 0.04	--,--
J0942-2551	(L2)	CARN	09:42:32.369	-25:51:37.58	-100.0 ± 2.3	19.5 ± 4.2	20.5 ± 1.8	--,--
J0942-4335	(M8)	CARN	09:42:33.406	-43:35:28.91	-97.13 ± 0.28	48.92 ± 0.28	19.89 ± 0.18	--,--
J0943-2258	(M5)	CARN	09:43:29.520	-22:58:46.61	-90.61 ± 0.14	6.40 ± 0.15	18.34 ± 0.09	--,--
J0946-5953	(M5)	CARN	09:46:41.890	-59:53:49.09	-86.66 ± 0.10	74.12 ± 0.10	20.65 ± 0.05	--,--
J0948-3321	(M5)	CARN	09:48:27.067	-33:21:16.43	-94.27 ± 0.10	25.37 ± 0.13	19.83 ± 0.07	--,--
J0951-3848	(M4)	CARN	09:51:49.865	-38:48:41.91	-125.21 ± 0.05	46.17 ± 0.07	26.67 ± 0.04	--,--
J1004-3436	(M4)	CARN	10:04:20.822	-34:36:02.01	-70.14 ± 0.08	14.90 ± 0.09	13.57 ± 0.05	--,--
J1020-4819	(M5)	CARN	10:20:18.955	-48:19:05.91	-110.23 ± 0.06	40.41 ± 0.06	22.96 ± 0.04	--,--
J1020-0633	(M5)	CARN	10:20:48.641	-06:33:19.98	-183.10 ± 0.46	-26.43 ± 0.70	33.19 ± 0.96	--,--
J1020-0634	(M5)	CARN	10:20:50.911	-06:34:40.49	-182.39 ± 0.15	-25.19 ± 0.13	31.56 ± 0.11	--,--
J1024-4110	(M8)	CARN	10:24:39.785	-41:10:14.09	-124.05 ± 0.19	59.62 ± 0.22	22.84 ± 0.15	--,--
J1028-4919	(M6)	CARN	10:28:39.286	-49:19:33.60	-116.59 ± 0.18	57.10 ± 0.17	23.25 ± 0.11	--,--
J1031-4127	(M5)	CARN	10:31:08.146	-41:27:48.06	-282.63 ± 0.06	55.07 ± 0.07	54.43 ± 0.05	--,--

Table 3 continued

Table 3 (*continued*)

Name	Spectral	Assoc.	R.A. ^b	Decl. ^b	$\mu_\alpha \cos \delta$	μ_δ	Parallax	Rad. Vel.	Ambiguous	Ref. ^d
	Type ^a		(hh:mm:ss.sss)	(dd:mm:ss.ss)	(mas yr ⁻¹)	(mas yr ⁻¹)	(mas)	(km s ⁻¹)	Assoc. ^c	
J1031-3613	(M6)	CARN	10:31:33.634	-36:13:05.85	-81.08 ± 0.22	17.02 ± 0.24	14.28 ± 0.15	-,-
J1038-5106	(M8)	CARN	10:38:01.730	-51:06:27.89	-123.68 ± 0.25	64.99 ± 0.24	23.02 ± 0.16	-,-
J1045-2130	(M8)	CARN	10:45:56.136	-21:30:38.47	-104.45 ± 0.98	1.13 ± 0.82	16.93 ± 0.55	-,-
J1052-3812	(M6)	CARN	10:52:17.983	-38:12:21.19	-171.27 ± 0.10	44.56 ± 0.12	28.01 ± 0.09	-,-
J1105-6014	(M5)	CARN	11:05:27.912	-60:14:39.49	-229.97 ± 0.21	78.52 ± 0.19	35.86 ± 0.12	-,-
J1106-2821	(M4)	CARN	11:06:22.178	-28:21:27.99	-133.61 ± 0.12	9.99 ± 0.10	21.94 ± 0.07	-,-
J1113-2628	(M2)	CARN	11:13:42.658	-26:28:26.54	-170.79 ± 0.09	4.69 ± 0.07	24.57 ± 0.05	11.2 ± 0.3	...	-,4
J0109-2441	M3	CARN	01:09:12.843	-24:41:20.53	300.21 ± 0.18	24.63 ± 0.13	49.07 ± 0.08	33,-
J1131-4418	(M5)	CARN	11:31:01.018	-44:18:54.26	-124.35 ± 0.11	5.45 ± 0.10	20.74 ± 0.08	-,-
J1141+4245	(M4)	CARN	11:41:43.826	+42:45:05.71	-575.65 ± 0.07	-89.97 ± 0.07	90.76 ± 0.05	-,-
J1150-2914	(L1)	CARN	11:50:42.857	-29:14:48.93	-171.09 ± 0.84	-1.73 ± 0.49	23.88 ± 0.60	-,-
J1205+6932	M4V	CARN	12:05:28.330	+69:32:21.75	-456.97 ± 0.06	-55.21 ± 0.05	64.70 ± 0.03	-3 ± 9	...	14,14
J1213-0432	L4	CARN	12:13:02.962	-04:32:44.27	-368.1 ± 2.2	-34.6 ± 1.4	59.5 ± 1.0	2,-
J1221+0616	(M6)	CARN	12:21:19.526	+06:16:57.84	-219.19 ± 0.21	-6.17 ± 0.14	29.61 ± 0.11	-,-
J1230-1323	G1/2V	CARN	12:30:04.493	-13:23:36.21	-266.02 ± 0.08	-46.71 ± 0.05	41.05 ± 0.05	1.3 ± 0.2	...	23,4
J1258-0826	(M5)	CARN	12:58:58.387	-08:26:32.69	-199.44 ± 0.18	-20.45 ± 0.09	27.11 ± 0.09	-,-
J1314+6622	M5.5	CARN	13:14:22.822	+66:22:33.70	-395.77 ± 0.16	60.75 ± 0.11	55.48 ± 0.08	18,-
J1316-1220	M3.5V	CARN	13:16:45.108	-12:20:21.18	-289.0 ± 2.1	-51.6 ± 2.1	45.5 ± 1.2	8,-
J1341+0805	(M7)	CARN	13:41:32.654	+08:05:04.67	-267.68 ± 0.37	-12.96 ± 0.21	40.36 ± 0.19	-,-
J1355+1403	F6V	CARN	13:55:49.685	+14:03:23.54	-290.89 ± 0.07	8.50 ± 0.07	40.86 ± 0.05	-10.7 ± 0.2	...	34,4
J1418-5528	(M4)	CARN	14:18:24.946	-55:28:38.98	-291.09 ± 0.08	-109.05 ± 0.10	46.91 ± 0.05	-,-
J1421-1618	M7.5	CARN	14:21:18.439	-16:18:21.37	-249.60 ± 0.42	-60.48 ± 0.32	39.76 ± 0.22	35,-
J1538-8745	(M6)	CARN	15:38:52.630	-87:45:53.14	-187.69 ± 0.15	-186.26 ± 0.17	40.66 ± 0.09	-,-
J1626-3812	(M6)	CARN	16:26:51.293	-38:12:36.60	-296.05 ± 0.23	-258.73 ± 0.16	71.42 ± 0.12	-,-
J1633-6808	(M8)	CARN	16:33:48.461	-68:08:53.09	-218.77 ± 0.17	-314.77 ± 0.27	65.67 ± 0.18	-,-
J1633-6808	(M8)	CARN	16:33:49.138	-68:08:54.12	-230.82 ± 0.10	-347.40 ± 0.16	65.36 ± 0.10	-,-
J1700+2521	M3.5	CARN	17:00:20.184	+25:21:05.02	-126.42 ± 0.05	132.32 ± 0.07	44.81 ± 0.04	36,-
J1854+1058	M3.5V	CARN	18:54:53.856	+10:58:45.06	29.48 ± 0.30	84.21 ± 0.28	53.88 ± 0.13	37,-
J1857-5559	K7Ve	CARN	18:57:30.557	-55:59:35.03	35.49 ± 0.09	-451.19 ± 0.07	81.16 ± 0.08	-16 ± 5	...	38,39
J2050-3424	(M5)	CARN	20:50:16.582	-34:24:47.20	335.61 ± 0.13	-296.94 ± 0.10	104.07 ± 0.09	...	CARN(82);BPMG(18)	-,-
J2347+2702	M9	CARN	23:47:37.214	+27:02:07.15	315.16 ± 0.30	15.20 ± 0.19	46.75 ± 0.19	40,-
J0226-6700	(M6)	CARN	02:26:11.544	-67:00:54.56	145.66 ± 0.14	60.63 ± 0.13	26.22 ± 0.08	-,-
J0252-2417	(M4)	CARN	02:52:29.430	-24:17:17.71	152.3 ± 2.2	53.4 ± 2.0	28.80 ± 0.97	-,-
J0021-4245	M6	CARN	00:21:11.101	-42:45:40.36	255.05 ± 0.09	-12.53 ± 0.09	37.40 ± 0.07	41,-
J0406+7915	M4.5	CARN	04:06:38.779	+79:15:55.16	277.25 ± 0.08	-404.46 ± 0.10	73.91 ± 0.06	1.4 ± 0.1	...	42,43
J0501-7856	(M5)	CARN	05:01:54.189	-78:56:10.40	80.16 ± 0.11	172.67 ± 0.13	29.73 ± 0.07	-,-
J0516+5640	(M7)	CARN	05:16:53.739	+56:40:12.89	140.54 ± 0.15	-408.28 ± 0.14	68.83 ± 0.11	-,-
J0519-4506	(L2)	CARN	05:19:28.796	-45:06:38.08	39.5 ± 1.9	63.9 ± 2.5	19.4 ± 1.1	-,-
J0520-3109	(M5)	CARN	05:20:04.183	-31:09:59.37	65.64 ± 0.05	88.96 ± 0.07	29.51 ± 0.03	-,-

Table 3 continued

Table 3 (*continued*)

Name	Spectral	Assoc.	R.A. ^b	Decl. ^b	$\mu_\alpha \cos \delta$	μ_δ	Parallax	Rad. Vel.	Ambiguous	Ref. ^d
	Type ^a		(hh:mm:ss.sss)	(dd:mm:ss.ss)	(mas yr ⁻¹)	(mas yr ⁻¹)	(mas)	(km s ⁻¹)	Assoc. ^c	
J0545-6453	(M5)	CARN	05:45:00.663	-64:53:58.86	42.21 ± 0.25	151.00 ± 0.27	24.07 ± 0.13	-,-
J0558-4849	(M3)	CARN	05:58:12.601	-48:49:54.27	32.11 ± 0.04	163.30 ± 0.04	34.36 ± 0.02	23.5 ± 0.3	...	-,4
J0601-3225	M4	CARN	06:01:25.578	-32:25:09.50	41.08 ± 0.07	140.62 ± 0.08	36.37 ± 0.05	21,-
J0605-6559	(M6)	CARN	06:05:26.147	-65:59:52.96	30.18 ± 0.19	115.23 ± 0.17	21.33 ± 0.08	-,-
J0608-5703	(M5)	CARN	06:08:36.154	-57:03:37.88	32.64 ± 0.40	153.52 ± 0.39	26.97 ± 0.18	-,-
J0633-4750	(M6)	CARN	06:33:37.866	-47:50:43.52	6.47 ± 0.13	96.24 ± 0.15	20.66 ± 0.07	-,-
J0637-4055	(M5)	CARN	06:37:58.429	-40:55:55.94	1.57 ± 0.11	102.58 ± 0.10	25.94 ± 0.06	-,-
J0258+2040	(M5)	HYA	02:58:06.445	+20:40:01.34	238.12 ± 0.22	-24.48 ± 0.24	30.59 ± 0.10	26.6 ± 0.4	...	-,5
J0259+2254	(M9)	HYA	02:59:44.942	+22:54:43.75	221.51 ± 0.84	-37.88 ± 0.71	30.09 ± 0.44	-,-
J0302+1931	(M4)	HYA	03:02:09.981	+19:31:13.37	236.66 ± 0.13	-29.07 ± 0.13	31.28 ± 0.07	-,-
J0311+2218	(M5)	HYA	03:11:56.663	+22:18:07.70	228.55 ± 0.20	-42.40 ± 0.16	31.16 ± 0.10	-,-
J0342+1216	M5.2V+L0	HYA	03:42:32.032	+12:16:22.34	196.95 ± 0.12	-9.14 ± 0.09	30.31 ± 0.07	35.4 ± 0.4	...	44,45
J0351+0722	(M5)	HYA	03:51:34.387	+07:22:22.99	173.38 ± 0.20	3.32 ± 0.12	27.64 ± 0.10	-,-
J0351+0722	(M5)	HYA	03:51:34.659	+07:22:25.12	172.27 ± 0.15	3.05 ± 0.09	27.58 ± 0.07	-,-
J0352+2028	(M6)	HYA	03:52:20.939	+20:28:40.65	147.95 ± 0.27	-36.28 ± 0.17	23.77 ± 0.14	-,-
J0352+1115	M1	HYA	03:52:34.522	+11:15:38.70	176.69 ± 0.12	-8.67 ± 0.09	28.60 ± 0.06	46,-
J0353+1719	(M5)	HYA	03:53:09.084	+17:19:44.05	138.98 ± 0.22	-30.08 ± 0.15	23.52 ± 0.10	35 ± 4	...	-,5
J0355+1439	M8.8V	HYA	03:55:20.346	+14:39:29.29	154.17 ± 0.47	-19.93 ± 0.35	27.17 ± 0.25	2,-
J0358+2710	(M8)	HYA	03:58:50.653	+27:10:32.92	140.63 ± 0.62	-59.28 ± 0.36	25.19 ± 0.40	-,-
J0410+2136	(M6)	HYA	04:10:37.618	+21:36:09.01	114.99 ± 0.23	-40.72 ± 0.17	20.66 ± 0.16	-,-
J0411+1505	(M7)	HYA	04:11:14.737	+15:05:10.56	123.28 ± 0.31	-24.86 ± 0.24	22.28 ± 0.18	-,-
J0415+0857	(M5)	HYA	04:15:48.203	+08:57:57.98	131.85 ± 0.14	-3.00 ± 0.10	24.77 ± 0.08	-,-
J0416+2052	(M8)	HYA	04:16:56.655	+20:52:35.65	119.03 ± 0.53	-38.95 ± 0.31	21.44 ± 0.28	-,-
J0419+1402	(M4)	HYA	04:19:57.835	+14:02:40.85	116.1 ± 1.8	-22.9 ± 1.6	21.39 ± 0.72	42 ± 4	...	-,5
J0427+2058	(M7)	HYA	04:27:53.188	+20:58:52.83	92.17 ± 0.32	-37.10 ± 0.24	18.87 ± 0.17	-,-
J0428+0756	(M4)	HYA	04:28:08.095	+07:56:44.78	98.78 ± 0.10	1.04 ± 0.07	19.78 ± 0.05	-,-
J0429+2529	M8V	HYA	04:29:47.362	+25:29:17.95	98.04 ± 0.66	-52.22 ± 0.45	20.83 ± 0.32	47,-
J0433+1451	(M5)	HYA	04:33:52.708	+14:51:02.75	101.79 ± 0.15	-25.50 ± 0.10	21.99 ± 0.10	33 ± 1	...	-,5
J0433+0537	(L1)	HYA	04:33:56.707	+05:37:23.65	107.9 ± 1.1	6.59 ± 0.67	21.45 ± 0.74	-,-
J0436+1151	M9	HYA	04:36:27.783	+11:51:24.06	100.35 ± 0.50	-8.42 ± 0.25	22.89 ± 0.26	35,-
J0437+2251	(M7)	HYA	04:37:05.212	+22:51:25.66	95.67 ± 0.46	-46.25 ± 0.23	20.99 ± 0.21	-,-
J0440+2536	(M4)	HYA	04:40:06.893	+25:36:44.67	105.17 ± 0.09	-62.96 ± 0.06	23.40 ± 0.04	35 ± 3	...	-,5
J0440+2325	(M6)	HYA	04:40:11.100	+23:25:13.60	89.51 ± 0.38	-45.84 ± 0.20	19.98 ± 0.16	-,-
J0441+0826	(M5)	HYA	04:41:43.076	+08:26:21.30	106.40 ± 0.11	-1.83 ± 0.06	23.53 ± 0.06	-,-
J0441+0826	(M5)	HYA	04:41:43.202	+08:26:17.10	101.38 ± 0.16	-1.05 ± 0.09	23.66 ± 0.08	-,-
J0441+1453	(M9)	HYA	04:41:45.261	+14:53:57.87	98.29 ± 0.97	-22.58 ± 0.51	21.85 ± 0.59	-,-
J0442+2027	M3.0V	HYA	04:42:30.399	+20:27:10.84	89.32 ± 0.16	-37.72 ± 0.06	20.44 ± 0.06	8,-
J0444+1902	(M5)	HYA	04:44:06.792	+19:02:07.26	88.81 ± 0.20	-34.38 ± 0.10	20.28 ± 0.10	-,-
J0444+1442	(M5)	HYA	04:44:08.502	+14:42:53.26	91.45 ± 0.15	-25.15 ± 0.07	21.83 ± 0.08	-,-

Table 3 continued

Table 3 (*continued*)

Name	Spectral	Assoc.	R.A. ^b	Decl. ^b	$\mu_\alpha \cos \delta$	μ_δ	Parallax	Rad. Vel.	Ambiguous	Ref. ^d
	Type ^a		(hh:mm:ss.sss)	(dd:mm:ss.ss)	(mas yr ⁻¹)	(mas yr ⁻¹)	(mas)	(km s ⁻¹)	Assoc. ^c	
J0444+2356	(M5)	HYA	04:44:31.721	+23:56:27.15	86.24 ± 0.14	-48.78 ± 0.06	19.50 ± 0.07	-,-
J0445+1443	(M8)	HYA	04:45:13.240	+14:43:26.32	82.14 ± 0.71	-22.30 ± 0.33	19.67 ± 0.36	-,-
J0445+1503	(M8)	HYA	04:45:33.158	+15:03:02.25	83.87 ± 0.42	-23.24 ± 0.25	20.77 ± 0.23	-,-
J0445+1246	(L1)	HYA	04:45:43.827	+12:46:31.25	99.6 ± 1.3	-16.34 ± 0.67	23.04 ± 0.79	-,-
J0446+1846	(M5)	HYA	04:46:15.344	+18:46:28.68	97.94 ± 0.26	-44.36 ± 0.13	22.94 ± 0.15	-,-
J0447+1719	(M7)	HYA	04:47:15.061	+17:19:49.10	95.00 ± 0.28	-30.71 ± 0.16	22.77 ± 0.17	-,-
J0447+1901	(M3)	HYA	04:47:56.721	+19:01:25.54	73.61 ± 0.08	-30.87 ± 0.05	18.56 ± 0.05	45 ± 2	...	-,4
J0447+1901	(M4)	HYA	04:47:56.871	+19:01:28.40	80.26 ± 0.13	-35.00 ± 0.07	18.27 ± 0.08	45 ± 2	...	-,5
J0448+2051	M6V	HYA	04:48:22.540	+20:51:42.75	76.42 ± 0.44	-37.17 ± 0.21	17.90 ± 0.24	48,-
J0449+0858	(M6)	HYA	04:49:04.188	+08:58:52.52	97.15 ± 0.15	-6.27 ± 0.09	23.36 ± 0.09	-,-
J0450+1808	(M6)	HYA	04:50:49.860	+18:08:27.74	88.76 ± 0.17	-35.44 ± 0.10	21.40 ± 0.10	-,-
J0451+2556	(M5)	HYA	04:51:18.939	+25:56:32.23	85.63 ± 0.18	-57.75 ± 0.09	20.77 ± 0.10	-,-
J0451+2436	(M5)	HYA	04:51:53.451	+24:36:35.59	86.45 ± 0.15	-55.10 ± 0.08	20.92 ± 0.09	-,-
J0452+1710	(M5)	HYA	04:52:22.000	+17:10:26.62	87.27 ± 0.22	-34.37 ± 0.11	21.91 ± 0.11	-,-
J0454+0744	(M5)	HYA	04:54:48.926	+07:44:19.96	98.90 ± 0.11	-0.54 ± 0.05	25.49 ± 0.06	-,-
J0455+2139	M8.5V	HYA	04:55:59.070	+21:39:59.00	77.28 ± 0.63	-44.66 ± 0.33	20.84 ± 0.32	48,-
J0457+2201	(M6)	HYA	04:57:27.004	+22:01:02.45	68.53 ± 0.23	-39.28 ± 0.14	18.34 ± 0.13	-,-
J0459+1920	(M5)	HYA	04:59:27.685	+19:20:36.94	79.46 ± 0.11	-41.15 ± 0.07	21.33 ± 0.08	-,-
J0459+1304	(M9)	HYA	04:59:32.632	+13:04:54.57	80.4 ± 1.1	-20.55 ± 0.65	20.74 ± 0.50	-,-
J0501+1741	(M5)	HYA	05:01:15.178	+17:41:37.89	85.97 ± 0.17	-39.74 ± 0.12	23.24 ± 0.11	-,-
J0502+1442	M8.9V	HYA	05:02:13.531	+14:42:36.42	72.93 ± 0.71	-25.27 ± 0.53	21.60 ± 0.46	2,-
J0504+1900	(M5)	HYA	05:04:06.262	+19:00:25.71	67.21 ± 0.17	-40.28 ± 0.09	22.09 ± 0.09	-,-
J0505+1034	(M5)	HYA	05:05:54.167	+10:34:50.70	79.56 ± 0.12	-11.38 ± 0.08	23.36 ± 0.07	-,-
J0507+1536	(M4)	HYA	05:07:09.281	+15:36:49.02	78.35 ± 0.11	-30.46 ± 0.08	22.28 ± 0.06	42.8 ± 0.7	...	-,4
J0508+1522	(M5)	HYA	05:08:15.492	+15:22:37.00	69.91 ± 0.19	-23.99 ± 0.12	20.02 ± 0.11	-,-
J0508+1415	(M7)	HYA	05:08:51.587	+14:15:10.99	87.87 ± 0.30	-27.96 ± 0.20	25.55 ± 0.16	-,-
J0514+1253	(M5)	HYA	05:14:53.007	+12:53:18.45	62.78 ± 0.24	-20.18 ± 0.15	20.15 ± 0.13	-,-
J0644-7820	(M5)	THA	06:44:30.434	-78:20:09.77	18.23 ± 0.16	52.20 ± 0.17	14.96 ± 0.09	-,-
J1044-8701	(M4)	THA	10:44:14.854	-87:01:36.17	-39.81 ± 0.09	42.01 ± 0.08	14.21 ± 0.05	-,-
J0113-3438	(M5)	THA	01:13:03.750	-34:38:19.36	110.10 ± 0.06	-60.11 ± 0.07	26.12 ± 0.05	-,-
J1737-8653	(M5)	THA	17:37:59.945	-86:53:17.56	-36.76 ± 0.11	-57.04 ± 0.16	15.98 ± 0.06	-,-
J1747-8846	M3.5	THA	17:47:27.158	-88:46:10.44	-35.75 ± 0.13	-60.20 ± 0.17	17.18 ± 0.08	21,-
J1829-8026	(M3)	THA	18:29:09.446	-80:26:45.10	-23.72 ± 0.06	-69.30 ± 0.08	16.68 ± 0.04	-,-
J0156-7457	(M5)	THA	01:56:30.754	-74:57:27.63	96.78 ± 0.15	-11.30 ± 0.15	23.21 ± 0.09	-,-
J1943-6016	(M4)	THA	19:43:09.890	-60:16:58.48	-4.11 ± 0.06	-82.68 ± 0.06	17.81 ± 0.05	-,-
J0015-2946	M4	THA	00:15:36.842	-29:46:01.78	108.15 ± 0.14	-79.43 ± 0.12	27.42 ± 0.10	0 ± 5	...	49,25
J2017-6214	(M4)	THA	20:17:53.124	-62:14:44.14	8.75 ± 0.09	-83.52 ± 0.12	18.16 ± 0.08	-,-
J2019-5027	(M5)	THA	20:19:49.819	-50:27:29.17	5.53 ± 0.10	-77.72 ± 0.09	16.97 ± 0.07	-,-
J2034-6634	(M4)	THA	20:34:30.703	-66:34:40.40	10.64 ± 0.05	-78.21 ± 0.07	16.87 ± 0.04	-,-

Table 3 continued

Table 3 (*continued*)

Name	Spectral	Assoc.	R.A. ^b	Decl. ^b	$\mu_\alpha \cos \delta$	μ_δ	Parallax	Rad. Vel.	Ambiguous	Ref. ^d
	Type ^a		(hh:mm:ss.sss)	(dd:mm:ss.ss)	(mas yr ⁻¹)	(mas yr ⁻¹)	(mas)	(km s ⁻¹)	Assoc. ^c	
J2043-6942	(M4)	THA	20:43:10.514	-69:42:47.51	14.22 ± 0.05	-82.06 ± 0.07	17.98 ± 0.04	-,-
J2110-8308	(M5)	THA	21:10:48.211	-83:08:17.21	22.19 ± 0.10	-72.77 ± 0.08	17.32 ± 0.06	-,-
J2309-3951	(M4)	THA	23:09:36.427	-39:51:10.81	71.66 ± 0.08	-80.41 ± 0.11	22.75 ± 0.07	-,-
J2327-3045	(M4)	THA	23:27:44.285	-30:45:41.08	75.67 ± 0.13	-73.35 ± 0.15	22.61 ± 0.09	-,-
J2341-3638	(M5)	THA	23:41:09.154	-36:38:18.99	92.53 ± 0.14	-83.32 ± 0.13	25.75 ± 0.09	-,-
J0249-8421	(M3)	THA	02:49:07.916	-84:21:04.45	69.93 ± 0.09	13.53 ± 0.09	17.21 ± 0.05	-,-
J0300-0746	(M5)	THA	03:00:25.937	-07:46:55.40	83.54 ± 0.18	-40.43 ± 0.15	19.96 ± 0.12	-,-
J0329-4803	(M5)	THA	03:29:03.801	-48:03:36.59	93.94 ± 0.08	-4.36 ± 0.11	23.97 ± 0.05	-,-
J0329-4803	(M5)	THA	03:29:04.353	-48:03:33.98	90.93 ± 0.08	-3.26 ± 0.10	23.94 ± 0.04	-,-
J0348-3738	(M2)	THA	03:48:40.509	-37:38:19.98	74.24 ± 0.04	-4.65 ± 0.07	18.75 ± 0.03	15.9 ± 0.9	...	-,5
J0352-8523	(M4)	THA	03:52:18.541	-85:23:05.97	57.16 ± 0.08	28.40 ± 0.08	15.60 ± 0.04	-,-
J0405-4014	M4.2	THA	04:05:39.705	-40:14:10.45	70.69 ± 0.81	3.8 ± 1.1	20.39 ± 0.52	...	THA(52);COL(47)	50,-
J0408-2744	(M4)	THA	04:08:22.360	-27:44:40.35	67.30 ± 0.38	-18.84 ± 0.50	18.42 ± 0.28	-,-
J0408-2744	(M5)	THA	04:08:22.473	-27:44:34.75	69.01 ± 0.12	-15.54 ± 0.16	18.85 ± 0.09	-,-
J0417-3347	B9V	THA	04:17:53.740	-33:47:54.14	61.57 ± 0.56	-7.75 ± 0.58	18.51 ± 0.35	17.6 ± 0.9	...	51,52
J0425-7630	(M4)	THA	04:25:22.437	-76:30:06.55	57.11 ± 0.11	34.47 ± 0.11	17.27 ± 0.05	-,-
J0425-4958	(M5)	THA	04:25:49.584	-49:58:41.66	59.54 ± 0.10	11.93 ± 0.11	17.61 ± 0.05	-,-
J0427-2455	(M5)	THA	04:27:26.311	-24:55:27.48	57.94 ± 0.09	-13.55 ± 0.10	17.28 ± 0.06	-,-
J0438-2702	(M5)	THA	04:38:45.731	-27:02:02.17	56.80 ± 0.07	-11.67 ± 0.10	18.37 ± 0.05	19.3 ± 0.1	...	-,5
J0030-3809	(M5)	THA	00:30:39.728	-38:09:57.65	92.74 ± 0.09	-63.44 ± 0.07	23.23 ± 0.06	-,-
J0455-5446	(M9)	THA	04:55:21.122	-54:46:15.72	53.60 ± 0.87	23.07 ± 0.80	18.94 ± 0.34	-,-
J0500-4514	(M4)	THA	05:00:19.131	-45:14:41.87	48.91 ± 0.07	12.92 ± 0.08	18.93 ± 0.04	-,-
J0506-5828	(M2)	THA	05:06:10.493	-58:28:28.30	50.02 ± 0.05	29.85 ± 0.05	18.70 ± 0.02	19.6 ± 0.7	...	-,4
J0519-7104	(M5)	THA	05:19:04.336	-71:04:03.58	43.21 ± 0.12	41.68 ± 0.14	17.14 ± 0.07	-,-
J0536-6555	(M6)	THA	05:36:03.336	-65:55:18.43	38.04 ± 0.17	39.93 ± 0.22	17.07 ± 0.10	-,-
J0538-7413	(M5)	THA	05:38:21.162	-74:13:54.84	39.28 ± 0.07	46.70 ± 0.10	16.68 ± 0.05	-,-
J0548-5211	(M5)	THA	05:48:09.957	-52:11:02.35	33.97 ± 0.09	26.32 ± 0.09	16.25 ± 0.04	-,-
J0552-5929	(M5)	THA	05:52:49.004	-59:29:07.53	32.55 ± 0.14	32.48 ± 0.13	15.28 ± 0.07	-,-
J0039-3817	(M4)	THA	00:39:35.477	-38:17:18.69	101.47 ± 0.10	-66.50 ± 0.07	24.92 ± 0.06	3.3 ± 0.4	...	-,5
J0607-6409	(M4)	THA	06:07:29.276	-64:09:31.81	27.50 ± 0.11	38.70 ± 0.09	15.35 ± 0.05	-,-
J0651-3033	(M4)	COL	06:51:50.842	-30:33:37.49	-0.39 ± 0.19	1.43 ± 0.24	15.14 ± 0.14	-,-
J0653-2806	(M3)	COL	06:53:31.301	-28:06:16.23	-2.26 ± 0.05	-0.97 ± 0.06	13.35 ± 0.04	-,-
J0655+2250	(M8)	COL	06:55:47.129	+22:50:19.94	-2.27 ± 0.55	-91.09 ± 0.46	24.01 ± 0.32	-,-
J0714-4009	(M4)	COL	07:14:42.298	-40:09:37.99	-9.22 ± 0.77	11.37 ± 0.91	14.25 ± 0.42	-,-
J0716-4118	(M5)	COL	07:16:43.217	-41:18:56.94	-8.24 ± 0.11	13.95 ± 0.12	15.46 ± 0.07	-,-
J0733-4019	(M4)	COL	07:33:34.188	-40:19:00.19	-10.13 ± 0.31	10.83 ± 0.35	13.05 ± 0.17	-,-
J0733-4018	(M4)	COL	07:33:34.231	-40:18:58.56	-13.03 ± 0.14	10.77 ± 0.15	13.74 ± 0.08	-,-
J2313+5937	(M2)	COL	23:13:23.734	+59:37:08.12	91.16 ± 0.06	2.61 ± 0.05	21.67 ± 0.03	-,-
J2319+7900	M3.5V	COL	23:19:25.603	+79:00:04.77	209.27 ± 0.08	61.60 ± 0.07	52.82 ± 0.05	8,-

Table 3 continued

Table 3 (*continued*)

Name	Spectral	Assoc.	R.A. ^b	Decl. ^b	$\mu_\alpha \cos \delta$	μ_δ	Parallax	Rad. Vel.	Ambiguous	Ref. ^d
	Type ^a		(hh:mm:ss.sss)	(dd:mm:ss.ss)	(mas yr ⁻¹)	(mas yr ⁻¹)	(mas)	(km s ⁻¹)	Assoc. ^c	
J0222-1046	F3V	COL	02:22:01.693	-10:46:40.40	153.19 ± 0.19	-82.48 ± 0.18	33.33 ± 0.10	12 ± 4	...	6,53
J2330+5916	(M4)	COL	23:30:02.885	+59:16:08.42	109.49 ± 0.08	-3.97 ± 0.06	26.82 ± 0.05	-,-
J0255+4746	(K7)	COL	02:55:43.621	+47:46:46.47	85.39 ± 0.09	-79.49 ± 0.11	19.97 ± 0.05	-,-
J0257+4907	(M5)	COL	02:57:21.531	+49:07:31.85	117.80 ± 0.15	-105.76 ± 0.14	29.18 ± 0.08	-,-
J0301-3607	(M5)	COL	03:01:56.827	-36:07:26.09	54.92 ± 0.09	-9.25 ± 0.10	13.28 ± 0.07	-,-
J0307-2750	(M4)	COL	03:07:49.175	-27:50:46.99	67.62 ± 0.09	-16.97 ± 0.10	16.77 ± 0.07	13.8 ± 0.8	...	-,5
J0316-3509	(M3)	COL	03:16:50.500	-35:09:38.15	83.88 ± 0.20	-14.04 ± 0.23	21.69 ± 0.12	...	COL(67);THA(33)	-,-
J0022+1203	M7.5	COL	00:22:13.948	+12:03:03.54	131.95 ± 0.48	-79.66 ± 0.30	28.19 ± 0.24	54,-
J0320+3942	M1.5Ve	COL	03:20:45.413	+39:42:59.38	126.7 ± 1.3	-129.25 ± 0.86	31.60 ± 0.51	31,-
J0326-3850	(M3)	COL	03:26:37.108	-38:50:15.96	49.48 ± 0.06	-2.65 ± 0.07	12.43 ± 0.04	-,-
J0341-2253	(M1)	COL	03:41:15.632	-22:53:08.07	51.45 ± 0.05	-15.23 ± 0.05	13.89 ± 0.04	18 ± 2	...	-,4
J0344-2005	(M4)	COL	03:44:33.867	-20:05:38.48	51.21 ± 0.08	-17.88 ± 0.07	14.20 ± 0.07	-,-
J0400-4256	(M4)	COL	04:00:10.071	-42:56:31.16	42.82 ± 0.06	4.55 ± 0.08	11.93 ± 0.04	-,-
J0400-4256	(M4)	COL	04:00:13.789	-42:56:34.86	43.19 ± 0.07	5.05 ± 0.09	12.03 ± 0.05	-,-
J0405-2809	(M4)	COL	04:05:57.128	-28:09:46.52	49.59 ± 0.07	-9.68 ± 0.10	15.21 ± 0.05	-,-
J0416-5841	(M8)	COL	04:16:57.560	-58:41:04.40	31.07 ± 0.60	18.17 ± 0.75	10.69 ± 0.30	-,-
J0419-4025	(M7)	COL	04:19:55.741	-40:25:34.39	40.83 ± 0.36	4.15 ± 0.50	12.71 ± 0.23	-,-
J0427-3327	M4.8	COL	04:27:45.692	-33:27:42.67	42.40 ± 0.10	-3.12 ± 0.12	16.15 ± 0.06	50,-
J0429-3608	(M4)	COL	04:29:17.911	-36:08:27.10	43.20 ± 0.07	1.75 ± 0.08	14.70 ± 0.04	-,-
J0430-4640	(M8)	COL	04:30:35.363	-46:40:21.16	67.83 ± 0.32	18.94 ± 0.37	22.63 ± 0.17	...	COL(64);CAR(22);THA(14)	-,-
J0432+7407	(M4)	COL	04:32:57.100	+74:07:00.30	78.23 ± 0.06	-134.38 ± 0.10	29.32 ± 0.05	-7 ± 7	...	-,5
J0432+7406	(M2)	COL	04:32:57.531	+74:06:58.06	78.38 ± 0.06	-124.92 ± 0.09	29.54 ± 0.04	-7 ± 7	...	-,4
J0440-1842	(M4)	COL	04:40:53.330	-18:42:35.44	37.00 ± 0.07	-15.20 ± 0.07	13.30 ± 0.05	21 ± 1	...	-,5
J0446-2627	(M5)	COL	04:46:34.105	-26:27:56.84	33.35 ± 0.08	-5.46 ± 0.12	12.11 ± 0.06	-,-
J0448-3821	(M4)	COL	04:48:00.020	-38:21:37.30	32.69 ± 0.07	7.34 ± 0.11	12.65 ± 0.05	-,-
J0449-5117	(M4)	COL	04:49:10.613	-51:17:45.63	27.21 ± 0.11	14.79 ± 0.15	10.36 ± 0.06	-,-
J0451-2725	(M4)	COL	04:51:03.968	-27:25:48.24	32.54 ± 0.37	-3.94 ± 0.41	12.88 ± 0.22	-,-
J0504-3151	(M5)	COL	05:04:18.897	-31:51:21.63	26.97 ± 0.11	1.01 ± 0.11	13.57 ± 0.07	-,-
J0505-1916	(M5)	COL	05:05:32.014	-19:16:36.27	36.25 ± 0.08	-17.30 ± 0.11	16.89 ± 0.07	-,-
J0507-4356	(M4)	COL	05:07:08.984	-43:56:23.78	30.64 ± 0.08	13.23 ± 0.11	12.98 ± 0.05	-,-
J0507-3856	(M4)	COL	05:07:49.358	-38:56:26.92	22.52 ± 0.18	7.79 ± 0.21	10.35 ± 0.10	-,-
J0507-4136	(M4)	COL	05:07:54.318	-41:36:06.13	25.51 ± 0.08	9.77 ± 0.08	10.76 ± 0.04	-,-
J0508-4557	(M8)	COL	05:08:16.368	-45:57:50.93	26.2 ± 1.1	15.6 ± 1.5	11.51 ± 0.58	-,-
J0509-4207	(M1)	COL	05:09:51.698	-42:07:43.76	24.42 ± 0.05	9.88 ± 0.05	10.54 ± 0.02	24 ± 4	...	-,4
J0510-3253	(M3)	COL	05:10:26.376	-32:53:06.75	26.26 ± 0.05	2.00 ± 0.06	12.31 ± 0.03	-,-
J0510-3253	(M4)	COL	05:10:26.439	-32:53:09.20	27.37 ± 0.08	2.64 ± 0.09	12.33 ± 0.05	-,-
J0514-2517	(M3)	COL	05:14:03.217	-25:17:03.83	31.23 ± 0.06	-7.54 ± 0.07	15.64 ± 0.04	-,-
J0516-3124	(M4)	COL	05:16:01.221	-31:24:45.70	34.25 ± 0.08	-0.73 ± 0.09	18.66 ± 0.05	-,-
J0517-1121	(M5)	COL	05:17:53.070	-11:21:20.43	27.59 ± 0.16	-23.01 ± 0.16	14.40 ± 0.11	-,-

Table 3 continued

Table 3 (*continued*)

Name	Spectral	Assoc.	R.A. ^b	Decl. ^b	$\mu_\alpha \cos \delta$	μ_δ	Parallax	Rad. Vel.	Ambiguous	Ref. ^d
	Type ^a		(hh:mm:ss.sss)	(dd:mm:ss.ss)	(mas yr ⁻¹)	(mas yr ⁻¹)	(mas)	(km s ⁻¹)	Assoc. ^c	
J0519-2811	(M5)	COL	05:19:25.775	-28:11:06.08	32.22 ± 0.09	-5.03 ± 0.10	17.60 ± 0.06	-, -
J0520-2042	(M8)	COL	05:20:48.087	-20:42:14.81	25.4 ± 2.0	-7.8 ± 2.3	11.9 ± 1.7	-, -
J0521-3307	(M2)	COL	05:21:55.937	-33:07:12.68	35.05 ± 0.04	1.94 ± 0.05	18.60 ± 0.03	25 ± 2	...	-, 4
J0521-3307	(M5)	COL	05:21:56.287	-33:07:12.51	33.23 ± 0.11	5.96 ± 0.13	18.62 ± 0.07	25 ± 2	...	-, 5
J0523-2019	(M4)	COL	05:23:09.514	-20:19:59.95	26.64 ± 0.06	-12.57 ± 0.07	14.85 ± 0.05	-, -
J0524-3418	(M1)	COL	05:24:03.011	-34:18:37.21	28.50 ± 0.05	4.75 ± 0.05	17.49 ± 0.03	22 ± 2	...	-, 4
J0526-3404	(M4)	COL	05:26:45.615	-34:04:24.35	30.55 ± 0.07	4.58 ± 0.09	16.94 ± 0.04	-, -
J0529-1957	(M5)	COL	05:29:08.327	-19:57:21.60	25.26 ± 0.08	-12.32 ± 0.11	15.17 ± 0.07	-, -
J0529-2852	(M4)	COL	05:29:25.326	-28:52:27.39	21.93 ± 0.06	-0.31 ± 0.06	12.63 ± 0.04	-, -
J0529-2852	(M5)	COL	05:29:28.398	-28:52:32.11	22.32 ± 0.10	-0.59 ± 0.11	12.73 ± 0.06	-, -
J0534-3239	M2.5	COL	05:34:48.617	-32:39:35.97	28.28 ± 0.04	3.17 ± 0.05	16.89 ± 0.03	25 ± 1	...	21, 4
J0536-3654	(M4)	COL	05:36:39.841	-36:54:07.79	18.83 ± 0.09	6.87 ± 0.09	12.36 ± 0.05	-, -
J0538-1616	(M5)	COL	05:38:08.198	-16:16:14.42	25.37 ± 0.10	-22.60 ± 0.11	17.81 ± 0.07	-, -
J0538-2940	(M5)	COL	05:38:50.908	-29:40:56.08	25.27 ± 0.09	-2.21 ± 0.11	18.02 ± 0.06	-, -
J0543-3335	(M3)	COL	05:43:38.142	-33:35:42.62	22.58 ± 0.05	4.39 ± 0.05	15.61 ± 0.03	-, -
J0543-2342	(M4)	COL	05:43:42.409	-23:42:41.74	20.76 ± 0.08	-7.34 ± 0.11	14.66 ± 0.07	-, -
J0549-3724	(M4)	COL	05:49:55.374	-37:24:28.72	14.60 ± 0.11	9.88 ± 0.13	10.53 ± 0.06	-, -
J0551-3925	(M6)	COL	05:51:36.190	-39:25:01.07	22.51 ± 0.17	13.32 ± 0.17	18.98 ± 0.09	-, -
J0553-3149	(M6)	COL	05:53:37.069	-31:49:12.08	19.53 ± 0.18	2.51 ± 0.21	15.67 ± 0.11	-, -
J0609-2537	(M4)	COL	06:09:43.333	-25:37:34.24	9.38 ± 0.06	-2.30 ± 0.08	10.95 ± 0.05	-, -
J0616-2543	(L1)	COL	06:16:56.248	-25:43:55.86	11.50 ± 0.93	-10.2 ± 1.3	19.40 ± 0.80	-, -
J0628-4415	(M4)	COL	06:28:50.556	-44:15:21.46	8.15 ± 0.08	17.02 ± 0.08	12.40 ± 0.04	-, -
J0629-2130	(M5)	COL	06:29:06.680	-21:30:50.91	4.56 ± 0.05	-9.25 ± 0.10	14.32 ± 0.06	-, -
J0629-4349	(M5)	COL	06:29:23.480	-43:49:23.11	8.14 ± 0.16	15.97 ± 0.18	12.14 ± 0.08	-, -
J0638-5604	(M2)	COL	06:38:06.729	-56:04:52.89	2.42 ± 0.09	27.33 ± 0.10	11.70 ± 0.05	-, -
J0640-7051	(M8)	CAR	06:40:18.552	-70:51:56.07	8.44 ± 0.33	53.08 ± 0.46	15.34 ± 0.22	-, -
J0641-5616	(M4)	CAR	06:41:15.979	-56:16:29.67	4.97 ± 0.07	35.72 ± 0.07	16.29 ± 0.03	-, -
J0646-7038	(M4)	CAR	06:46:24.300	-70:38:02.42	3.52 ± 0.08	40.24 ± 0.08	12.22 ± 0.04	-, -
J0658-6311	(M7)	CAR	06:58:20.251	-63:11:34.62	2.43 ± 0.54	32.13 ± 0.46	11.89 ± 0.23	-, -
J0700-6203	(M5)	CAR	07:00:40.507	-62:03:41.72	1.45 ± 0.12	32.41 ± 0.13	11.94 ± 0.06	-, -
J0708-6058	(M4)	CAR	07:08:57.434	-60:58:50.79	-1.42 ± 0.07	29.69 ± 0.06	11.55 ± 0.03	-, -
J0715-6555	(M5)	CAR	07:15:17.050	-65:55:48.14	-1.77 ± 0.11	33.35 ± 0.09	11.26 ± 0.05	-, -
J0724-5922	(M4)	CAR	07:24:29.074	-59:22:22.17	-11.88 ± 0.09	39.17 ± 0.08	16.13 ± 0.05	-, -
J0736-6705	(M4)	CAR	07:36:01.507	-67:05:40.47	-8.46 ± 0.42	38.47 ± 0.46	12.09 ± 0.26	-, -
J0744-6458	(M2)	CAR	07:44:11.038	-64:58:04.78	-8.37 ± 0.07	32.84 ± 0.06	12.68 ± 0.03	20 ± 3	...	-, 4
J0759-5035	(M5)	CAR	07:59:41.383	-50:35:59.76	-17.50 ± 0.15	20.32 ± 0.15	13.88 ± 0.07	-, -
J0804-6316	(M2)	CAR	08:04:05.299	-63:16:39.11	-17.33 ± 0.05	32.35 ± 0.05	12.80 ± 0.02	-, -
J0806-7444	(M2)	CAR	08:06:36.019	-74:44:24.26	-16.34 ± 0.05	49.44 ± 0.05	14.53 ± 0.03	17 ± 1	...	-, 4
J0808-5420	(M5)	CAR	08:08:58.070	-54:20:54.09	-21.31 ± 0.15	24.51 ± 0.13	14.91 ± 0.07	-, -

Table 3 continued

Table 3 (*continued*)

Name	Spectral	Assoc.	R.A. ^b	Decl. ^b	$\mu_\alpha \cos \delta$	μ_δ	Parallax	Rad. Vel.	Ambiguous	Ref. ^d
	Type ^a		(hh:mm:ss.sss)	(dd:mm:ss.ss)	(mas yr ⁻¹)	(mas yr ⁻¹)	(mas)	(km s ⁻¹)	Assoc. ^c	
J0810-5015	(M5)	CAR	08:10:20.501	-50:15:43.32	-19.63 ± 0.12	18.55 ± 0.12	13.62 ± 0.07	-,-
J0811-6656	(M4)	CAR	08:11:11.909	-66:56:39.64	-14.62 ± 0.09	28.71 ± 0.08	10.43 ± 0.05	-,-
J0811-5003	(M5)	CAR	08:11:48.434	-50:03:18.24	-18.35 ± 0.14	18.76 ± 0.16	13.32 ± 0.07	-,-
J0814-6007	(M5)	CAR	08:14:45.098	-60:07:24.01	-31.95 ± 0.16	60.22 ± 0.13	25.83 ± 0.09	-,-
J0815-6359	(M5)	CAR	08:15:40.836	-63:59:39.39	-21.12 ± 0.16	32.27 ± 0.12	13.73 ± 0.07	-,-
J0819-6414	(M5)	CAR	08:19:26.102	-64:14:25.85	-14.23 ± 0.60	27.46 ± 0.52	11.07 ± 0.28	-,-
J0824-5522	(M8)	CAR	08:24:05.966	-55:22:03.07	-23.14 ± 0.44	22.96 ± 0.50	14.06 ± 0.23	-,-
J0839-6954	(M5)	CAR	08:39:47.225	-69:54:23.02	-24.05 ± 0.09	37.40 ± 0.10	13.11 ± 0.06	-,-
J0841-5745	(M5)	CAR	08:41:47.825	-57:45:31.41	-33.88 ± 0.14	28.25 ± 0.14	17.45 ± 0.07	-,-
J0841-7113	(M5)	CAR	08:41:59.887	-71:13:16.47	-21.06 ± 0.10	33.67 ± 0.10	11.81 ± 0.06	-,-
J0842-7113	(M4)	CAR	08:42:00.830	-71:13:21.12	-20.83 ± 0.09	33.53 ± 0.09	11.75 ± 0.05	-,-
J0842-5743	(M5)	CAR	08:42:15.989	-57:43:04.32	-25.98 ± 0.13	23.35 ± 0.13	13.76 ± 0.06	-,-
J0844-6158	(M5)	CAR	08:44:19.915	-61:58:42.10	-19.87 ± 0.14	24.09 ± 0.12	10.77 ± 0.07	-,-
J0848-6307	(M5)	CAR	08:48:48.926	-63:07:34.60	-29.93 ± 0.16	30.12 ± 0.15	14.12 ± 0.08	-,-
J0858-6113	(M4)	CAR	08:58:07.327	-61:13:21.16	-30.65 ± 0.08	24.87 ± 0.07	14.16 ± 0.04	-,-
J0858-6113	(M4)	CAR	08:58:07.978	-61:13:26.83	-30.28 ± 0.08	25.36 ± 0.08	14.21 ± 0.04	-,-
J0900-6751	(M8)	CAR	09:00:06.662	-67:51:06.39	-28.4 ± 1.1	30.86 ± 0.99	13.87 ± 0.59	-,-
J0901-5221	(M4)	CAR	09:01:20.494	-52:21:12.68	-27.72 ± 0.08	12.82 ± 0.08	12.21 ± 0.05	-,-
J0904-7137	(M5)	CAR	09:04:22.968	-71:37:14.93	-26.37 ± 0.11	34.00 ± 0.11	12.35 ± 0.06	-,-
J0908-5831	(M2)	CAR	09:08:37.387	-58:31:51.68	-24.98 ± 0.05	16.63 ± 0.05	10.21 ± 0.03	-,-
J0917-7444	A0V	CAR	09:17:27.454	-74:44:03.97	-29.89 ± 0.19	35.87 ± 0.20	12.93 ± 0.09	55,-
J0918-5452	M4	CAR	09:18:01.546	-54:52:32.85	-52.3 ± 1.1	26.8 ± 1.1	18.87 ± 0.67	21,-
J0918-6101	(L1)	CAR	09:18:56.294	-61:01:18.73	-29.0 ± 3.2	20.0 ± 3.9	14.9 ± 1.8	-,-
J0923-7340	(M3)	CAR	09:23:46.973	-73:40:54.67	-30.92 ± 0.05	35.78 ± 0.06	13.08 ± 0.03	-,-
J0923-7340	(M5)	CAR	09:23:48.161	-73:40:46.90	-32.31 ± 0.08	34.66 ± 0.10	13.15 ± 0.05	-,-
J0928-6414	M4	CAR	09:28:23.292	-64:14:54.63	-30.65 ± 0.07	20.27 ± 0.06	11.24 ± 0.04	21,-
J0930-4927	(M4)	CAR	09:30:17.810	-49:27:39.59	-32.03 ± 0.09	8.16 ± 0.08	11.23 ± 0.05	-,-
J0931-7327	(M3)	CAR	09:31:54.403	-73:27:36.84	-32.13 ± 0.07	33.03 ± 0.07	12.78 ± 0.04	-,-
J0934-7405	(M4)	CAR	09:34:04.238	-74:05:36.06	-33.14 ± 0.09	33.83 ± 0.09	12.87 ± 0.05	-,-
J0934-5653	(M8)	CAR	09:34:23.376	-56:53:08.70	-37.6 ± 1.0	15.31 ± 0.74	11.37 ± 0.59	-,-
J0935-6221	(M4)	CAR	09:35:20.489	-62:21:59.97	-31.31 ± 0.10	17.86 ± 0.09	11.99 ± 0.06	-,-
J0939-6119	B9IV/V	CAR	09:39:20.921	-61:19:40.66	-42.29 ± 0.39	19.45 ± 0.33	15.21 ± 0.18	20 ± 4	...	55,53
J0940-6745	(M5)	CAR	09:40:36.547	-67:45:16.47	-35.60 ± 0.17	24.32 ± 0.19	13.05 ± 0.09	-,-
J0942-5601	(M4)	CAR	09:42:13.795	-56:01:35.97	-34.13 ± 0.10	11.32 ± 0.10	12.32 ± 0.05	-,-
J0948-5201	(M5)	CAR	09:48:29.465	-52:01:59.55	-34.37 ± 0.22	6.90 ± 0.18	11.29 ± 0.11	-,-
J0949-7138	(M4)	CAR	09:49:00.754	-71:38:02.95	-36.10 ± 0.13	28.56 ± 0.13	12.63 ± 0.07	-,-
J0950-5828	(M4)	CAR	09:50:00.598	-58:28:18.42	-36.19 ± 0.08	12.70 ± 0.08	12.76 ± 0.04	-,-
J1003-5924	(M3)	CAR	10:03:58.493	-59:24:02.49	-31.46 ± 0.09	11.79 ± 0.09	10.19 ± 0.05	-,-
J1005-7136	(M4)	CAR	10:05:22.723	-71:36:58.56	-35.55 ± 0.10	21.21 ± 0.10	11.48 ± 0.06	...	CAR(93);LCC(7)	-,-

Table 3 continued

Table 3 (*continued*)

Name	Spectral	Assoc.	R.A. ^b	Decl. ^b	$\mu_\alpha \cos \delta$	μ_δ	Parallax	Rad. Vel.	Ambiguous	Ref. ^d
	Type ^a		(hh:mm:ss.sss)	(dd:mm:ss.ss)	(mas yr ⁻¹)	(mas yr ⁻¹)	(mas)	(km s ⁻¹)	Assoc. ^c	
J1005-7137	(M0)	CAR	10:05:25.358	-71:37:28.01	-36.43 ± 0.17	22.76 ± 0.16	11.30 ± 0.09	-,-
J1005-5730	(M4)	CAR	10:05:38.016	-57:30:40.02	-55.68 ± 0.09	17.98 ± 0.08	17.45 ± 0.05	-,-
J1013-5557	(M5)	CAR	10:13:58.020	-55:57:06.09	-50.78 ± 0.15	11.30 ± 0.15	15.40 ± 0.08	-,-
J1020-7105	(M4)	CAR	10:20:37.262	-71:05:24.84	-37.18 ± 0.12	20.56 ± 0.12	11.18 ± 0.07	-,-
J1020-6311	M4	CAR	10:20:44.501	-63:11:21.24	-43.19 ± 0.66	12.67 ± 0.64	13.81 ± 0.38	21,-
J1021-6226	(M3)	CAR	10:21:15.451	-62:26:04.09	-38.48 ± 0.11	11.67 ± 0.10	11.95 ± 0.07	-,-
J1030-6252	(M4)	CAR	10:30:21.727	-62:52:42.97	-51.93 ± 0.07	13.52 ± 0.07	16.11 ± 0.04	-,-
J1037-7329	(M4)	CAR	10:37:57.406	-73:29:41.29	-46.17 ± 0.08	22.85 ± 0.07	13.47 ± 0.04	-,-
J1038-5954	(M4)	CAR	10:38:44.362	-59:54:43.70	-36.81 ± 0.08	6.95 ± 0.08	10.96 ± 0.05	...	CAR(58);LCC(42)	-,-
J1041-6541	(M6)	CAR	10:41:05.827	-65:41:10.88	-42.58 ± 0.51	11.37 ± 0.46	12.54 ± 0.26	...	CAR(90);LCC(10)	-,-
J1041-7602	(M4)	CAR	10:41:32.899	-76:02:25.67	-44.66 ± 0.09	23.52 ± 0.07	12.85 ± 0.05	-,-
J1113-6448	M2	CAR	11:13:40.726	-64:48:59.31	-55.44 ± 0.05	5.07 ± 0.04	14.67 ± 0.03	21,-
J1116-6626	(M8)	CAR	11:16:17.630	-66:26:19.37	-50.8 ± 1.1	5.93 ± 0.72	12.82 ± 0.64	-,-
J0224-7633	(M9)	CAR	02:24:12.271	-76:33:19.90	67.7 ± 2.0	10.8 ± 1.3	15.75 ± 0.82	-,-
J0315-7723	F5IV-V	CAR	03:15:58.204	-77:23:17.47	113.16 ± 0.16	62.54 ± 0.14	34.12 ± 0.08	14.6 ± 0.2	CAR(91);COL(9)	6,4
J0413-8408	(M5)	CAR	04:13:29.045	-84:08:26.61	44.38 ± 0.17	40.41 ± 0.24	14.06 ± 0.10	-,-
J0427-7719	(M8)	CAR	04:27:21.639	-77:19:03.68	51.40 ± 0.49	45.94 ± 0.63	18.94 ± 0.28	...	CAR(89);ABDMG(11)	-,-
J0524-7109	(M6)	CAR	05:24:02.040	-71:09:28.53	36.03 ± 0.23	50.03 ± 0.20	18.69 ± 0.14	-,-
J0524-7038	(M5)	CAR	05:24:08.573	-70:38:05.65	35.24 ± 0.11	52.99 ± 0.15	18.55 ± 0.06	-,-
J0552-5302	(M4)	CAR	05:52:28.962	-53:02:58.93	24.72 ± 0.11	36.42 ± 0.10	20.33 ± 0.05	...	CAR(87);COL(13)	-,-
J0608-8133	(M5)	CAR	06:08:52.059	-81:33:04.60	18.12 ± 0.07	64.19 ± 0.10	16.90 ± 0.05	-,-
J0610-6129	F0III/IV	CAR	06:10:52.922	-61:29:58.79	14.66 ± 0.05	34.12 ± 0.05	13.03 ± 0.03	55,-
J0626-7516	(M2)	CAR	06:26:22.041	-75:16:39.80	11.84 ± 0.04	47.38 ± 0.05	13.40 ± 0.02	16 ± 2	...	-,4
J1126-3824	(M3)	TWA	11:26:51.254	-38:24:55.62	-60.84 ± 0.10	-15.51 ± 0.08	14.53 ± 0.07	-,-
J1218-4528	(M4)	TWA	12:18:18.624	-45:28:41.68	-50.20 ± 0.09	-19.21 ± 0.05	12.23 ± 0.07	-,-
J1230-4402	(M3)	TWA	12:30:05.141	-44:02:36.31	-51.82 ± 0.09	-21.74 ± 0.06	12.66 ± 0.06	-,-
J1230-4404	(M4)	TWA	12:30:05.734	-44:04:32.12	-51.59 ± 0.10	-21.61 ± 0.07	12.74 ± 0.07	-,-
J1237-4419	(M5)	TWA	12:37:04.961	-44:19:19.69	-43.83 ± 0.18	-18.27 ± 0.19	11.35 ± 0.13	-,-
J1240-4633	(M5)	TWA	12:40:05.645	-46:33:59.01	-49.26 ± 0.15	-21.68 ± 0.16	12.33 ± 0.10	-,-
J1242-4952	(M8)	TWA	12:42:30.662	-49:52:24.79	-45.1 ± 1.1	-21.54 ± 0.89	11.17 ± 0.83	...	TWA(52);LCC(46)	-,-
J1250-4231	(M4)	TWA	12:50:47.705	-42:31:49.06	-39.40 ± 0.14	-19.60 ± 0.11	10.11 ± 0.09	...	TWA(50);LCC(34);UCL(16)	-,-
J1250-4231	(M3)	TWA	12:50:49.097	-42:31:23.80	-38.78 ± 0.15	-20.78 ± 0.12	10.26 ± 0.10	...	TWA(62);LCC(28);UCL(10)	-,-
J1153+2410	(M5)	CBER	11:53:45.506	+24:10:15.41	-11.87 ± 0.18	-9.84 ± 0.15	11.86 ± 0.14	-,-
J1155+2528	(M1)	CBER	11:55:30.540	+25:28:32.54	-12.77 ± 0.06	-9.63 ± 0.04	12.37 ± 0.04	1.6 ± 0.8	...	-,4
J1205+2501	M8V	CBER	12:05:35.465	+25:01:31.17	-12.9 ± 1.1	-9.73 ± 0.72	11.40 ± 0.64	1,-
J1208+3106	(K8)	CBER	12:08:36.086	+31:06:09.64	-11.89 ± 0.07	-8.07 ± 0.05	11.24 ± 0.04	-0.5 ± 0.7	...	-,4
J1210+2625	M9V	CBER	12:10:40.925	+26:25:32.13	-11.28 ± 0.64	-8.29 ± 0.76	12.20 ± 0.43	1,-
J1214+2314	(M4)	CBER	12:14:26.513	+23:14:02.35	-11.28 ± 0.09	-8.92 ± 0.08	10.99 ± 0.05	-,-
J1217+2436	M9V	CBER	12:17:10.438	+24:36:07.24	-11.5 ± 3.8	-6.8 ± 2.3	11.4 ± 2.5	1,-

Table 3 continued

Table 3 (*continued*)

Name	Spectral	Assoc.	R.A. ^b	Decl. ^b	$\mu_\alpha \cos \delta$	μ_δ	Parallax	Rad. Vel.	Ambiguous	Ref. ^d
	Type ^a		(hh:mm:ss.sss)	(dd:mm:ss.ss)	(mas yr ⁻¹)	(mas yr ⁻¹)	(mas)	(km s ⁻¹)	Assoc. ^c	
J1219+3109	M8V	CBER	12:19:52.414	+31:09:57.70	-11.87 ± 0.79	-10.56 ± 0.50	12.51 ± 0.43	1,-
J1224+2653	(M2)	CBER	12:24:11.215	+26:53:16.50	-11.25 ± 0.05	-9.42 ± 0.04	11.58 ± 0.04	0 ± 2	...	-,4
J1229+2146	(M2)	CBER	12:29:24.900	+21:46:49.61	-12.08 ± 0.06	-9.82 ± 0.04	12.12 ± 0.04	1 ± 1	...	-,4
J1233+3107	M9V	CBER	12:33:51.588	+31:07:05.04	-11.26 ± 0.95	-8.58 ± 0.64	11.59 ± 0.66	1,-
J1235+2750	(M5)	CBER	12:35:52.310	+27:50:41.15	-11.79 ± 0.19	-8.55 ± 0.12	11.32 ± 0.13	-,-
J1237+3108	M7V	CBER	12:37:27.564	+31:08:02.16	-11.45 ± 0.22	-8.24 ± 0.15	11.42 ± 0.16	1,-
J1238+2333	(M2)	CBER	12:38:11.441	+23:33:21.97	-12.04 ± 0.07	-10.34 ± 0.04	11.45 ± 0.04	-1 ± 2	...	-,4
J1244+2456	(M3)	CBER	12:44:29.974	+24:56:02.55	-12.22 ± 0.05	-8.76 ± 0.04	12.12 ± 0.04	-,-
J1244+2547	M7V	CBER	12:44:31.567	+25:47:20.77	-12.22 ± 0.36	-7.83 ± 0.24	12.11 ± 0.26	1,-
J1247+2445	M7V	CBER	12:47:22.661	+24:45:48.49	-11.82 ± 0.63	-9.35 ± 0.39	12.21 ± 0.32	1,-
J1249+2521	K5V	CBER	12:49:00.406	+25:21:35.43	-12.71 ± 0.08	-8.69 ± 0.06	12.29 ± 0.06	56,-
J1249+2709	(M0)	CBER	12:49:24.175	+27:09:57.79	-11.28 ± 0.07	-7.83 ± 0.06	11.15 ± 0.05	-1 ± 2	...	-,4
J1251+2132	(M6)	CBER	12:51:26.786	+21:32:43.48	-11.99 ± 0.27	-9.36 ± 0.16	11.59 ± 0.14	-,-
J1255+2255	(M6)	CBER	12:55:55.378	+22:55:12.58	-11.04 ± 0.26	-8.52 ± 0.16	11.15 ± 0.13	-1 ± 2	...	-,-
J1257+2639	(M5)	CBER	12:57:48.602	+26:39:36.55	-12.34 ± 0.09	-7.74 ± 0.07	11.82 ± 0.06	-,-
J1257+2449	(M4)	CBER	12:57:56.546	+24:49:17.95	-12.18 ± 0.12	-8.24 ± 0.08	12.04 ± 0.06	-,-
J1259+2531	(M5)	CBER	12:59:03.074	+25:31:07.57	-11.43 ± 0.12	-8.24 ± 0.11	11.17 ± 0.10	-,-
J0519+0725	(M6)	THOR	05:19:08.495	+07:25:28.00	9.57 ± 0.35	-32.87 ± 0.28	10.34 ± 0.22	-,-
J0519+0909	(M5)	THOR	05:19:26.189	+09:09:54.34	11.92 ± 0.32	-35.72 ± 0.24	10.18 ± 0.18	-,-
J0520+0511	K0	THOR	05:20:17.962	+05:11:51.58	11.94 ± 0.25	-35.16 ± 0.19	10.72 ± 0.14	57,-
J0522+0545	(M8)	THOR	05:22:32.862	+05:45:23.84	2.0 ± 1.7	-24.5 ± 1.5	10.57 ± 0.89	-,-
J0523+0459	(M6)	THOR	05:23:39.549	+04:59:30.47	10.2 ± 1.0	-34.53 ± 0.76	10.50 ± 0.34	-,-
J0527+0626	(M6)	THOR	05:27:28.062	+06:26:43.32	8.93 ± 0.40	-32.37 ± 0.30	10.01 ± 0.20	-,-
J0539+0848	(M5)	THOR	05:39:04.466	+08:48:20.38	9.74 ± 0.18	-38.62 ± 0.16	10.92 ± 0.15	-,-
J0542+1539	(M5)	THOR	05:42:16.729	+15:39:43.49	5.71 ± 0.23	-39.86 ± 0.18	10.52 ± 0.14	-,-
J0304-3919	(M5)	XFOR	03:04:15.712	-39:19:12.94	40.64 ± 0.09	-5.53 ± 0.10	10.13 ± 0.06	-,-
J0321-3521	(M6)	XFOR	03:21:01.960	-35:21:21.95	37.90 ± 0.14	-5.58 ± 0.21	10.01 ± 0.11	-,-
J0323-3652	(M4)	XFOR	03:23:48.483	-36:52:39.02	41.46 ± 0.09	-5.45 ± 0.12	10.50 ± 0.06	-,-
J0325-3706	(M4)	XFOR	03:25:24.072	-37:06:06.05	38.56 ± 0.06	-4.46 ± 0.09	10.17 ± 0.05	-,-
J1141-7315	(M5)	EPSC	11:41:17.069	-73:15:36.90	-40.60 ± 0.09	5.67 ± 0.08	10.42 ± 0.05	...	EPSC(71);LCC(28)	-,-
J1143-7418	(M3)	EPSC	11:43:29.506	-74:18:37.87	-41.28 ± 0.07	-3.03 ± 0.07	10.06 ± 0.04	...	EPSC(91);LCC(9)	-,-
J1200-7444	(M3)	EPSC	12:00:02.525	-74:44:06.79	-42.05 ± 0.08	-5.70 ± 0.07	10.07 ± 0.05	-,-
J1220-7135	(M2)	EPSC	12:20:33.854	-71:35:18.96	-41.78 ± 0.10	-8.57 ± 0.07	10.77 ± 0.06	7 ± 1	EPSC(85);LCC(15)	-,-
J1220-7353	(M2)	EPSC	12:20:36.038	-73:53:02.97	-40.62 ± 0.07	-9.33 ± 0.05	10.01 ± 0.04	-,-
J1222-7001	(M3)	EPSC	12:22:00.521	-70:01:03.94	-41.31 ± 0.10	-10.47 ± 0.06	10.01 ± 0.05	...	EPSC(62);LCC(38)	-,-
J1222-7137	M2	EPSC	12:22:22.222	-71:37:04.25	-42.95 ± 0.04	-9.96 ± 0.04	10.52 ± 0.03	...	EPSC(85);LCC(15)	21,-
J1222-7410	(M5)	EPSC	12:22:48.475	-74:10:20.57	-42.57 ± 0.15	-9.27 ± 0.13	10.60 ± 0.09	-,-
J1225-7551	(M4)	EPSC	12:25:58.094	-75:51:11.83	-41.23 ± 0.11	-10.46 ± 0.11	10.05 ± 0.07	-,-
J1232-7654	(M2)	EPSC	12:32:47.878	-76:54:24.05	-41.8 ± 1.7	-13.5 ± 1.3	11.69 ± 0.91	-,-

Table 3 continued

Table 3 (*continued*)

Name	Spectral	Assoc.	R.A. ^b	Decl. ^b	$\mu_\alpha \cos \delta$	μ_δ	Parallax	Rad. Vel.	Ambiguous	Ref. ^d
	Type ^a		(hh:mm:ss.sss)	(dd:mm:ss.ss)	(mas yr ⁻¹)	(mas yr ⁻¹)	(mas)	(km s ⁻¹)	Assoc. ^c	
J0520+2504	(M4)	118TAU	05:20:36.223	+25:04:04.00	9.41 ± 0.18	-42.55 ± 0.11	10.18 ± 0.10	-,-
J1019-6440	(M3)	LCC	10:19:03.079	-64:40:51.87	-34.31 ± 0.09	12.02 ± 0.08	11.48 ± 0.04	15.8 ± 0.7	...	-,5
J1022-6216	(M5)	LCC	10:22:03.722	-62:16:28.44	-36.89 ± 0.18	10.92 ± 0.16	11.90 ± 0.10	...	LCC(53);CAR(47)	-,-
J1026-5955	(M2)	LCC	10:26:46.538	-59:55:26.59	-33.33 ± 0.10	6.93 ± 0.10	10.04 ± 0.06	...	LCC(50);CAR(50)	-,-
J1040-6302	(M6)	LCC	10:40:05.741	-63:02:39.08	-29.84 ± 0.79	2.99 ± 0.63	11.26 ± 0.45	-,-
J1040-6716	(M8)	LCC	10:40:20.083	-67:16:46.07	-33.0 ± 1.2	11.73 ± 0.98	10.79 ± 0.59	-,-
J1044-6314	(M8)	LCC	10:44:43.075	-63:14:26.20	-38.4 ± 1.1	6.73 ± 0.84	11.45 ± 0.47	...	LCC(77);CAR(23)	-,-
J1052-6818	(M9)	LCC	10:52:09.058	-68:18:42.09	-42.6 ± 1.2	7.9 ± 1.1	13.15 ± 0.69	-,-
J1104-6949	(M3)	LCC	11:04:23.731	-69:49:21.78	-40.49 ± 0.07	2.56 ± 0.06	10.19 ± 0.04	-,-
J1104-6711	(M0)	LCC	11:04:34.013	-67:11:51.84	-38.82 ± 0.04	9.74 ± 0.04	10.78 ± 0.02	16 ± 1	LCC(91);CAR(9)	-,4
J1126-5934	(M4)	LCC	11:26:58.838	-59:34:47.70	-40.02 ± 0.08	-0.86 ± 0.07	10.64 ± 0.05	-,-
J1131-6855	(M2)	LCC	11:31:57.842	-68:55:18.33	-41.44 ± 0.06	-2.16 ± 0.06	10.22 ± 0.04	-,-
J1132-5650	(M4)	LCC	11:32:17.081	-56:50:08.87	-40.16 ± 0.10	-6.04 ± 0.08	10.02 ± 0.07	-,-
J1136-6927	(M2)	LCC	11:36:16.730	-69:27:51.54	-42.67 ± 0.09	0.46 ± 0.07	10.14 ± 0.05	-,-
J1136-6053	(M3)	LCC	11:36:22.330	-60:53:14.59	-43.83 ± 0.06	-2.52 ± 0.06	11.32 ± 0.04	-,-
J1142-5708	(M5)	LCC	11:42:17.038	-57:08:02.72	-40.19 ± 0.11	-7.23 ± 0.09	10.01 ± 0.07	-,-
J1149-5948	(K3)	LCC	11:49:58.114	-59:48:02.99	-43.5 ± 1.7	-4.6 ± 1.4	11.7 ± 1.3	-,-
J1150-5032	(M8)	LCC	11:50:55.416	-50:32:45.32	-40.60 ± 0.87	-10.45 ± 0.58	10.31 ± 0.55	-,-
J1152-7041	(M5)	LCC	11:52:11.856	-70:41:55.93	-41.54 ± 0.14	-5.24 ± 0.14	10.12 ± 0.08	-,-
J1152-6645	(M4)	LCC	11:52:17.791	-66:45:45.67	-41.55 ± 0.09	-6.25 ± 0.08	10.17 ± 0.05	-,-
J1153-6711	(M4)	LCC	11:53:28.939	-67:11:12.99	-43.13 ± 0.08	-6.39 ± 0.07	10.50 ± 0.05	-,-
J1154-5403	(M4)	LCC	11:54:17.354	-54:03:40.86	-42.17 ± 0.10	-10.25 ± 0.09	10.28 ± 0.07	-,-
J1154-5324	(M0)	LCC	11:54:31.666	-53:24:32.81	-40.95 ± 0.05	-10.49 ± 0.04	10.50 ± 0.03	14 ± 2	...	-,4
J1154-5956	(M4)	LCC	11:54:56.650	-59:56:47.57	-44.07 ± 0.08	-5.33 ± 0.08	11.69 ± 0.05	-,-
J1159-6041	(M5)	LCC	11:59:29.510	-60:41:06.62	-38.78 ± 0.15	-5.58 ± 0.13	10.48 ± 0.09	-,-
J1202-6213	(M5)	LCC	12:02:12.161	-62:13:50.85	-39.55 ± 0.17	-4.80 ± 0.18	10.47 ± 0.12	-,-
J1202-6409	(M5)	LCC	12:02:28.099	-64:09:09.85	-47.30 ± 0.19	-5.19 ± 0.14	12.01 ± 0.11	-,-
J1203-6905	(M2)	LCC	12:03:02.023	-69:05:12.83	-38.38 ± 0.06	-0.68 ± 0.05	10.36 ± 0.04	-,-
J1206-6554	(M8)	LCC	12:06:42.727	-65:54:00.30	-38.8 ± 2.1	-5.7 ± 1.1	10.30 ± 0.84	-,-
J1210-6226	(M4)	LCC	12:10:01.334	-62:26:43.03	-41.11 ± 0.09	-10.12 ± 0.08	10.16 ± 0.06	-,-
J1210-6244	(M3)	LCC	12:10:09.161	-62:44:05.49	-41.89 ± 0.09	-10.09 ± 0.08	10.30 ± 0.06	-,-
J1210-5321	(M7)	LCC	12:10:56.491	-53:21:59.72	-38.20 ± 0.43	-11.65 ± 0.33	10.26 ± 0.33	-,-
J1212-5801	(M3)	LCC	12:12:22.099	-58:01:10.57	-41.66 ± 0.07	-12.10 ± 0.05	10.29 ± 0.04	-,-
J1213-6447	(K5)	LCC	12:13:19.500	-64:47:50.23	-46.08 ± 0.36	-7.52 ± 0.32	11.74 ± 0.22	14 ± 1	...	-,4
J1213-6448	(K7)	LCC	12:13:20.902	-64:48:59.62	-46.83 ± 0.04	-7.22 ± 0.04	12.25 ± 0.03	14 ± 3	...	-,4
J1217-6409	M2	LCC	12:17:40.056	-64:09:39.19	-37.58 ± 0.68	-6.11 ± 0.50	10.96 ± 0.38	21,-
J1217-5718	(M5)	LCC	12:17:54.026	-57:18:11.97	-35.70 ± 0.56	-10.79 ± 0.44	11.88 ± 0.36	-,-
J1217-5855	(M0)	LCC	12:17:58.070	-58:55:56.82	-41.10 ± 0.11	-11.89 ± 0.09	10.00 ± 0.08	-,-
J1218-6621	(M6)	LCC	12:18:47.633	-66:21:43.85	-40.80 ± 0.36	-10.49 ± 0.22	10.06 ± 0.19	-,-

Table 3 continued

Table 3 (*continued*)

Name	Spectral	Assoc.	R.A. ^b	Decl. ^b	$\mu_\alpha \cos \delta$	μ_δ	Parallax	Rad. Vel.	Ambiguous	Ref. ^d
	Type ^a		(hh:mm:ss.sss)	(dd:mm:ss.ss)	(mas yr ⁻¹)	(mas yr ⁻¹)	(mas)	(km s ⁻¹)	Assoc. ^c	
J1219-5520	(M5)	LCC	12:19:13.241	-55:20:20.01	-37.97 ± 0.25	-12.31 ± 0.20	10.08 ± 0.21	-,-
J1221-5813	(M4)	LCC	12:21:10.975	-58:13:12.09	-35.69 ± 0.58	-8.29 ± 0.61	10.31 ± 0.43	-,-
J1221-6754	(M2)	LCC	12:21:58.800	-67:54:54.91	-42.60 ± 0.07	-11.10 ± 0.05	10.43 ± 0.04	-,-
J1222-6330	(M8)	LCC	12:22:07.915	-63:30:53.87	-36.3 ± 1.4	-8.4 ± 1.0	10.77 ± 0.88	-,-
J1222-5636	(M5)	LCC	12:22:42.262	-56:36:11.59	-34.90 ± 0.36	-10.65 ± 0.29	10.20 ± 0.28	-,-
J1225-5944	(M8)	LCC	12:25:04.747	-59:44:33.73	-37.92 ± 0.60	-12.45 ± 0.56	10.11 ± 0.46	-,-
J1225-6721	(M4)	LCC	12:25:11.950	-67:21:44.97	-40.71 ± 0.10	-11.22 ± 0.07	10.06 ± 0.06	-,-
J1225-6529	(M6)	LCC	12:25:25.258	-65:29:27.68	-37.17 ± 0.43	-7.04 ± 0.25	10.01 ± 0.20	-,-
J1225-5747	(M5)	LCC	12:25:34.997	-57:47:11.95	-39.92 ± 0.14	-10.59 ± 0.12	10.45 ± 0.11	-,-
J1227-6505	(M8)	LCC	12:27:13.886	-65:05:55.24	-36.1 ± 1.3	-10.04 ± 0.74	10.10 ± 0.68	-,-
J1228-6300	(M8)	LCC	12:28:19.234	-63:00:54.65	-35.3 ± 2.9	-1.4 ± 2.0	10.9 ± 1.7	-,-
J1229-6001	(K9)	LCC	12:29:14.342	-60:01:13.04	-39.51 ± 0.04	-13.75 ± 0.04	10.02 ± 0.03	-,-
J1231-5456	(M4)	LCC	12:31:08.446	-54:56:44.57	-35.55 ± 0.14	-12.66 ± 0.11	10.14 ± 0.11	-,-
J1232-6456	(K6)	LCC	12:32:42.485	-64:56:51.45	-41.74 ± 0.05	-13.73 ± 0.04	10.38 ± 0.04	13 ± 1	...	-4
J1233-6848	(M5)	LCC	12:33:24.734	-68:48:55.60	-41.43 ± 0.13	-12.51 ± 0.11	10.06 ± 0.09	...	LCC(92);EPSC(8)	-,-
J1233-5923	(M5)	LCC	12:33:28.963	-59:23:46.98	-37.05 ± 0.19	-8.40 ± 0.18	10.09 ± 0.15	13.9 ± 0.9	...	-,5
J1233-5634	(M5)	LCC	12:33:59.438	-56:34:48.22	-33.41 ± 0.22	-13.02 ± 0.20	10.18 ± 0.16	-,-
J1234-5827	(M8)	LCC	12:34:05.830	-58:27:49.69	-38.65 ± 0.55	-14.53 ± 0.49	10.26 ± 0.45	-,-
J1235-7043	(M5)	LCC	12:35:15.245	-70:43:08.00	-43.72 ± 0.11	-12.64 ± 0.09	10.71 ± 0.07	...	LCC(89);EPSC(11)	-,-
J1235-6818	(M4)	LCC	12:35:57.055	-68:18:01.19	-36.96 ± 0.30	-8.18 ± 0.24	10.25 ± 0.18	-,-
J1236-5301	(M3)	LCC	12:36:13.567	-53:01:33.07	-38.40 ± 0.08	-15.80 ± 0.06	10.12 ± 0.07	-,-
J1236-5638	(M5)	LCC	12:36:31.704	-56:38:15.36	-37.84 ± 0.13	-12.10 ± 0.12	10.15 ± 0.11	-,-
J1236-6310	(M5)	LCC	12:36:43.752	-63:10:57.06	-37.92 ± 0.25	-9.88 ± 0.15	10.20 ± 0.12	-,-
J1238-5559	(M4)	LCC	12:38:04.265	-55:59:48.26	-37.05 ± 0.10	-23.27 ± 0.09	10.08 ± 0.09	-,-
J1238-5530	(M3)	LCC	12:38:32.971	-55:30:34.32	-40.19 ± 0.06	-14.40 ± 0.05	10.56 ± 0.06	-,-
J1239-5337	M2.5	LCC	12:39:20.998	-53:37:57.40	-45.00 ± 0.09	-14.92 ± 0.06	12.20 ± 0.08	8 ± 3	...	21,5
J1239-5539	F5V	LCC	12:39:21.154	-55:39:14.82	-40.26 ± 0.20	-16.58 ± 0.21	10.26 ± 0.19	12 ± 1	...	55,4
J1241-5720	(M2)	LCC	12:41:22.584	-57:20:45.59	-40.44 ± 0.05	-15.92 ± 0.04	10.18 ± 0.04	-,-
J1241-5834	(M5)	LCC	12:41:28.354	-58:34:15.78	-43.95 ± 0.16	-17.40 ± 0.14	10.34 ± 0.12	-,-
J1241-4641	(M5)	LCC	12:41:29.501	-46:41:14.56	-38.13 ± 0.19	-16.00 ± 0.25	10.41 ± 0.20	...	LCC(74);TWA(21);UCL(5)	-,-
J1241-4641	(M3)	LCC	12:41:31.250	-46:41:04.55	-38.93 ± 0.12	-16.86 ± 0.16	10.01 ± 0.09	...	LCC(79);TWA(16)	-,-
J1242-6943	(M4)	LCC	12:42:13.042	-69:43:48.63	-39.50 ± 0.14	-12.77 ± 0.10	10.06 ± 0.08	...	LCC(85);EPSC(15)	-,-
J1242-7034	(M5)	LCC	12:42:55.714	-70:34:20.97	-40.46 ± 0.12	-13.20 ± 0.12	10.06 ± 0.08	...	LCC(64);EPSC(36)	-,-
J1245-6232	(M4)	LCC	12:45:09.545	-62:32:35.42	-39.89 ± 0.07	-13.51 ± 0.07	10.16 ± 0.05	-,-
J1245-6232	(M2)	LCC	12:45:10.092	-62:32:36.63	-41.67 ± 0.29	-16.19 ± 0.26	10.05 ± 0.21	-,-
J1247-5946	(M5)	LCC	12:47:08.818	-59:46:09.14	-40.97 ± 0.08	-16.45 ± 0.08	10.54 ± 0.06	-,-
J1247-7031	(M2)	LCC	12:47:35.998	-70:31:14.02	-40.25 ± 0.05	-14.24 ± 0.05	10.01 ± 0.03	...	LCC(86);EPSC(14)	-,-
J1248-6828	(M3)	LCC	12:48:31.802	-68:28:54.11	-41.16 ± 0.07	-14.97 ± 0.07	10.54 ± 0.05	-,-
J1248-5747	(M5)	LCC	12:48:46.661	-57:47:37.28	-38.36 ± 0.14	-13.51 ± 0.13	10.27 ± 0.12	-,-

Table 3 continued

Table 3 (*continued*)

Name	Spectral	Assoc.	R.A. ^b	Decl. ^b	$\mu_\alpha \cos \delta$	μ_δ	Parallax	Rad. Vel.	Ambiguous	Ref. ^d
	Type ^a		(hh:mm:ss.sss)	(dd:mm:ss.ss)	(mas yr ⁻¹)	(mas yr ⁻¹)	(mas)	(km s ⁻¹)	Assoc. ^c	
J1248-6446	(M3)	LCC	12:48:47.863	-64:46:11.92	-40.45 ± 0.07	-15.82 ± 0.06	10.23 ± 0.05	-,-
J1248-6446	(M3)	LCC	12:48:52.721	-64:46:10.96	-40.52 ± 0.08	-15.45 ± 0.07	10.32 ± 0.06	-,-
J1248-5949	(M1)	LCC	12:48:54.869	-59:49:47.90	-41.58 ± 0.04	-17.15 ± 0.04	10.63 ± 0.03	11 ± 6	...	-,4
J1249-6152	(M8)	LCC	12:49:14.237	-61:52:27.69	-43.3 ± 1.1	-10.7 ± 1.0	11.11 ± 0.66	-,-
J1249-4758	(M3)	LCC	12:49:46.409	-47:58:32.31	-38.78 ± 0.11	-17.57 ± 0.08	10.05 ± 0.08	...	LCC(88);TWA(8)	-,-
J1250-6044	(K7)	LCC	12:50:47.652	-60:44:05.90	-31.68 ± 0.17	-14.62 ± 0.26	10.46 ± 0.13	-,-
J1250-5717	(M7)	LCC	12:50:52.231	-57:17:05.07	-36.78 ± 0.53	-13.03 ± 0.42	10.07 ± 0.44	-,-
J1252-6159	(M5)	LCC	12:52:14.496	-61:59:16.35	-41.02 ± 0.18	-16.42 ± 0.16	10.26 ± 0.13	-,-
J1253-6014	(M2)	LCC	12:53:17.894	-60:14:00.01	-32.96 ± 0.77	-15.90 ± 0.75	11.23 ± 0.71	-,-
J1254-5818	(M5)	LCC	12:54:39.230	-58:18:17.58	-40.68 ± 0.14	-17.93 ± 0.15	10.36 ± 0.13	-,-
J1255-6356	(M4)	LCC	12:55:07.632	-63:56:37.05	-39.28 ± 0.08	-16.56 ± 0.08	10.14 ± 0.05	-,-
J1255-7417	(M3)	LCC	12:55:55.070	-74:17:20.57	-40.45 ± 0.47	-6.31 ± 0.14	10.53 ± 0.11	-,-
J1257-6651	(M1)	LCC	12:57:41.767	-66:51:36.98	-37.55 ± 0.47	-13.57 ± 0.43	10.19 ± 0.29	-,-
J1258-6906	(M4)	LCC	12:58:17.436	-69:06:21.91	-41.91 ± 0.11	-16.79 ± 0.11	10.61 ± 0.08	-,-
J1300-6926	(M3)	LCC	13:00:04.452	-69:26:20.27	-47.42 ± 0.06	-20.22 ± 0.06	12.01 ± 0.04	-,-
J1304-5950	(M4)	LCC	13:04:38.520	-59:50:58.25	-45.57 ± 0.95	-16.95 ± 0.35	11.33 ± 0.40	-,-
J1305-4811	(M3)	LCC	13:05:20.875	-48:11:11.61	-34.5 ± 1.2	-25.9 ± 1.1	11.4 ± 1.0	...	LCC(87);UCL(9)	-,-
J1306-4815	(M9)	LCC	13:06:03.756	-48:15:33.15	-34.4 ± 2.9	-20.8 ± 1.2	11.5 ± 1.1	...	LCC(77);TWA(13);UCL(10)	-,-
J1307-6844	(M2)	LCC	13:07:17.534	-68:44:10.78	-39.38 ± 0.06	-17.51 ± 0.05	10.15 ± 0.04	-,-
J1308-6844	(M0)	LCC	13:08:30.610	-68:44:49.02	-39.18 ± 0.05	-17.72 ± 0.04	10.21 ± 0.03	-,-
J1308-5053	(M2)	LCC	13:08:32.542	-50:53:31.66	-40.24 ± 0.08	-20.10 ± 0.06	10.86 ± 0.04	14 ± 3	...	-,4
J1309-5720	(K8)	LCC	13:09:02.102	-57:20:01.26	-41.58 ± 0.03	-17.51 ± 0.04	10.48 ± 0.03	12 ± 1	...	-,4
J1310-5945	(M4)	LCC	13:10:53.328	-59:45:28.80	-46.27 ± 0.06	-22.90 ± 0.07	11.99 ± 0.06	-,-
J1311-4924	(M4)	LCC	13:11:38.990	-49:24:38.38	-37.56 ± 0.11	-20.52 ± 0.09	10.11 ± 0.07	...	LCC(93);UCL(5)	-,-
J1311-6700	(M5)	LCC	13:11:53.777	-67:00:33.70	-41.42 ± 0.21	-20.30 ± 0.22	10.16 ± 0.17	-,-
J1312-5440	(M3)	LCC	13:12:18.518	-54:40:32.59	-34.93 ± 0.52	-18.08 ± 0.37	10.56 ± 0.29	-,-
J1312-5447	(M8)	LCC	13:12:34.668	-54:47:26.97	-37.2 ± 1.7	-22.0 ± 1.2	10.0 ± 1.1	-,-
J1313-5314	(M4)	LCC	13:13:31.219	-53:14:51.96	-42.30 ± 0.17	-20.09 ± 0.21	11.66 ± 0.11	...	LCC(93);UCL(7)	-,-
J1313-5807	(M3)	LCC	13:13:42.490	-58:07:22.17	-50.36 ± 0.24	-27.67 ± 0.28	13.21 ± 0.21	-,-
J1316-6948	(M4)	LCC	13:16:24.982	-69:48:52.18	-40.90 ± 0.29	-18.02 ± 0.28	10.12 ± 0.21	-,-
J1316-4917	(M4)	LCC	13:16:57.646	-49:17:40.95	-38.94 ± 0.13	-21.25 ± 0.12	10.53 ± 0.10	...	LCC(86);UCL(10)	-,-
J1317-6207	(K8)	LCC	13:17:32.834	-62:07:12.08	-38.18 ± 0.04	-19.85 ± 0.05	10.18 ± 0.04	10 ± 2	...	-,4
J1317-5455	(M4)	LCC	13:17:56.083	-54:55:41.54	-43.94 ± 0.11	-21.94 ± 0.11	11.97 ± 0.06	...	LCC(94);UCL(6)	-,-
J1318-5916	(M8)	LCC	13:18:03.612	-59:16:36.76	-34.79 ± 0.73	-19.39 ± 0.79	10.20 ± 0.63	-,-
J1318-5057	(M4)	LCC	13:18:23.052	-50:57:29.74	-38.35 ± 0.10	-22.02 ± 0.09	10.24 ± 0.06	-,-
J1319-6831	M1.5	LCC	13:19:56.765	-68:31:14.31	-39.93 ± 0.14	-18.58 ± 0.12	10.59 ± 0.09	21,-
J1324-7020	(M5)	LCC	13:24:35.059	-70:20:26.45	-38.70 ± 0.13	-20.89 ± 0.11	10.37 ± 0.08	-,-
J1325-5111	(M3)	LCC	13:25:58.044	-51:11:44.87	-39.69 ± 0.62	-20.60 ± 0.52	11.14 ± 0.35	12.4 ± 0.5	LCC(92);UCL(8)	-,5
J1326-4627	(M4)	LCC	13:26:25.010	-46:27:34.65	-35.52 ± 0.15	-22.66 ± 0.19	10.04 ± 0.11	...	LCC(70);UCL(22);TWA(8)	-,-

Table 3 continued

Table 3 (*continued*)

Name	Spectral	Assoc.	R.A. ^b	Decl. ^b	$\mu_\alpha \cos \delta$	μ_δ	Parallax	Rad. Vel.	Ambiguous	Ref. ^d
	Type ^a		(hh:mm:ss.sss)	(dd:mm:ss.ss)	(mas yr ⁻¹)	(mas yr ⁻¹)	(mas)	(km s ⁻¹)	Assoc. ^c	
J1327-4719	(M2)	LCC	13:27:27.598	-47:19:08.04	-39.64 ± 0.12	-25.62 ± 0.11	11.03 ± 0.08	...	LCC(49);TWA(33);UCL(18)	,,-
J1327-4902	(M2)	LCC	13:27:32.674	-49:02:22.33	-37.79 ± 0.09	-23.17 ± 0.13	10.30 ± 0.06	...	LCC(83);UCL(14)	,,-
J1331-6047	(M5)	LCC	13:31:06.202	-60:47:57.39	-39.32 ± 0.09	-18.92 ± 0.12	10.75 ± 0.09	,,-
J1331-4706	(M4)	LCC	13:31:57.691	-47:06:14.68	-37.65 ± 0.19	-26.45 ± 0.20	10.30 ± 0.14	...	LCC(74);UCL(20);TWA(7)	,,-
J1332-7147	(M5)	LCC	13:32:11.585	-71:47:38.60	-36.41 ± 0.09	-20.90 ± 0.10	10.14 ± 0.06	,,-
J1333-6508	(M3)	LCC	13:33:51.828	-65:08:33.33	-36.98 ± 0.05	-21.88 ± 0.06	10.16 ± 0.04	,,-
J1334-5624	(M3)	LCC	13:34:07.166	-56:24:27.00	-48.04 ± 0.11	-29.69 ± 0.19	12.51 ± 0.08	...	LCC(90);UCL(10)	,,-
J1334-5624	(M2)	LCC	13:34:07.277	-56:24:26.31	-47.50 ± 0.49	-30.08 ± 0.62	12.48 ± 0.35	...	LCC(91);UCL(8)	,,-
J1334-5959	(M4)	LCC	13:34:46.375	-59:59:40.99	-36.51 ± 0.06	-22.10 ± 0.09	10.28 ± 0.07	,,-
J1337-6749	(M3)	LCC	13:37:54.907	-67:49:49.93	-32.86 ± 0.87	-19.61 ± 0.78	10.15 ± 0.66	,,-
J1339-5613	(M8)	LCC	13:39:00.701	-56:13:27.10	-36.5 ± 1.8	-21.2 ± 2.0	10.5 ± 1.1	...	LCC(95);UCL(5)	,,-
J1339-4718	(M3)	LCC	13:39:32.366	-47:18:00.82	-36.08 ± 0.12	-24.28 ± 0.11	10.09 ± 0.09	...	LCC(62);UCL(37)	,,-
J1343-5156	(M4)	LCC	13:43:11.381	-51:56:11.61	-36.81 ± 0.15	-24.91 ± 0.11	10.42 ± 0.07	...	LCC(84);UCL(16)	,,-
J1344-6412	(M4)	LCC	13:44:07.378	-64:12:36.70	-35.24 ± 0.07	-23.82 ± 0.08	10.02 ± 0.06	,,-
J1350-5217	(M5)	LCC	13:50:40.277	-52:17:34.74	-36.06 ± 0.17	-25.75 ± 0.18	10.27 ± 0.09	...	LCC(78);UCL(22)	,,-
J1351-5223	(M3)	LCC	13:51:50.395	-52:23:27.77	-35.98 ± 0.13	-25.95 ± 0.16	10.21 ± 0.08	...	LCC(77);UCL(23)	,,-
J1352-5123	(M5)	LCC	13:52:19.046	-51:23:58.08	-36.94 ± 0.21	-22.58 ± 0.20	10.23 ± 0.13	...	LCC(58);UCL(42)	,,-
J1400-5517	(M2)	LCC	14:00:40.699	-55:17:37.77	-35.30 ± 0.07	-27.74 ± 0.16	10.28 ± 0.06	...	LCC(82);UCL(18)	,,-
J0120-6241	(M5)	OCT	01:20:36.925	-62:41:38.85	33.78 ± 0.14	41.63 ± 0.10	14.48 ± 0.07	,,-
J2119-8237	(M5)	OCT	21:19:46.178	-82:37:26.53	33.89 ± 0.10	-5.84 ± 0.13	10.64 ± 0.06	,,-
J2231-5709	(K6)	OCT	22:31:11.455	-57:09:11.39	35.17 ± 0.05	3.21 ± 0.05	10.06 ± 0.03	,,-
J2335-6441	F2IV/V	OCT	23:35:13.078	-64:41:20.61	33.03 ± 0.05	14.68 ± 0.06	10.91 ± 0.03	55,-
J0241-5725	(M4)	OCT	02:41:18.984	-57:25:17.71	17.92 ± 0.10	30.52 ± 0.13	11.64 ± 0.08	4 ± 2	...	,,5
J0241-5725	M3	OCT	02:41:19.160	-57:25:18.17	14.73 ± 0.07	29.64 ± 0.08	11.36 ± 0.05	4 ± 2	...	21,4
J0327-3756	(M5)	OCT	03:27:37.460	-37:56:41.23	6.93 ± 0.10	30.38 ± 0.12	13.18 ± 0.07	,,-
J0334-4957	(M6)	OCT	03:34:38.936	-49:57:50.35	9.44 ± 0.16	28.57 ± 0.19	10.89 ± 0.09	,,-
J0340-5207	(M4)	OCT	03:40:12.240	-52:07:09.39	0.90 ± 0.07	40.25 ± 0.09	12.90 ± 0.04	,,-
J0025-6237	(M5)	OCT	00:25:05.997	-62:37:06.80	32.27 ± 0.10	18.45 ± 0.09	11.84 ± 0.07	,,-
J0407-5043	(M5)	OCT	04:07:27.941	-50:43:53.52	0.31 ± 0.14	28.39 ± 0.15	10.09 ± 0.07	,,-
J0411-4044	(M5)	OCT	04:11:32.000	-40:44:24.67	-0.77 ± 0.17	24.87 ± 0.18	10.89 ± 0.10	,,-
J0411-4044	(M5)	OCT	04:11:33.165	-40:44:22.58	-0.01 ± 0.10	27.48 ± 0.11	10.69 ± 0.06	,,-
J0414-7025	(M4)	OCT	04:14:01.260	-70:25:23.08	-1.39 ± 0.09	33.90 ± 0.09	10.29 ± 0.04	,,-
J0429-5138	(M4)	OCT	04:29:33.898	-51:38:51.38	-6.58 ± 0.13	37.15 ± 0.14	12.80 ± 0.06	,,-
J0430-3304	(M3)	OCT	04:30:46.345	-33:04:02.96	-4.81 ± 0.12	23.40 ± 0.15	10.71 ± 0.08	,,-
J0430-3605	(M4)	OCT	04:30:46.592	-36:05:14.67	-5.58 ± 0.11	24.44 ± 0.14	11.05 ± 0.07	,,-
J0433-3650	(M4)	OCT	04:33:05.243	-36:50:37.43	-3.99 ± 0.12	23.48 ± 0.14	10.00 ± 0.07	,,-
J0446-3452	(M4)	OCT	04:46:28.855	-34:52:04.29	-8.12 ± 0.09	23.34 ± 0.16	10.48 ± 0.06	,,-
J0501-3550	(M3)	OCT	05:01:13.769	-35:50:44.52	-11.60 ± 0.06	18.85 ± 0.07	10.30 ± 0.04	,,-
J0501-7058	(M5)	OCT	05:01:50.405	-70:58:46.57	-10.12 ± 0.82	33.29 ± 0.92	11.69 ± 0.47	,,-

Table 3 continued

Table 3 (*continued*)

Name	Spectral	Assoc.	R.A. ^b	Decl. ^b	$\mu_\alpha \cos \delta$	μ_δ	Parallax	Rad. Vel.	Ambiguous	Ref. ^d
	Type ^a		(hh:mm:ss.sss)	(dd:mm:ss.ss)	(mas yr ⁻¹)	(mas yr ⁻¹)	(mas)	(km s ⁻¹)	Assoc. ^c	
J0516-3225	(M4)	OCT	05:16:43.922	-32:25:53.33	-13.32 ± 0.08	21.17 ± 0.08	10.44 ± 0.04	-,-
J0516-3226	(M4)	OCT	05:16:44.387	-32:26:03.01	-14.55 ± 0.10	21.62 ± 0.10	10.39 ± 0.06	-,-
J0555-4457	(M8)	OCT	05:55:23.733	-44:57:36.66	-16.4 ± 1.4	21.8 ± 1.9	11.40 ± 0.79	-,-
J0422+1629	(M8)	TAU	04:22:48.299	+16:29:21.63	6.6 ± 3.2	-14.7 ± 2.7	11.0 ± 1.9	-,-
J0426+2531	(M8)	TAU	04:26:37.031	+25:31:28.65	0.9 ± 2.1	-20.5 ± 1.5	10.8 ± 1.1	-,-
J0436+1310	(M8)	TAU	04:36:20.896	+13:10:58.02	14.8 ± 2.9	-13.4 ± 1.7	10.5 ± 1.9	-,-
J0453+2237	(M9)	TAU	04:53:59.226	+22:37:53.79	1.7 ± 3.3	-19.1 ± 1.4	10.8 ± 1.3	-,-
J0459+2628	(M8)	TAU	04:59:32.852	+26:28:03.85	-1.9 ± 3.8	-18.8 ± 2.1	10.9 ± 2.1	-,-
J1339-3306	(M5)	UCL	13:39:48.245	-33:06:20.33	-36.09 ± 0.19	-27.32 ± 0.19	10.12 ± 0.11	-,-
J1351-3742	(K9)	UCL	13:51:45.622	-37:42:00.88	-37.53 ± 0.08	-27.10 ± 0.10	10.51 ± 0.05	3 ± 2	...	-,25
J1354-4204	(M4)	UCL	13:54:03.886	-42:04:35.73	-25.02 ± 0.25	-20.21 ± 0.25	10.39 ± 0.22	-,-
J1355-4307	(M8)	UCL	13:55:51.986	-43:07:02.50	-27.9 ± 1.3	-19.3 ± 1.6	10.4 ± 1.6	...	UCL(93);LCC(7)	-,-
J1357-3759	(M3)	UCL	13:57:58.070	-37:59:34.80	-42.28 ± 0.11	-31.28 ± 0.10	12.45 ± 0.07	-,-
J1358-3315	(M4)	UCL	13:58:50.256	-33:15:21.06	-39.90 ± 0.13	-30.35 ± 0.12	11.30 ± 0.07	-,-
J1414-3805	(M4)	UCL	14:14:14.753	-38:05:27.62	-34.62 ± 0.21	-27.51 ± 0.22	10.39 ± 0.14	-,-
J1415-3548	(M8)	UCL	14:15:18.307	-35:48:18.91	-28.4 ± 1.5	-29.2 ± 1.5	10.7 ± 1.2	-,-
J1416-4030	(M3)	UCL	14:16:03.060	-40:30:34.66	-33.26 ± 0.53	-27.22 ± 0.42	10.86 ± 0.31	-,-
J1417-4018	(M5)	UCL	14:17:32.616	-40:18:56.30	-34.38 ± 0.18	-29.36 ± 0.16	10.14 ± 0.08	-,-
J1421-4904	(M3)	UCL	14:21:51.106	-49:04:38.89	-34.27 ± 0.16	-28.27 ± 0.14	10.02 ± 0.08	...	UCL(95);LCC(5)	-,-
J1432-4016	(M4)	UCL	14:32:22.615	-40:16:27.47	-37.73 ± 0.16	-33.23 ± 0.16	12.35 ± 0.32	-,-
J1435-3422	(M1)	UCL	14:35:17.786	-34:22:50.73	-36.46 ± 0.11	-36.24 ± 0.13	11.89 ± 0.05	3 ± 1	...	-,4
J1437-3409	(M2)	UCL	14:37:13.188	-34:09:21.38	-30.55 ± 0.13	-31.61 ± 0.09	10.07 ± 0.06	-,-
J1439-3527	(M4)	UCL	14:39:15.214	-35:27:12.14	-34.46 ± 0.18	-33.58 ± 0.15	10.82 ± 0.09	-,-
J1440-4838	(M5)	UCL	14:40:44.650	-48:38:25.39	-37.75 ± 0.28	-36.26 ± 0.23	11.10 ± 0.14	-,-
J1441-3329	(M5)	UCL	14:41:13.860	-33:29:56.91	-35.74 ± 0.23	-36.10 ± 0.17	11.85 ± 0.11	-,-
J1446-5055	K6Ve	UCL	14:46:20.134	-50:55:45.43	-32.50 ± 0.69	-36.45 ± 0.50	10.77 ± 0.24	7 ± 1	...	58,4
J1446-4540	(M4)	UCL	14:46:24.298	-45:40:07.27	-43.00 ± 0.19	-41.52 ± 0.20	12.59 ± 0.10	-,-
J1447-5042	(M5)	UCL	14:47:23.122	-50:42:43.68	-39.76 ± 0.21	-38.08 ± 0.17	11.97 ± 0.10	-,-
J1448-3224	(M4)	UCL	14:48:58.754	-32:24:08.93	-34.43 ± 0.18	-32.00 ± 0.15	10.13 ± 0.10	-,-
J1449-3810	(M3)	UCL	14:49:19.442	-38:10:18.84	-28.91 ± 0.15	-30.29 ± 0.13	10.12 ± 0.14	-,-
J1453-4619	(M8)	UCL	14:53:03.715	-46:19:43.60	-29.7 ± 2.0	-22.0 ± 1.2	10.07 ± 0.81	-,-
J1453-3354	(M4)	UCL	14:53:57.329	-33:54:35.43	-32.91 ± 0.14	-30.83 ± 0.11	10.15 ± 0.07	-,-
J1454-3833	(M5)	UCL	14:54:11.326	-38:33:14.37	-35.0 ± 1.1	-39.73 ± 0.82	14.18 ± 0.61	-,-
J1458-5816	(M2)	UCL	14:58:47.496	-58:16:23.30	-35.94 ± 0.08	-32.87 ± 0.08	10.81 ± 0.04	...	UCL(93);LCC(7)	-,-
J1458-2631	(M6)	UCL	14:58:51.437	-26:31:45.07	-29.29 ± 0.71	-27.95 ± 0.51	10.15 ± 0.42	-,-
J1506-3725	(M6)	UCL	15:06:17.136	-37:25:36.18	-31.74 ± 0.46	-34.82 ± 0.41	10.50 ± 0.30	-,-
J1508-3627	(M4)	UCL	15:08:11.282	-36:27:19.04	-33.37 ± 0.20	-33.84 ± 0.15	10.19 ± 0.15	-,-
J1509-4047	(M4)	UCL	15:09:23.335	-40:47:05.53	-33.64 ± 0.13	-39.12 ± 0.11	11.02 ± 0.08	-,-
J1510-3902	(M5)	UCL	15:10:53.050	-39:02:59.77	-24.4 ± 1.1	-29.88 ± 0.75	11.55 ± 0.64	-,-

Table 3 continued

Table 3 (*continued*)

Name	Spectral	Assoc.	R.A. ^b	Decl. ^b	$\mu_\alpha \cos \delta$	μ_δ	Parallax	Rad. Vel.	Ambiguous	Ref. ^d
	Type ^a		(hh:mm:ss.sss)	(dd:mm:ss.ss)	(mas yr ⁻¹)	(mas yr ⁻¹)	(mas)	(km s ⁻¹)	Assoc. ^c	
J1515-2527	(M4)	UCL	15:15:34.747	-25:27:02.01	-26.85 ± 0.17	-32.39 ± 0.12	10.30 ± 0.09	...	UCL(92);USCO(8)	-,-
J1517-3334	(M3)	UCL	15:17:58.258	-33:34:43.19	-32.85 ± 0.28	-41.40 ± 0.21	12.43 ± 0.21	-,-
J1524-3309	(M8)	UCL	15:24:53.938	-33:09:33.04	-33.0 ± 1.2	-37.74 ± 0.87	10.20 ± 0.97	-,-
J1525-4121	(M4)	UCL	15:25:05.988	-41:21:08.06	-31.21 ± 0.16	-38.86 ± 0.12	11.34 ± 0.08	-,-
J1530-3317	(M5)	UCL	15:30:05.638	-33:17:37.32	-27.83 ± 0.33	-35.90 ± 0.24	11.73 ± 0.20	-,-
J1531-3504	(M3)	UCL	15:31:09.569	-35:04:57.75	-21.00 ± 0.57	-27.72 ± 0.43	10.16 ± 0.40	-,-
J1531-4711	M4	UCL	15:31:24.898	-47:11:11.32	-30.88 ± 0.83	-34.36 ± 0.50	10.21 ± 0.40	21,-
J1531-4711	M4	UCL	15:31:24.902	-47:11:12.15	-24.29 ± 0.26	-33.96 ± 0.13	10.09 ± 0.10	21,-
J1531-3517	(M4)	UCL	15:31:59.688	-35:17:55.80	-25.55 ± 0.20	-34.18 ± 0.14	10.08 ± 0.16	-,-
J1533-4018	(M4)	UCL	15:33:46.056	-40:18:02.93	-27.92 ± 0.17	-37.65 ± 0.11	10.49 ± 0.09	-,-
J1537-3322	M5.5	UCL	15:37:01.063	-33:22:56.02	-25.57 ± 0.68	-31.11 ± 0.46	10.75 ± 0.40	59,-
J1537-5322	K7	UCL	15:37:17.570	-53:22:28.16	-30.16 ± 0.07	-39.38 ± 0.07	10.69 ± 0.04	3.5 ± 0.7	...	21,4
J1538-4953	(M5)	UCL	15:38:42.487	-49:53:04.23	-35.02 ± 0.74	-43.17 ± 0.47	11.68 ± 0.29	-,-
J1541-3051	(M6)	UCL	15:41:06.110	-30:51:49.60	-23.79 ± 0.88	-35.97 ± 0.60	11.97 ± 0.83	...	UCL(88);USCO(12)	-,-
J1541-3003	(M5)	UCL	15:41:20.748	-30:03:13.56	-24.21 ± 0.32	-33.06 ± 0.25	10.28 ± 0.24	...	UCL(85);USCO(15)	-,-
J1542-4319	(M8)	UCL	15:42:07.946	-43:19:08.68	-22.5 ± 1.9	-35.2 ± 1.4	10.57 ± 0.85	-,-
J1545-5250	(M3)	UCL	15:45:10.442	-52:50:42.17	-27.86 ± 0.10	-36.99 ± 0.10	10.06 ± 0.05	-,-
J1555-3708	(M4)	UCL	15:55:12.022	-37:08:11.60	-28.69 ± 0.14	-41.63 ± 0.09	11.10 ± 0.07	-,-
J1555-3634	(M2)	UCL	15:55:47.614	-36:34:00.76	-27.03 ± 0.11	-39.43 ± 0.07	10.67 ± 0.05	-,-
J1556-3643	K6	UCL	15:56:02.470	-36:43:47.85	-26.77 ± 0.09	-40.46 ± 0.05	10.58 ± 0.04	60,-
J1556-3643	(M3)	UCL	15:56:03.389	-36:43:55.92	-27.09 ± 0.24	-37.95 ± 0.14	10.71 ± 0.11	-,-
J1557-4744	(M5)	UCL	15:57:04.973	-47:44:21.76	-30.13 ± 0.24	-44.27 ± 0.15	11.86 ± 0.10	-,-
J1557-4009	(M4)	UCL	15:57:48.439	-40:09:07.21	-26.09 ± 0.19	-38.21 ± 0.11	10.23 ± 0.08	-,-
J1558-5029	(M2)	UCL	15:58:19.682	-50:29:10.69	-29.57 ± 0.15	-43.71 ± 0.11	11.38 ± 0.06	-,-
J1559-5147	(M3)	UCL	15:59:14.042	-51:47:23.87	-26.80 ± 0.09	-40.91 ± 0.06	10.52 ± 0.04	-,-
J1602-3537	(M5)	UCL	16:02:54.941	-35:37:25.38	-25.95 ± 0.32	-39.32 ± 0.18	10.79 ± 0.17	-,-
J1604-5259	(M2)	UCL	16:04:26.844	-52:59:32.67	-31.08 ± 0.07	-43.91 ± 0.05	11.78 ± 0.04	3 ± 3	...	-,4
J1607-3554	(M5)	UCL	16:07:59.443	-35:54:18.72	-21.04 ± 0.66	-34.34 ± 0.29	10.16 ± 0.23	-,-
J1615-2854	(M5)	UCL	16:15:02.050	-28:54:02.71	-24.10 ± 0.22	-38.76 ± 0.15	10.59 ± 0.11	-,-
J1618-3839	(M4)	UCL	16:18:37.718	-38:39:10.97	-26.66 ± 0.19	-33.43 ± 0.13	10.35 ± 0.11	-2 ± 1	...	-,5
J1620-4641	(M2)	UCL	16:20:31.229	-46:41:57.31	-23.92 ± 0.12	-43.29 ± 0.08	10.53 ± 0.06	-,-
J1623-3902	(M3)	UCL	16:23:46.723	-39:02:01.68	-20.95 ± 0.23	-38.77 ± 0.17	10.17 ± 0.12	-,-
J1633-4122	(M6)	UCL	16:33:59.765	-41:22:10.19	-21.76 ± 0.90	-33.86 ± 0.93	10.14 ± 0.36	-,-
J1634-3201	(M5)	UCL	16:34:23.268	-32:01:07.64	-20.75 ± 0.45	-34.22 ± 0.26	10.03 ± 0.20	-,-
J1642-3257	(M5)	UCL	16:42:06.595	-32:57:31.47	-18.47 ± 0.36	-39.92 ± 0.19	11.42 ± 0.17	-,-
J1651-3843	(M4)	UCL	16:51:58.454	-38:43:30.29	-19.96 ± 0.21	-46.00 ± 0.13	11.33 ± 0.11	-,-
J1556-2028	(M8)	USCO	15:56:47.354	-20:28:07.90	-9.5 ± 1.3	-22.54 ± 0.87	10.1 ± 1.6	-,-
J1557-2024	(M4)	USCO	15:57:00.905	-20:24:48.63	-18.5 ± 1.0	-24.20 ± 0.65	10.59 ± 0.67	-3 ± 7	...	-,5
J1603-1340	(M7)	USCO	16:03:35.196	-13:40:45.79	-10.2 ± 1.3	-26.96 ± 0.76	11.36 ± 0.75	-,-

Table 3 continued

Table 3 (*continued*)

Name	Spectral Type ^a	Assoc.	R.A. ^b (hh:mm:ss.sss)	Decl. ^b (dd:mm:ss.ss)	$\mu_\alpha \cos \delta$ (mas yr ⁻¹)	μ_δ (mas yr ⁻¹)	Parallax (mas)	Rad. Vel. (km s ⁻¹)	Ambiguous Assoc. ^c	Ref. ^d
J1608-2406	(M5)	USCO	16:08:19.075	-24:06:26.86	-13.41 ± 0.80	-21.50 ± 0.41	10.23 ± 0.40	-, -
J1609-2539	(M5)	USCO	16:09:26.938	-25:39:08.55	-15.23 ± 0.72	-23.42 ± 0.41	10.38 ± 0.33	-, -
J1617-2123	(M7)	USCO	16:17:53.222	-21:23:56.21	-4.60 ± 0.67	-23.85 ± 0.51	10.03 ± 0.36	-, -

^a Spectral types between parentheses were estimated from the absolute *Gaia G*-band magnitude.

^b J2000 position at epoch 2015 from the *Gaia* DR2 catalog.

^c List of associations in ambiguous cases with their relative probabilities (%) between parentheses.

References—(1) West et al. 2011; (2) Bardalez Gagliuffi et al. 2014; (3) Cruz & Reid 2002; (4) Lindegren et al. 2018; (5) Co-moving star; (6) Gray et al. 2006; (7) Phan Bao et al. 2008; (8) Alonso-Floriano et al. 2015; (9) Stephenson 1986; (10) Reid et al. 1995; (11) Abt & Cardona 1984; (12) Wilson 1953; (13) Abt & Morrell 1995; (14) Newton et al. 2014; (15) Scholz et al. 2005; (16) Malo et al. 2014a; (17) Wright et al. 2003; (18) Reid et al. 2004; (19) Jeffries 1995; (20) Houk 1982; (21) Riaz et al. 2006; (22) Herbig et al. 1986; (23) Houk & Smith-Moore 1988; (24) Reid et al. 2007; (25) Kunder et al. 2017; (26) Desidera et al. 2015; (27) Gray et al. 2003; (28) Fleming et al. 1988; (29) Schlieder et al. 2012; (30) Gaidos et al. 2014; (31) Lépine et al. 2013; (32) Kirkpatrick et al. 2008; (33) Koen et al. 2010; (34) van Belle & von Braun 2009; (35) Faherty et al. 2009; (36) Cook et al. 2016; (37) Kirkpatrick et al. 1991; (38) Evans et al. 1964; (39) Duflot et al. 1995; (40) Allen et al. 2007; (41) Dieterich et al. 2014; (42) Law et al. 2008; (43) Deshpande et al. 2013; (44) Bowler et al. 2015; (45) Shkolnik et al. 2012; (46) Pesch 1968; (47) Guieu et al. 2006; (48) Luhman 2006; (49) Jones & West 2016; (50) Rodriguez et al. 2013; (51) Royer et al. 2007; (52) Evans 1967; (53) Gontcharov 2006; (54) Cruz et al. 2003; (55) Houk & Cowley 1975; (56) Upgren 1962; (57) Gagné et al. 2015b; (58) Torres et al. 2006; (59) Comerón et al. 2013; (60) Krautter et al. 1997.

Table 4. Co-moving systems identified in this work.

<i>Gaia</i> DR2	Assoc.	Separation	R.A. ^a	Decl. ^a	$\mu_\alpha \cos \delta$	μ_δ	Parallax	Rad. Vel.
Source ID		($''$)	(hh:mm:ss.sss)	(dd:mm:ss.ss)	(mas yr $^{-1}$)	(mas yr $^{-1}$)	(mas)	(km s $^{-1}$)
5000558409016727296	THA	...	00:39:35.477	-38:17:18.69	101.47 \pm 0.10	-66.50 \pm 0.07	24.92 \pm 0.06	(2.7 \pm 0.7)
5000558443376465408	...	19.9	00:39:35.930	-38:16:59.55	99.45 \pm 0.08	-64.46 \pm 0.07	24.85 \pm 0.04	1.7 \pm 4.0
2371914419569514752	ABDMG	...	01:06:25.510	-14:17:28.82	101.82 \pm 0.11	-98.76 \pm 0.08	22.02 \pm 0.05	(9.5 \pm 1.8)
2371914419569515136	...	22.6	01:06:26.260	-14:17:48.57	99.93 \pm 0.08	-94.63 \pm 0.06	22.01 \pm 0.04	8.0 \pm 0.3
292521529517547776	ABDMG	...	01:39:58.869	+26:11:00.80	138.98 \pm 0.26	-146.21 \pm 0.12	31.02 \pm 0.08	(-4.0 \pm 1.4)
292521529517332224	...	8.0	01:39:59.341	+26:11:05.74	135.06 \pm 0.18	-151.91 \pm 0.09	30.85 \pm 0.05	-8.9 \pm 10.1
4941694920153720448	ABDMG	...	01:48:47.900	-48:31:16.38	110.54 \pm 0.06	-53.67 \pm 0.06	25.62 \pm 0.04	(21.7 \pm 1.2)
4941706636824503680	...	72.0	01:48:41.060	-48:30:52.75	110.90 \pm 0.04	-53.97 \pm 0.04	25.54 \pm 0.02	20.9 \pm 1.3
93806419367308544	ABDMG	...	01:53:31.897	+19:17:36.37	78.11 \pm 0.72	-97.50 \pm 0.62	19.98 \pm 0.35	(-0.2 \pm 1.2)
93806419367307904	ABDMG	7.4	01:53:31.904	+19:17:43.77	77.85 \pm 0.91	-106.97 \pm 0.73	18.88 \pm 0.42	(2.3 \pm 1.2)
4738546128147329536	OCT	...	02:41:18.984	-57:25:17.71	17.92 \pm 0.10	30.52 \pm 0.13	11.64 \pm 0.08	(8.4 \pm 0.8)
4738546128148599296	OCT	1.5	02:41:19.160	-57:25:18.17	14.73 \pm 0.07	29.64 \pm 0.08	11.36 \pm 0.05	4.4 \pm 1.8
22338438439701760	BPMG	...	02:44:22.804	+10:57:34.20	73.85 \pm 0.18	-58.41 \pm 0.15	21.32 \pm 0.09	(12.4 \pm 1.2)
22338644598132096	...	20.9	02:44:21.444	+10:57:40.21	67.39 \pm 0.28	-56.04 \pm 0.24	20.51 \pm 0.14	4.4 \pm 1.8
108421402801188864	HYA	...	02:58:06.445	+20:40:01.34	238.12 \pm 0.22	-24.48 \pm 0.24	30.59 \pm 0.10	(28.8 \pm 1.7)
108421608959951488	...	14.7	02:58:05.480	+20:40:06.95	233.96 \pm 0.15	-31.29 \pm 0.13	30.62 \pm 0.09	28.1 \pm 0.4
5071668498910478336	COL	...	03:07:49.175	-27:50:46.99	67.62 \pm 0.09	-16.97 \pm 0.10	16.77 \pm 0.07	(16.5 \pm 0.7)
5071668533270215040	...	59.3	03:07:50.927	-27:49:52.43	65.22 \pm 0.13	-18.38 \pm 0.16	18.44 \pm 0.12	...
4833875985299919360	THA	...	03:29:03.801	-48:03:36.59	93.94 \pm 0.08	-4.36 \pm 0.11	23.97 \pm 0.05	(14.4 \pm 0.6)
4833875985299919232	THA	6.1	03:29:04.353	-48:03:33.98	90.93 \pm 0.08	-3.26 \pm 0.10	23.94 \pm 0.04	(14.3 \pm 0.6)
5087228577012243200	COL	...	03:41:15.632	-22:53:08.07	51.45 \pm 0.05	-15.23 \pm 0.05	13.89 \pm 0.04	17.6 \pm 1.6
5087979238513395072	...	25.0	03:41:16.186	-22:52:44.23	49.73 \pm 0.06	-16.44 \pm 0.06	13.92 \pm 0.04	17.1 \pm 4.3
71504509626338048	ABDMG	...	03:45:52.818	+27:33:24.60	41.76 \pm 0.42	-116.99 \pm 0.26	17.86 \pm 0.31	(4.9 \pm 1.4)
71505918375609728	...	69.5	03:45:58.005	+27:33:33.48	41.37 \pm 0.11	-117.99 \pm 0.07	17.65 \pm 0.08	-41.6 \pm 3.3
4673548429552928384	ABDMG	...	03:46:25.083	-62:46:23.25	53.74 \pm 0.08	18.48 \pm 0.08	18.17 \pm 0.04	(27.7 \pm 1.0)
4673547673638684416	ABDMG	31.9	03:46:29.412	-62:46:11.77	53.00 \pm 0.11	17.74 \pm 0.11	18.14 \pm 0.06	(27.7 \pm 1.0)
4856719640741737216	THA	...	03:48:40.509	-37:38:19.98	74.24 \pm 0.04	-4.65 \pm 0.07	18.75 \pm 0.03	(15.5 \pm 0.6)
4856719713756945664	...	86.2	03:48:35.980	-37:37:12.62	80.68 \pm 0.27	-5.01 \pm 0.32	18.98 \pm 0.17	...
3277175602945236608	HYA	...	03:51:34.387	+07:22:22.99	173.38 \pm 0.20	3.32 \pm 0.12	27.64 \pm 0.10	(35.9 \pm 1.7)
3277175602945236352	HYA	4.6	03:51:34.659	+07:22:25.12	172.27 \pm 0.15	3.05 \pm 0.09	27.58 \pm 0.07	(35.8 \pm 1.7)
43615328469218176	HYA	...	03:53:09.084	+17:19:44.05	138.98 \pm 0.22	-30.08 \pm 0.15	23.52 \pm 0.10	(35.5 \pm 2.0)
43615122310787840	...	17.5	03:53:10.202	+17:19:37.05	143.79 \pm 0.14	-29.56 \pm 0.09	23.09 \pm 0.06	...
4841643450834660608	COL	...	04:00:10.071	-42:56:31.16	42.82 \pm 0.06	4.55 \pm 0.08	11.93 \pm 0.04	(20.8 \pm 0.8)
4841643382115183360	COL	41.0	04:00:13.789	-42:56:34.86	43.19 \pm 0.07	5.05 \pm 0.09	12.03 \pm 0.05	(20.9 \pm 0.8)
4889147197876478464	THA	...	04:08:22.360	-27:44:40.35	67.30 \pm 0.38	-18.84 \pm 0.50	18.42 \pm 0.28	(17.1 \pm 0.5)
4889194133279088640	THA	5.8	04:08:22.473	-27:44:34.75	69.01 \pm 0.12	-15.54 \pm 0.16	18.85 \pm 0.09	(16.7 \pm 0.5)
4840770472960569728	OCT	...	04:11:32.000	-40:44:24.67	-0.77 \pm 0.17	24.87 \pm 0.18	10.89 \pm 0.09	(14.3 \pm 0.6)
4840770472961988608	OCT	2.8	04:11:33.165	-40:44:22.58	-0.01 \pm 0.10	27.48 \pm 0.11	10.69 \pm 0.05	(14.1 \pm 0.6)
3310634974432619648	HYA	...	04:19:57.835	+14:02:40.85	116.06 \pm 1.77	-22.86 \pm 1.60	21.39 \pm 0.72	(39.0 \pm 2.0)
3310634944368705664	...	34.4	04:19:57.827	+14:02:06.44	115.39 \pm 0.53	-19.30 \pm 0.31	21.97 \pm 0.18	...
4839371237040134528	ABDMG	...	04:23:57.766	-43:08:59.53	37.11 \pm 0.05	-32.23 \pm 0.08	25.25 \pm 0.04	31.4 \pm 4.2
4839368423837856640	ABDMG	65.7	04:24:01.237	-43:08:05.88	35.90 \pm 0.04	-33.36 \pm 0.06	25.27 \pm 0.03	31.8 \pm 1.0
151170517969728000	TAU	...	04:26:37.031	+25:31:28.65	0.95 \pm 2.07	-20.55 \pm 1.49	10.80 \pm 1.14	(15.3 \pm 2.9)
151170101356829440	...	67.2	04:26:32.858	+25:30:52.21	-3.82 \pm 0.37	-19.99 \pm 0.25	7.29 \pm 0.19	...
501985332196022144	COL	...	04:32:57.100	+74:07:00.30	78.23 \pm 0.06	-134.38 \pm 0.10	29.32 \pm 0.05	(-9.1 \pm 0.5)
501985336493825792	COL	2.9	04:32:57.531	+74:06:58.06	78.38 \pm 0.06	-124.92 \pm 0.09	29.54 \pm 0.04	-7.3 \pm 6.6
3309420014084185600	HYA	...	04:33:52.708	+14:51:02.75	101.79 \pm 0.15	-25.50 \pm 0.10	21.99 \pm 0.10	(40.2 \pm 2.0)
3309419984020071552	...	33.6	04:33:51.028	+14:50:39.56	101.54 \pm 0.80	-24.09 \pm 0.53	22.67 \pm 0.88	...
4891725758804028672	THA	...	04:38:45.731	-27:02:02.17	56.80 \pm 0.07	-11.67 \pm 0.10	18.37 \pm 0.05	(18.4 \pm 0.5)
4891725758804030208	...	23.0	04:38:44.007	-27:02:01.97	56.15 \pm 0.04	-10.87 \pm 0.05	18.35 \pm 0.03	18.2 \pm 0.3

Table 4 continued

Table 4 (continued)

<i>Gaia</i> DR2	Assoc.	Separation	R.A. ^a	Decl. ^a	$\mu_\alpha \cos \delta$	μ_δ	Parallax	Rad. Vel.
Source ID		($''$)	(hh:mm:ss.sss)	(dd:mm:ss.ss)	(mas yr $^{-1}$)	(mas yr $^{-1}$)	(mas)	(km s $^{-1}$)
148184656704340352	HYA	...	04:40:06.893	+25:36:44.67	105.17 \pm 0.09	-62.96 \pm 0.06	23.40 \pm 0.04	(39.2 \pm 1.9)
148183866430358016	...	80.2	04:40:09.341	+25:35:31.66	99.05 \pm 0.09	-61.29 \pm 0.06	22.62 \pm 0.05	35.0 \pm 2.9
2978678571329039488	COL	...	04:40:53.330	-18:42:35.44	37.00 \pm 0.07	-15.20 \pm 0.07	13.30 \pm 0.05	(22.3 \pm 1.0)
2978678635751304192	...	36.1	04:40:50.894	-18:42:25.26	35.80 \pm 0.19	-14.04 \pm 0.18	12.48 \pm 0.13	21.0 \pm 1.1
3292367795624174592	HYA	...	04:41:43.076	+08:26:21.30	106.40 \pm 0.11	-1.83 \pm 0.06	23.53 \pm 0.06	(41.4 \pm 1.8)
3292367795624174720	HYA	4.6	04:41:43.202	+08:26:17.10	101.38 \pm 0.16	-1.05 \pm 0.09	23.66 \pm 0.08	(41.6 \pm 1.8)
4881308710764495744	COL	...	04:46:34.105	-26:27:56.84	33.35 \pm 0.08	-5.46 \pm 0.12	12.11 \pm 0.06	(23.2 \pm 1.0)
4881308710762664576	...	2.3	04:46:34.249	-26:27:55.57	33.53 \pm 0.08	-3.63 \pm 0.11	12.16 \pm 0.06	...
3409855590918086400	HYA	...	04:47:56.721	+19:01:25.54	73.61 \pm 0.08	-30.87 \pm 0.05	18.56 \pm 0.05	45.1 \pm 1.9
3409855590918757760	HYA	3.6	04:47:56.871	+19:01:28.40	80.26 \pm 0.13	-35.00 \pm 0.07	18.27 \pm 0.08	(41.3 \pm 2.0)
4784133288986121728	COL	...	04:49:10.613	-51:17:45.63	27.21 \pm 0.11	14.79 \pm 0.15	10.36 \pm 0.06	(20.6 \pm 0.8)
4784133082827764608	...	14.0	04:49:11.054	-51:17:59.01	27.34 \pm 0.11	14.12 \pm 0.15	10.46 \pm 0.06	...
3405240704393700608	BPMG	...	04:51:07.314	+16:22:48.15	23.36 \pm 0.23	-45.61 \pm 0.10	15.26 \pm 0.11	(17.4 \pm 1.6)
3405240498233928704	...	1.6	04:51:07.398	+16:22:47.09	26.53 \pm 0.18	-45.90 \pm 0.09	15.05 \pm 0.10	...
3405240738753437056	...	32.3	04:51:07.697	+16:23:20.03	26.71 \pm 0.13	-45.96 \pm 0.07	15.44 \pm 0.07	...
2960561231044409856	ABDMG	...	05:03:49.884	-24:23:07.93	25.98 \pm 0.08	-40.17 \pm 0.10	17.04 \pm 0.06	(28.7 \pm 1.1)
2960561059245715968	...	47.7	05:03:53.300	-24:23:17.92	24.96 \pm 0.11	-38.22 \pm 0.14	16.87 \pm 0.08	...
4875262084006357888	COL	...	05:04:18.897	-31:51:21.63	26.97 \pm 0.11	1.01 \pm 0.11	13.57 \pm 0.07	(22.0 \pm 1.1)
4875262084006358016	...	1.9	05:04:18.848	-31:51:19.82	25.16 \pm 0.23	-1.73 \pm 0.24	13.58 \pm 0.13	...
200653214143138816	ABDMG	...	05:04:41.454	+40:24:00.79	15.93 \pm 0.18	-116.73 \pm 0.14	16.42 \pm 0.09	(0.6 \pm 1.3)
200653214147471360	...	2.7	05:04:41.342	+40:23:58.36	15.02 \pm 0.09	-114.78 \pm 0.07	16.35 \pm 0.05	8.2 \pm 6.0
4826952051342945792	COL	...	05:10:26.376	-32:53:06.75	26.26 \pm 0.05	2.00 \pm 0.05	12.31 \pm 0.03	(23.1 \pm 1.1)
4826952051340919936	COL	2.6	05:10:26.439	-32:53:09.20	27.37 \pm 0.08	2.64 \pm 0.09	12.33 \pm 0.05	(23.6 \pm 1.1)
4826580622570992768	OCT	...	05:16:43.922	-32:25:53.33	-13.32 \pm 0.08	21.17 \pm 0.08	10.44 \pm 0.04	(15.0 \pm 0.6)
4826580622571056896	OCT	11.3	05:16:44.387	-32:26:03.01	-14.55 \pm 0.10	21.62 \pm 0.10	10.39 \pm 0.06	(15.3 \pm 0.6)
2905965427842036480	CARN	...	05:20:04.183	-31:09:59.37	65.64 \pm 0.05	88.96 \pm 0.07	29.51 \pm 0.03	(26.4 \pm 1.2)
2905965427842909824	...	6.6	05:20:04.691	-31:10:00.46	59.25 \pm 0.03	95.91 \pm 0.04	29.52 \pm 0.02	40.3 \pm 0.2
3209947476293720448	BPMG	...	05:20:43.632	-05:46:53.18	9.39 \pm 0.08	-37.44 \pm 0.07	23.95 \pm 0.04	(21.3 \pm 1.4)
3209947441933983744	...	51.4	05:20:40.420	-05:47:11.65	9.57 \pm 0.10	-36.92 \pm 0.08	23.88 \pm 0.06	33.2 \pm 0.2
4826381331791369600	COL	...	05:21:55.937	-33:07:12.68	35.05 \pm 0.04	1.94 \pm 0.04	18.60 \pm 0.02	24.8 \pm 2.0
4826381336088651392	COL	4.4	05:21:56.287	-33:07:12.51	33.23 \pm 0.11	5.96 \pm 0.13	18.62 \pm 0.07	(24.1 \pm 1.1)
2906679938602481408	COL	...	05:29:25.326	-28:52:27.39	21.93 \pm 0.06	-0.31 \pm 0.06	12.63 \pm 0.04	(23.7 \pm 1.2)
2906668221931697024	COL	40.6	05:29:28.398	-28:52:32.11	22.32 \pm 0.10	-0.59 \pm 0.11	12.73 \pm 0.06	(23.8 \pm 1.2)
2972006013216383744	ABDMG	...	05:42:30.126	-15:35:02.00	5.28 \pm 0.23	-92.18 \pm 0.27	24.55 \pm 0.09	(27.1 \pm 1.1)
2972006013216383616	ABDMG	1.1	05:42:30.178	-15:35:02.14	8.10 \pm 0.72	-91.83 \pm 0.77	26.98 \pm 0.50	(27.6 \pm 1.1)
3428409475977567616	ABDMG	...	05:45:06.670	+23:50:08.94	3.72 \pm 0.09	-113.34 \pm 0.07	16.81 \pm 0.05	(9.9 \pm 1.4)
3428409475974489088	ABDMG	3.2	05:45:06.899	+23:50:09.73	2.94 \pm 0.10	-111.73 \pm 0.08	16.73 \pm 0.05	(10.0 \pm 1.4)
2970964466468213888	ABDMG	...	05:45:35.068	-16:30:34.23	15.38 \pm 0.14	-59.25 \pm 0.15	17.42 \pm 0.09	(27.2 \pm 1.1)
2970964397748737280	ABDMG	2.6	05:45:35.095	-16:30:36.77	14.07 \pm 0.07	-59.88 \pm 0.08	17.44 \pm 0.05	(27.2 \pm 1.1)
480586331955742464	ABDMG	...	05:45:45.441	+66:38:28.13	20.97 \pm 0.05	-145.30 \pm 0.07	23.85 \pm 0.05	(-13.4 \pm 1.1)
480586263236265600	ABDMG	11.2	05:45:46.897	+66:38:20.99	23.92 \pm 0.05	-148.69 \pm 0.07	23.89 \pm 0.05	(-13.0 \pm 1.1)
2997190533209842560	ABDMG	...	06:02:21.074	-13:55:17.47	-5.70 \pm 0.35	-91.18 \pm 0.34	21.35 \pm 0.18	(26.2 \pm 1.1)
2997190322755484032	...	20.4	06:02:21.892	-13:55:34.03	-6.38 \pm 0.07	-92.85 \pm 0.08	22.15 \pm 0.04	26.0 \pm 0.3
2997190258331936384	ABDMG	108.5	06:02:25.913	-13:56:39.99	-8.15 \pm 0.22	-83.79 \pm 0.23	22.25 \pm 0.11	(27.2 \pm 1.1)
5569783378378984960	CARN	...	06:37:58.429	-40:55:55.94	1.57 \pm 0.11	102.58 \pm 0.10	25.94 \pm 0.06	(25.0 \pm 1.3)
5569783309659510400	...	21.6	06:38:00.311	-40:55:59.49	-0.90 \pm 0.07	100.53 \pm 0.06	25.95 \pm 0.03	...
5584657949640130048	COL	...	07:33:34.188	-40:19:00.19	-10.13 \pm 0.31	10.83 \pm 0.35	13.05 \pm 0.17	(22.0 \pm 0.9)
5584657983995678080	COL	1.7	07:33:34.231	-40:18:58.56	-13.03 \pm 0.14	10.77 \pm 0.15	13.74 \pm 0.08	(22.8 \pm 0.9)
5530787819813761024	ABDMG	...	07:41:49.814	-46:30:17.04	-28.97 \pm 0.09	-5.21 \pm 0.09	15.88 \pm 0.05	(31.1 \pm 0.9)
5530787824113814144	...	1.5	07:41:49.946	-46:30:16.44	-32.00 \pm 0.13	1.79 \pm 0.14	16.17 \pm 0.09	...
5711228333749523712	ABDMG	...	07:57:05.117	-22:26:43.83	-34.95 \pm 0.11	-71.91 \pm 0.18	23.04 \pm 0.10	(27.3 \pm 1.0)
5711228333756189440	...	1.2	07:57:05.041	-22:26:43.34	-28.97 \pm 0.33	-66.45 \pm 0.37	23.21 \pm 0.23	...
5221537843653900288	CAR	...	08:41:59.887	-71:13:16.47	-21.06 \pm 0.10	33.67 \pm 0.10	11.81 \pm 0.06	(20.7 \pm 0.6)

Table 4 continued

Table 4 (*continued*)

<i>Gaia</i> DR2	Assoc.	Separation	R.A. ^a	Decl. ^a	$\mu_\alpha \cos \delta$	μ_δ	Parallax	Rad. Vel.
Source ID		($''$)	(hh:mm:ss.sss)	(dd:mm:ss.ss)	(mas yr $^{-1}$)	(mas yr $^{-1}$)	(mas)	(km s $^{-1}$)
5221537843653900544	CAR	6.5	08:42:00.830	-71:13:21.12	-20.83 ± 0.09	33.53 ± 0.09	11.75 ± 0.05	(20.7 ± 0.6)
5298428169260191104	CAR	...	08:58:07.327	-61:13:21.16	-30.65 ± 0.08	24.87 ± 0.07	14.16 ± 0.04	(20.6 ± 0.6)
5298428169260191232	CAR	7.4	08:58:07.978	-61:13:26.83	-30.28 ± 0.08	25.36 ± 0.08	14.21 ± 0.04	(20.5 ± 0.6)
5310284340601424256	ABDMG	...	09:16:19.306	-54:40:44.64	-57.80 ± 0.10	0.08 ± 0.10	17.09 ± 0.05	(28.1 ± 0.9)
5310284340601424000	...	2.6	09:16:19.323	-54:40:47.28	-60.51 ± 0.08	2.78 ± 0.08	17.14 ± 0.04	...
5217812354662194048	CAR	...	09:23:46.973	-73:40:54.67	-30.92 ± 0.05	35.78 ± 0.06	13.08 ± 0.03	(18.9 ± 0.6)
5217812354662195328	CAR	9.2	09:23:48.161	-73:40:46.90	-32.31 ± 0.08	34.66 ± 0.09	13.15 ± 0.05	(19.1 ± 0.6)
5217846817480160640	CAR	...	09:31:37.363	-73:45:03.85	-32.18 ± 0.13	34.99 ± 0.13	12.68 ± 0.08	(19.0 ± 0.6)
5217846851839896704	...	55.0	09:31:24.756	-73:44:48.83	-34.44 ± 0.06	31.97 ± 0.06	12.79 ± 0.03	22.4 ± 0.8
5217846851839896832	...	53.3	09:31:25.097	-73:44:50.14	-31.59 ± 0.11	34.24 ± 0.11	13.00 ± 0.06	...
5218453026345066368	CAR	...	09:49:00.754	-71:38:02.95	-36.10 ± 0.13	28.56 ± 0.13	12.63 ± 0.07	(18.9 ± 0.6)
5218453026341853952	...	1.5	09:49:00.441	-71:38:03.16	-39.14 ± 0.10	23.58 ± 0.12	12.81 ± 0.05	...
5230321567172871040	CAR	...	10:05:22.723	-71:36:58.56	-35.55 ± 0.10	21.21 ± 0.10	11.48 ± 0.06	(19.0 ± 0.6)
5230321361014440704	CAR	32.0	10:05:25.358	-71:37:28.01	-36.43 ± 0.17	22.76 ± 0.16	11.30 ± 0.09	(19.4 ± 0.6)
5251591482193147776	LCC	...	10:19:03.079	-64:40:51.87	-34.31 ± 0.09	12.02 ± 0.08	11.48 ± 0.04	(17.7 ± 3.3)
5251591477884660352	...	21.9	10:19:04.701	-64:40:32.59	-37.19 ± 0.08	14.35 ± 0.07	11.46 ± 0.05	...
5251591482193162112	...	21.4	10:19:04.993	-64:40:34.34	-33.54 ± 0.09	12.28 ± 0.08	11.40 ± 0.06	...
3778570737913769216	CARN	...	10:20:48.641	-06:33:19.98	-183.10 ± 0.46	-26.43 ± 0.70	33.19 ± 0.96	(16.7 ± 1.0)
3778569191725543296	CARN	87.3	10:20:50.911	-06:34:40.49	-182.39 ± 0.15	-25.19 ± 0.13	31.56 ± 0.11	(17.2 ± 1.0)
804745827527463808	ABDMG	...	10:22:14.707	+41:14:24.34	-119.93 ± 0.98	-140.08 ± 1.07	25.96 ± 0.95	(-9.3 ± 1.5)
804739952015901056	...	63.1	10:22:10.397	+41:13:44.17	-120.57 ± 0.11	-138.14 ± 0.13	25.85 ± 0.07	-5.3 ± 0.2
778323802898879104	ABDMG	...	10:57:14.628	+41:42:52.93	-103.51 ± 0.07	-116.11 ± 0.08	23.55 ± 0.07	(-11.4 ± 1.5)
778323807194120448	...	1.9	10:57:14.562	+41:42:54.70	-109.52 ± 0.14	-123.84 ± 0.11	24.25 ± 0.09	-12.9 ± 4.5
3532609608824947840	CARN	...	11:13:42.658	-26:28:26.54	-170.79 ± 0.09	4.69 ± 0.07	24.57 ± 0.05	11.2 ± 0.3
3532611086293698560	...	43.7	11:13:43.136	-26:27:43.33	-172.90 ± 0.10	7.38 ± 0.07	24.62 ± 0.05	...
5375889038308656128	CARN	...	11:31:01.018	-44:18:54.26	-124.35 ± 0.11	5.45 ± 0.10	20.74 ± 0.08	(10.9 ± 0.9)
5375889003948915072	...	19.4	11:30:59.820	-44:19:08.74	-124.93 ± 0.08	4.82 ± 0.07	20.69 ± 0.05	...
5226891709370645376	EPSC	...	11:41:17.069	-73:15:36.90	-40.60 ± 0.09	5.67 ± 0.08	10.42 ± 0.05	(12.1 ± 2.2)
5226891709370642944	...	30.4	11:41:22.115	-73:15:58.04	-40.74 ± 0.12	5.93 ± 0.11	10.40 ± 0.07	...
3599411399841262592	CARN	...	11:56:08.009	-04:09:32.51	-149.87 ± 0.14	-13.09 ± 0.07	20.44 ± 0.09	(5.9 ± 0.8)
3599411399842474368	...	3.8	11:56:07.958	-04:09:36.18	-152.46 ± 0.10	-13.20 ± 0.05	20.56 ± 0.05	0.4 ± 0.3
6053080174073021696	LCC	...	12:13:19.500	-64:47:50.23	-46.08 ± 0.36	-7.52 ± 0.32	11.74 ± 0.22	14.4 ± 1.3
6053080105353531520	LCC	70.0	12:13:20.902	-64:48:59.62	-46.83 ± 0.04	-7.22 ± 0.04	12.25 ± 0.03	14.3 ± 2.8
6053316942658822272	LCC	...	12:17:40.056	-64:09:39.19	-37.58 ± 0.68	-6.11 ± 0.50	10.96 ± 0.38	(16.0 ± 4.3)
6053316942666110720	...	5.2	12:17:39.372	-64:09:41.92	-38.09 ± 0.08	-10.21 ± 0.07	9.23 ± 0.05	...
5861194641755494528	LCC	...	12:27:13.886	-65:05:55.24	-36.14 ± 1.34	-10.04 ± 0.74	10.10 ± 0.68	(14.6 ± 4.3)
5861194641755890048	...	15.2	12:27:14.987	-65:06:08.80	-35.59 ± 3.26	-4.03 ± 1.87	6.19 ± 1.84	...
6145304323118631680	TWA	...	12:30:05.141	-44:02:36.31	-51.82 ± 0.08	-21.74 ± 0.06	12.66 ± 0.06	(8.0 ± 1.4)
61453043429765430784	TWA	116.0	12:30:05.734	-44:04:32.12	-51.59 ± 0.10	-21.61 ± 0.07	12.74 ± 0.07	(8.0 ± 1.4)
6074516458849906560	LCC	...	12:31:08.446	-54:56:44.57	-35.55 ± 0.14	-12.66 ± 0.11	10.14 ± 0.11	(13.9 ± 4.3)
6074516458869049088	...	0.8	12:31:08.433	-54:56:43.80	-34.20 ± 1.18	-14.63 ± 0.25	9.95 ± 0.35	...
6058441770683656064	LCC	...	12:33:28.963	-59:23:46.98	-37.05 ± 0.19	-8.40 ± 0.18	10.09 ± 0.15	(14.3 ± 4.4)
6058441766355347200	...	2.9	12:33:29.278	-59:23:45.34	-38.80 ± 0.04	-11.01 ± 0.04	9.72 ± 0.03	14.0 ± 0.9
6073201958364804352	LCC	...	12:33:59.438	-56:34:48.22	-33.41 ± 0.22	-13.02 ± 0.20	10.18 ± 0.16	(14.6 ± 4.4)
6073202027084283392	...	35.0	12:33:58.204	-56:34:14.72	-34.31 ± 0.07	-15.25 ± 0.07	8.73 ± 0.06	...
6053654393972419584	LCC	...	12:36:43.752	-63:10:57.06	-37.92 ± 0.25	-9.88 ± 0.15	10.20 ± 0.12	(14.9 ± 4.3)
6053654393972421504	...	11.5	12:36:43.789	-63:10:45.59	-39.24 ± 0.05	-9.98 ± 0.05	10.36 ± 0.03	12.3 ± 0.6
6074733165726906112	LCC	...	12:39:20.998	-53:37:57.40	-45.00 ± 0.09	-14.92 ± 0.06	12.20 ± 0.08	(11.9 ± 4.3)
6074733165726906368	...	1.5	12:39:20.940	-53:37:58.78	-48.56 ± 0.11	-17.93 ± 0.07	12.31 ± 0.09	8.0 ± 2.7
6129159884655362944	LCC	...	12:41:29.501	-46:41:14.56	-38.13 ± 0.19	-16.00 ± 0.25	10.41 ± 0.20	(10.3 ± 3.9)
6129159919015101824	LCC	20.6	12:41:31.250	-46:41:04.55	-38.93 ± 0.12	-16.86 ± 0.16	10.01 ± 0.09	(10.5 ± 3.9)
6055197867775111936	LCC	...	12:45:09.545	-62:32:35.42	-39.89 ± 0.07	-13.51 ± 0.07	10.16 ± 0.05	(14.4 ± 4.4)
6055197867775111808	LCC	4.0	12:45:10.092	-62:32:36.63	-41.67 ± 0.29	-16.19 ± 0.26	10.05 ± 0.21	(14.0 ± 4.4)

Table 4 *continued*

Table 4 (continued)

<i>Gaia</i> DR2	Assoc.	Separation	R.A. ^a	Decl. ^a	$\mu_\alpha \cos \delta$	μ_δ	Parallax	Rad. Vel.
Source ID		($''$)	(hh:mm:ss.sss)	(dd:mm:ss.ss)	(mas yr $^{-1}$)	(mas yr $^{-1}$)	(mas)	(km s $^{-1}$)
6060965630906108672	ABDMG	...	12:45:16.615	-57:21:36.95	-200.18 ± 0.10	-140.60 ± 0.10	50.33 ± 0.09	(19.4 ± 1.0)
6060965699625586176	...	21.8	12:45:14.028	-57:21:30.84	-201.03 ± 0.05	-131.55 ± 0.05	50.49 ± 0.05	14.8 ± 0.2
5861825550891696000	LCC	...	12:48:47.863	-64:46:11.92	-40.45 ± 0.07	-15.82 ± 0.06	10.23 ± 0.05	(13.9 ± 4.2)
5861825349107118976	LCC	31.1	12:48:52.721	-64:46:10.96	-40.52 ± 0.08	-15.45 ± 0.07	10.32 ± 0.06	(14.1 ± 4.2)
6127918089350574848	LCC	...	12:49:46.409	-47:58:32.31	-38.78 ± 0.11	-17.57 ± 0.08	10.05 ± 0.08	(10.8 ± 4.1)
6127917333436329344	...	33.0	12:49:49.511	-47:58:43.07	-37.95 ± 0.09	-18.19 ± 0.07	9.84 ± 0.06	...
6139583907716775936	TWA	...	12:50:47.705	-42:31:49.06	-39.40 ± 0.14	-19.60 ± 0.11	10.11 ± 0.09	(8.6 ± 1.4)
6139584010795996160	TWA	29.6	12:50:49.097	-42:31:23.80	-38.78 ± 0.15	-20.78 ± 0.12	10.26 ± 0.10	(7.6 ± 1.4)
6060533277994568960	LCC	...	12:50:52.231	-57:17:05.07	-36.78 ± 0.53	-13.03 ± 0.42	10.07 ± 0.44	(13.3 ± 4.4)
6060533282301705088	...	0.7	12:50:52.181	-57:17:04.50	-38.67 ± 0.35	-14.17 ± 0.35	9.87 ± 0.33	...
5838505428954577536	LCC	...	12:55:55.070	-74:17:20.57	-40.45 ± 0.47	-6.31 ± 0.14	10.53 ± 0.11	(17.5 ± 3.6)
5838505463323964416	...	1.1	12:55:55.062	-74:17:19.48	-43.81 ± 0.22	-6.53 ± 0.18	10.41 ± 0.13	...
6067650695944221696	LCC	...	13:12:18.518	-54:40:32.59	-34.93 ± 0.52	-18.08 ± 0.37	10.56 ± 0.29	(11.2 ± 4.3)
6067650627224743424	...	102.2	13:12:07.511	-54:41:08.98	-33.66 ± 1.78	-19.77 ± 1.64	7.45 ± 0.95	4.9 ± 5.0
6067650970822132224	...	98.5	13:12:17.993	-54:38:54.17	-28.54 ± 0.07	-12.07 ± 0.06	7.72 ± 0.04	11.8 ± 2.1
6067650695933955968	...	1.0	13:12:18.502	-54:40:31.62	-30.86 ± 0.25	-17.06 ± 0.14	9.17 ± 0.09	...
6067650970822131584	...	86.9	13:12:18.553	-54:39:05.70	-28.91 ± 0.07	-13.24 ± 0.06	7.77 ± 0.04	11.5 ± 1.2
6063021369724033152	LCC	...	13:13:42.490	-58:07:22.17	-50.36 ± 0.24	-27.67 ± 0.28	13.21 ± 0.21	(14.2 ± 4.3)
6063020996104392576	...	19.7	13:13:40.004	-58:07:23.16	-54.15 ± 0.05	-32.49 ± 0.06	9.21 ± 0.05	...
6063021374031904384	...	0.7	13:13:42.449	-58:07:21.56	-52.84 ± 0.91	-33.02 ± 0.74	10.24 ± 0.31	...
6070093879495884672	LCC	...	13:25:58.044	-51:11:44.87	-39.69 ± 0.62	-20.60 ± 0.52	11.14 ± 0.35	(10.7 ± 4.1)
6070094085654316416	...	70.0	13:25:55.931	-51:10:37.71	-32.69 ± 0.09	-21.13 ± 0.10	8.65 ± 0.06	12.4 ± 0.5
6062897988210000512	LCC	...	13:34:07.166	-56:24:27.00	-48.04 ± 0.11	-29.69 ± 0.19	12.51 ± 0.08	(14.7 ± 4.1)
6062898091306143360	LCC	1.1	13:34:07.277	-56:24:26.31	-47.50 ± 0.49	-30.08 ± 0.62	12.48 ± 0.35	(14.4 ± 4.1)
6115448562335145600	UCL	...	13:51:45.302	-37:41:56.32	-35.49 ± 0.15	-27.15 ± 0.17	10.64 ± 0.10	(4.8 ± 3.0)
6115448562335144704	UCL	5.9	13:51:45.622	-37:42:00.88	-37.53 ± 0.08	-27.10 ± 0.10	10.51 ± 0.05	(3.9 ± 3.0)
5786595011112442880	ABDMG	...	14:15:41.498	-77:43:06.56	-66.18 ± 0.07	-61.65 ± 0.07	17.28 ± 0.04	(20.2 ± 1.0)
5786595011112450560	ABDMG	19.9	14:15:42.072	-77:42:46.73	-66.01 ± 0.06	-63.29 ± 0.06	17.14 ± 0.04	(20.1 ± 1.0)
5986939704885434880	UCL	...	15:31:24.902	-47:11:12.15	-24.29 ± 0.26	-33.96 ± 0.13	10.09 ± 0.10	(4.3 ± 4.1)
5986939704898034432	UCL	0.8	15:31:24.898	-47:11:11.32	-30.88 ± 0.83	-34.36 ± 0.50	10.21 ± 0.40	(4.5 ± 4.1)
6010503476008900480	UCL	...	15:56:02.470	-36:43:47.85	-26.77 ± 0.09	-40.46 ± 0.05	10.58 ± 0.04	(2.0 ± 3.9)
6010503407289419776	UCL	13.7	15:56:03.389	-36:43:55.92	-27.09 ± 0.24	-37.95 ± 0.14	10.71 ± 0.11	(1.5 ± 3.9)
6246927372513025408	USCO	...	15:57:00.905	-20:24:48.63	-18.54 ± 1.03	-24.20 ± 0.65	10.59 ± 0.67	(-5.9 ± 4.0)
6246927372513024128	...	11.4	15:57:00.836	-20:24:59.94	-17.68 ± 0.25	-26.70 ± 0.18	8.52 ± 0.16	-3.2 ± 7.5
5997293767212191360	UCL	...	16:18:37.718	-38:39:10.97	-26.66 ± 0.19	-33.43 ± 0.13	10.35 ± 0.11	(2.4 ± 3.9)
5997293771501339648	...	9.6	16:18:38.529	-38:39:12.33	-25.74 ± 0.10	-33.57 ± 0.07	10.32 ± 0.06	-3.1 ± 2.5
6018064886202720512	UCL	...	16:23:46.723	-39:02:01.68	-20.95 ± 0.23	-38.77 ± 0.17	10.17 ± 0.12	(1.5 ± 3.8)
6018064920562460672	...	27.4	16:23:48.247	-39:01:40.85	-21.34 ± 0.16	-37.51 ± 0.12	9.75 ± 0.08	...
6024647078192864640	UCL	...	16:34:23.268	-32:01:07.64	-20.75 ± 0.45	-34.22 ± 0.26	10.03 ± 0.20	(-0.3 ± 3.6)
6024647078207418368	...	0.6	16:34:23.269	-32:01:08.29	-20.78 ± 0.34	-30.06 ± 0.22	9.22 ± 0.15	...
5935776710115544832	BPMG	...	16:57:21.408	-53:43:29.18	-16.20 ± 0.16	-85.70 ± 0.14	19.82 ± 0.14	(0.3 ± 1.5)
5935776714456619008	...	11.0	16:57:20.245	-53:43:32.91	-10.85 ± 0.19	-84.09 ± 0.14	19.76 ± 0.12	0.5 ± 0.4
5814416056916139520	BPMG	...	17:02:09.319	-67:34:46.27	-20.27 ± 0.04	-99.48 ± 0.06	24.22 ± 0.04	(4.8 ± 1.4)
5814416056916140800	BPMG	12.8	17:02:09.818	-67:34:33.84	-20.46 ± 0.05	-99.24 ± 0.08	24.18 ± 0.05	(4.8 ± 1.4)
5945104588806333824	BPMG	...	17:48:33.744	-53:06:12.72	-1.93 ± 0.08	-56.13 ± 0.07	12.97 ± 0.05	(0.8 ± 1.5)
5945104490030338432	...	31.5	17:48:33.737	-53:06:44.26	-6.73 ± 0.37	-57.24 ± 0.25	13.05 ± 0.11	11.2 ± 3.4
5957941528881789568	BPMG	...	17:49:43.591	-40:05:36.22	-2.47 ± 0.11	-76.47 ± 0.09	19.50 ± 0.06	(-4.2 ± 1.5)
5957941352697849856	...	59.1	17:49:48.694	-40:05:44.13	-2.45 ± 0.24	-80.25 ± 0.21	21.41 ± 0.16	...
6421577304161210496	ABDMG	...	19:18:48.816	-69:10:22.45	14.96 ± 0.07	-92.23 ± 0.09	16.16 ± 0.06	(13.7 ± 1.2)
6421577304161210240	...	2.7	19:18:49.314	-69:10:22.80	11.45 ± 0.07	-91.97 ± 0.10	16.35 ± 0.07	...
6745746523539748096	BPMG	...	19:24:59.364	-32:04:31.70	19.82 ± 0.16	-50.09 ± 0.16	14.65 ± 0.11	(-6.0 ± 1.3)
6745746523539747456	...	2.0	19:24:59.489	-32:04:32.92	12.14 ± 0.16	-51.57 ± 0.16	13.90 ± 0.11	...
6754492966739292928	BPMG	...	19:48:16.548	-27:20:32.77	25.41 ± 0.11	-53.28 ± 0.06	15.42 ± 0.06	-5.8 ± 1.0

Table 4 continued

Table 4 (*continued*)

<i>Gaia</i> DR2	Assoc.	Separation	R.A. ^a	Decl. ^a	$\mu_\alpha \cos \delta$	μ_δ	Parallax	Rad. Vel.
Source ID		($''$)	(hh:mm:ss.sss)	(dd:mm:ss.ss)	(mas yr $^{-1}$)	(mas yr $^{-1}$)	(mas)	(km s $^{-1}$)
6754492932379552896	BPMG	7.2	19:48:17.076	-27:20:34.33	24.88 ± 0.28	-52.80 ± 0.17	15.03 ± 0.17	(-6.7 ± 1.2)
1975678603914496000	ABDMG	...	22:06:05.726	+47:34:02.99	97.19 ± 0.06	-58.49 ± 0.06	27.08 ± 0.04	(-24.4 ± 1.0)
1975678603914495616	...	3.4	22:06:05.801	+47:34:06.35	101.39 ± 0.06	-65.71 ± 0.06	26.90 ± 0.04	...
2832918891813969408	ABDMG	...	22:44:41.405	+17:54:16.02	82.11 ± 0.16	-80.73 ± 0.09	20.76 ± 0.07	-13.4 ± 1.5
2832918887518987904	ABDMG	3.4	22:44:41.635	+17:54:17.02	82.70 ± 0.30	-81.84 ± 0.20	20.11 ± 0.11	-13.0 ± 0.5
2865683170091662592	ABDMG	...	23:34:27.425	+27:39:41.88	94.38 ± 0.10	-75.82 ± 0.07	20.38 ± 0.07	(-13.9 ± 1.2)
2865683204451400576	...	61.9	23:34:22.865	+27:39:54.37	96.46 ± 0.06	-76.64 ± 0.05	20.18 ± 0.05	...
2328250334633289856	ABDMG	...	23:48:50.609	-28:07:17.30	96.65 ± 0.08	-105.23 ± 0.08	22.61 ± 0.05	6.9 ± 0.2
2328250059757795072	...	74.7	23:48:55.663	-28:07:50.62	100.12 ± 0.67	-104.69 ± 0.65	23.40 ± 0.39	...

^a J2000 position at epoch 2015 from the *Gaia* DR2 catalog.

Table 5. New bona fide members.

Name	Spectral Type ^a	Assoc.	R.A. ^b	Decl. ^b	MIST	Co-moving
			(hh:mm:ss.sss)	(dd:mm:ss.ss)	Age (Myr)	
New Bona Fide Members						
gam02 Ari	A2IV	ABDMG	01:53:31.90	+19:17:36.4	4–300	...
gam01 Ari	A0V	ABDMG	01:53:31.90	+19:17:43.8	4–300	...
HD 14691	F3V	COL	02:22:01.69	-10:46:40.4	10–3000	...
iot Hyi	F5IV-V	CAR	03:15:58.20	-77:23:17.5	> 10	...
ups04 Eri	B9V	THA	04:17:53.74	-33:47:54.1	1–200	...
HD 36169	G8V	ABDMG	05:29:03.29	-19:08:35.9	30–1000	...
HD 43199	F0III/IV	CAR	06:10:52.92	-61:29:58.8
HD 80950	A0V	CAR	09:17:27.45	-74:44:04.0	5–900	...
m Car	B9IV/V	CAR	09:39:20.92	-61:19:40.7	2–600	...
HD 102438	G6V	ABDMG	11:47:15.49	-30:17:15.0	30–1000	...
HD 108799	G1/2V	CARN	12:30:04.49	-13:23:36.2	30–1000	...
HD 109965	F5V	LCC	12:39:21.15	-55:39:14.8	> 10	...
HD 121560	F6V	CARN	13:55:49.68	+14:03:23.5	40–700	...
alf Cir	A7V	BPMG	14:42:29.95	-64:58:34.1	10–400	...
HD 213429	F8V	BPMG	22:31:18.48	-06:33:20.2	20–300	...
phi Gru	F4V	ABDMG	23:18:10.06	-40:49:29.6
Comovers with Known Bona Fide Members						
2MASS J00393534-3817176	(M4)	THA	00:39:35.48	-38:17:18.7	...	2M0039-3816 ^c
2MASS J01484771-4831156	(M5)	ABDMG	01:48:47.90	-48:31:16.4	...	GSC 08044-00859
UCAC3 222-12335	(M5)	HYA	02:58:06.45	+20:40:01.3	...	47 Ari
UCAC4 311-003056	(M4)	COL	03:07:49.18	-27:50:47.0	...	HD 19545
UCAC4 262-003815	(M2)	THA	03:48:40.51	-37:38:20.0	...	CCDM J03486-3737
2MASS J03530890+1719444	(M5)	HYA	03:53:09.08	+17:19:44.1	...	HD 24357
2MASS J04195770+1402413	(M4)	HYA	04:19:57.83	+14:02:40.8	...	h Tau
UCAC3 126-11943	(M5)	THA	04:38:45.73	-27:02:02.2	...	HIP 21632
2MASS J04400675+2536457	(M4)	HYA	04:40:06.89	+25:36:44.7	...	HD 283810
2MASS J10190316-6440520	(M3)	LCC	10:19:03.08	-64:40:51.9	...	CCDM J10191-6441
2MASS J13255810-5111444	(M3)	LCC	13:25:58.04	-51:11:44.9	...	HD 116651
2MASS J16572144-5343277	(M5)	BPMG	16:57:21.41	-53:43:29.2	...	2M1657-5343 ^d
2MASS J16183775-3839104	(M4)	UCL	16:18:37.72	-38:39:11.0	...	HIP 79908

Table 5 continued

Table 5 (*continued*)

Name	Spectral Type ^a	Assoc.	R.A. ^b (hh:mm:ss.sss)	Decl. ^b (dd:mm:ss.ss)	MIST	Co-moving
UCAC3 74-428746	(M2)	BPMG	17:48:33.74	-53:06:12.7	...	HD 161460
HD 223340	K1V	ABDMG	23:48:50.61	-28:07:17.3	...	del Scl

^a Spectral types between parentheses were estimated from the absolute *Gaia* G-band magnitude.

^b J2000 position at epoch 2015 from the *Gaia* DR2 catalog.

^c The full name of this object is 2MASS J00393579-3816584.

^d The full name of this object is 2MASS J16572029-5343316.

JG wrote the codes, manuscript, generated figures and led all analysis; *JKF* provided help with parsing the *Gaia* DR2 data as well as general comments.

Software: BANYAN Σ (Gagné et al. 2018).

REFERENCES

- Abt, H. A., & Cardona, O. 1984, The Astrophysical Journal, 276, 266
- Abt, H. A., & Morrell, N. I. 1995, Astrophysical Journal Supplement v.99, 99, 135
- Alam, S., Albareti, F. D., Allende Prieto, C., et al. 2015, The Astrophysical Journal Supplement Series, 219, 12
- Allen, P. R., Cruz, K. K., Koerner, D. W., McElwain, M. W., & Reid, N. I. 2007, The Astronomical Journal, 133, 971
- Allers, K. N., & Liu, M. C. 2013, The Astrophysical Journal, 772, 79
- Alonso-Floriano, F. J., Morales, J. C., Caballero, J. A., et al. 2015, Astronomy and Astrophysics, 577, A128
- Babusiaux, C., van Leeuwen, F., Barstow, M., et al. 2018, Astronomy & Astrophysics, doi:10.1051/0004-6361/201832843
- Bardalez Gagliuffi, D. C., Burgasser, A. J., Gelino, C. R., et al. 2014, The Astrophysical Journal, 794, 143
- Bell, C. P. M., Mamajek, E. E., & Naylor, T. 2015, Monthly Notices of the Royal Astronomical Society, 454, 593
- Böhringer, H., Schuecker, P., Guzzo, L., et al. 2004, Astronomy and Astrophysics, 425, 367
- Boller, T., Freyberg, M. J., Trümper, J., et al. 2016, Astronomy & Astrophysics, 588, A103
- Bouvier, J., Kendall, T. R., Meeus, G., et al. 2008, Astronomy and Astrophysics, 481, 661
- Bowler, B. P., Liu, M. C., Shkolnik, E. L., & Tamura, M. 2015, The Astrophysical Journal Supplement, 216, 7
- Bowler, B. P., Liu, M. C., Mawet, D., et al. 2017, The Astronomical Journal, 153, 18
- Brandt, T. D., & Huang, C. X. 2015, The Astrophysical Journal, 807, 24
- Chambers, K. C., Magnier, E. A., Metcalfe, N., et al. 2016, arXiv.org, arXiv:1612.05560
- Choi, J., Dotter, A., Conroy, C., et al. 2016, The Astrophysical Journal, 823, 102
- Comerón, F., Spezzi, L., Lopez Martí, B., & Merín, B. 2013, Astronomy and Astrophysics, 554, A86
- Cook, N. J., Pinfield, D. J., Marocco, F., et al. 2016, Monthly Notices of the Royal Astronomical Society, 457, 2192
- Cropper, M., Katz, D., Sartoretti, P., & et al. 2018, Astronomy & Astrophysics, doi:10.1051/0004-6361/201832763
- Cruz, K. K., Lowrance, P., Reid, N. I., Liebert, J., & Kirkpatrick, D. J. 2003, The Astronomical Journal, 126, 2421
- Cruz, K. K., & Reid, N. I. 2002, The Astronomical Journal, 123, 2828
- Cruz, K. L., Reid, I. N., Kirkpatrick, J. D., et al. 2007, The Astronomical Journal, 133, 439
- Davenport, J. R. A., Becker, A. C., Kowalski, A. F., et al. 2012, The Astrophysical Journal, 748, 58
- Deshpande, R., Blake, C. H., Bender, C. F., et al. 2013, The Astronomical Journal, 146, 156
- Desidera, S., Covino, E., Messina, S., et al. 2015, Astronomy & Astrophysics, 573, A126
- Desrochers, M.-E., Artigau, É., Gagné, J., et al. 2018, The Astrophysical Journal, 852, 55
- Dieterich, S. B., Henry, T. J., Jao, W.-C., et al. 2014, The Astronomical Journal, 147, 94

- Duflot, M., Figon, P., & Meyssonnier, N. 1995, *Astronomy and Astrophysics Supplement*, 114, 269
- Evans, D. S. 1967, Determination of Radial Velocities and their Applications, 30, 57
- Evans, D. S., Laing, J. D., Menzies, A., & Stoy, R. H. 1964, Royal Observatory bulletins ; no. 85; Royal Observatory bulletins. Series E ; no. 85., 85, 207
- Evans, D. W., Riello, M., De Angeli, F., et al. 2018, *Astronomy & Astrophysics*, doi:10.1051/0004-6361/201832756
- Faherty, J. K., Cruz, K. K., Burgasser, A. J., et al. 2009, *The Astronomical Journal*, 137, 1
- Faherty, J. K., Gagné, J., Burgasser, A. J., et al. 2018, arXiv.org, arXiv:1805.01573
- Faherty, J. K., Riedel, A. R., Cruz, K. K., et al. 2016, *The Astrophysical Journal Supplement Series*, 225, 10
- Fleming, T. A., Liebert, J., Gioia, I. M., & Maccacaro, T. 1988, *The Astrophysical Journal*, 331, 958
- Gagné, J., Faherty, J. K., & Fontaine, G. 2018a, arXiv.org, arXiv:1804.05248
- Gagné, J., Lafrenière, D., Doyon, R., Malo, L., & Artigau, É. 2015a, *The Astrophysical Journal*, 798, 73
- Gagné, J., Roy-Loubier, O., Faherty, J. K., Doyon, R., & Malo, L. 2018b, arXiv.org, 1804.03093v1
- Gagné, J., Schneider, A., & Cushing, M. 2018, Finder Charts Python Package v1.0, Zenodo, doi:10.5281/zenodo.1237017
- Gagné, J., Faherty, J. K., Cruz, K. L., et al. 2015b, *The Astrophysical Journal Supplement Series*, 219, 33
- Gagné, J., Faherty, J. K., Mamajek, E. E., et al. 2017, *The Astrophysical Journal Supplement Series*, 228, 18
- Gagné, J., Mamajek, E. E., Malo, L., et al. 2018, *The Astrophysical Journal*, 856, 23
- Gaia Collaboration, Brown, A. G. A., Vallenari, A., et al. 2018, *Astronomy & Astrophysics*, doi:10.1051/0004-6361/201833051
- . 2016, *Astronomy and Astrophysics*, 595, A2
- Gaidos, E., Mann, A. W., Lépine, S., et al. 2014, *Monthly Notices of the Royal Astronomical Society*, 443, 2561
- Galicher, R., Marois, C., Macintosh, B., et al. 2016, *Astronomy and Astrophysics*, 594, A63
- Gontcharov, G. A. 2006, *Astronomy Letters*, 32, 759
- Gray, R. O., Corbally, C. J., Garrison, R. F., et al. 2006, *The Astronomical Journal*, 132, 161
- Gray, R. O., Corbally, C. J., Garrison, R. F., McFadden, M. T., & Robinson, P. E. 2003, *The Astronomical Journal*, 126, 2048
- Guieu, S., Dougados, C., Monin, J.-L., Magnier, E., & Martín, E. L. 2006, *Astronomy and Astrophysics*, 446, 485
- Hambly, N. C., Cropper, M., Boudreault, S., et al. 2018, *Astronomy & Astrophysics*, doi:10.1051/0004-6361/201832716
- Hawley, S. L., Covey, K. R., Knapp, G. R., et al. 2002, *The Astronomical Journal*, 123, 3409
- Herbig, G. H., Vrba, F. J., & Rydgren, A. E. 1986, *Astronomical Journal*, 91, 575
- Houk, N. 1982, Michigan Catalogue of Two-dimensional Spectral Types for the HD stars. Volume 3. Declinations -40 to -26.
- Houk, N., & Cowley, A. P. 1975, University of Michigan Catalogue of two-dimensional spectral types for the HD stars. Volume I. Declinations -90 to -53., I
- Houk, N., & Smith-Moore, M. 1988, Michigan Catalogue of Two-dimensional Spectral Types for the HD Stars. Volume 4, 4
- Jeffries, R. D. 1995, *Monthly Notices of the Royal Astronomical Society*, 273, 559
- Jones, D. O., & West, A. A. 2016, *The Astrophysical Journal*, 817, 1
- Jones, J., White, R. J., Boyajian, T. S., et al. 2015, *American Astronomical Society*, 225, 112.03
- Kenyon, S. J., & Hartmann, L. 1995, *Astrophysical Journal Supplement v.101*, 101, 117
- Kirkpatrick, D. J., Henry, T. J., & McCarthy, D. W. J. 1991, *Astrophysical Journal Supplement Series*, 77, 417
- Kirkpatrick, D. J., Lowrance, P., Cruz, K. K., et al. 2008, *The Astrophysical Journal*, 689, 1295
- Koen, C., Kilkenney, D., van Wyk, F., & Marang, F. 2010, *Monthly Notices of the Royal Astronomical Society*, 403, 1949
- Kraus, A. L., Shkolnik, E. L., Allers, K. N., & Liu, M. C. 2014, *The Astronomical Journal*, 147, 146
- Krautter, J., Wichmann, R., Schmitt, J. H. M. M., et al. 1997, *A & A Supplement series*, 123, 329
- Kunder, A., Kordopatis, G., Steinmetz, M., et al. 2017, *The Astronomical Journal*, 153, 75
- Law, N. M., Hodgkin, S. T., & Mackay, C. D. 2008, *Monthly Notices of the Royal Astronomical Society*, 384, 150
- Lawrence, A., Warren, S. J., Almaini, O., et al. 2007, *Monthly Notices of the Royal Astronomical Society*, 379, 1599
- Lépine, S., Hilton, E. J., Mann, A. W., et al. 2013, *The Astronomical Journal*, 145, 102
- Lindgren, L., Hernández, J., Bombrun, A., et al. 2018, *Astronomy & Astrophysics*, doi:10.1051/0004-6361/201832727
- Luhman, K. L. 2006, *The Astrophysical Journal*, 645, 676

- Luhman, K. L., Stauffer, J. R., & Mamajek, E. E. 2005, *The Astrophysical Journal*, 628, L69
- Luri, X., A Brown, A. G., Sarro, L., et al. 2018, *Astronomy & Astrophysics*, doi:10.1051/0004-6361/201832964
- Malo, L., Artigau, É., Doyon, R., et al. 2014a, *The Astrophysical Journal*, 788, 81
- Malo, L., Doyon, R., Feiden, G. A., et al. 2014b, *The Astrophysical Journal*, 792, 37
- Malo, L., Doyon, R., Lafrenière, D., et al. 2013, *The Astrophysical Journal*, 762, 88
- Mamajek, E. 2016, A New Candidate Young Stellar Group at d=121 pc Associated with 118 Tauri, doi:10.6084/m9.figshare.3122689.v1
- Marois, C., Macintosh, B., Barman, T. S., et al. 2008, *Science*, 322, 1348
- Martin, D. C., Fanson, J., Schiminovich, D., et al. 2005, *The Astrophysical Journal*, 619, L1
- McMahon, R. G., Banerji, M., Gonzalez, E., et al. 2013, *The Messenger*, 154, 35
- Mignard, F., Klioner, S., Lindegren, L., et al. 2018, *Astronomy & Astrophysics*, doi:10.1051/0004-6361/201832916
- Murphy, S. J., & Lawson, W. A. 2015, *Monthly Notices of the Royal Astronomical Society*, 447, 1267
- Murphy, S. J., Lawson, W. A., & Bessell, M. S. 2013, *Monthly Notices of the Royal Astronomical Society*, 435, 1325
- Newton, E. R., Charbonneau, D., Irwin, J., et al. 2014, *The Astronomical Journal*, 147, 20
- Ochsenbein, F., Bauer, P., & Marcout, J. 2000, *Astronomy and Astrophysics Supplement*, 143, 23
- Pecaut, M. J., & Mamajek, E. E. 2016, *Monthly Notices of the Royal Astronomical Society*, 461, 794
- Perryman, M. A. C., Lindegren, L., Kovalevsky, J., et al. 1997, *Astronomy and Astrophysics* 323, 323, L49
- Pesch, P. 1968, *The Astrophysical Journal*, 151, 605
- Phan Bao, N., Bessell, M. S., Martín, E. L., et al. 2008, *Monthly Notices of the Royal Astronomical Society*, 383, 831
- Platais, I., Kozhurina-Platais, V., & van Leeuwen, F. 1998, *The Astronomical Journal*, 116, 2423
- Pöhnl, H., & Paunzen, E. 2010, *Astronomy & Astrophysics*, 514, A81
- Rameau, J., Chauvin, G., Lagrange, A.-M., et al. 2013, *The Astrophysical Journal Letters*, 772, L15
- Reid, N. I., Cruz, K. K., & Allen, P. R. 2007, *The Astronomical Journal*, 133, 2825
- Reid, N. I., Gizis, J. E., & Hawley, S. L. 1995, *The Astronomical Journal*, 110, 1838
- Reid, N. I., Cruz, K. K., Lowrance, P., et al. 2004, *The Astronomical Journal*, 128, 463
- Riaz, B., Gizis, J. E., & Harvin, J. 2006, *The Astronomical Journal*, 132, 866
- Ricker, G. R., Winn, J. N., Vanderspek, R., et al. 2015, *Journal of Astronomical Telescopes*, 1, 014003
- Riello, M., De Angeli, F., Evans, D. W., et al. 2018, *Astronomy & Astrophysics*, doi:10.1051/0004-6361/201832712
- Rodriguez, D., Bessell, M. S., Zuckerman, B., & Kastner, J. H. 2011, *The Astrophysical Journal*, 727, 62
- Rodriguez, D., Zuckerman, B., Kastner, J. H., et al. 2013, *The Astrophysical Journal*, 774, 101
- Royer, F., Zorec, J., & Gómez, A. E. 2007, *Astronomy and Astrophysics*, 463, 671
- Sartoretti, P., Katz, D., Cropper, M., et al. 2018, *Astronomy & Astrophysics*, doi:10.1051/0004-6361/201832836
- Saumon, D., & Marley, M. S. 2008, *The Astrophysical Journal*, 689, 1327
- Schlieder, J. E., Lépine, S., Rice, E., et al. 2012, *The Astronomical Journal*, 143, 114
- Schmidt, S. J., Cruz, K. K., Bongiorno, B. J., Liebert, J., & Reid, N. I. 2007, *The Astronomical Journal*, 133, 2258
- Schmidt, S. J., Hawley, S. L., West, A. A., et al. 2015, *The Astronomical Journal*, 149, 158
- Scholz, R. D., Meusinger, H., & Jahreiß, H. 2005, *Astronomy and Astrophysics*, 442, 211
- Shkolnik, E. L., Allers, K. N., Kraus, A. L., Liu, M. C., & Flagg, L. 2017, *The Astronomical Journal*, 154, 69
- Shkolnik, E. L., Anglada-Escude, G., Liu, M. C., et al. 2012, *The Astrophysical Journal*, 758, 56
- Shkolnik, E. L., Liu, M. C., Reid, I. N., Dupuy, T., & Weinberger, A. J. 2011, *The Astrophysical Journal*, 727, 6
- Silaj, J., & Landstreet, J. D. 2014, *Astronomy and Astrophysics*, 566, A132
- Skrutskie, M. F., Cutri, R. M., Stiening, R., et al. 2006, *The Astronomical Journal*, 131, 1163
- Smart, R. L., Marocco, F., Caballero, J. A., et al. 2017, *Monthly Notices of the Royal Astronomical Society*, 469, 401
- Soderblom, D. R., Hillenbrand, L. A., Jeffries, R. D., Mamajek, E. E., & Naylor, T. 2014, *Protostars and Planets VI*, 219
- Song, I., Zuckerman, B., & Bessell, M. S. 2012, *The Astronomical Journal*, 144, 8
- Soubiran, C., Jasniewicz, G., Chemin, L., et al. 2018, *Astronomy & Astrophysics*, doi:10.1051/0004-6361/201832795
- Stephenson, C. B. 1986, *Astronomical Journal*, 92, 139

- Torres, C. A. O., Quast, G. R., da Silva, L., et al. 2006, *Astronomy and Astrophysics*, 460, 695
- Torres, C. A. O., Quast, G. R., Melo, C. H. F., & Sterzik, M. F. 2008, *Handbook of Star Forming Regions*, I, 757
- Upgren, A. R. 1962, *Astronomical Journal*, 67, 37
- van Altena, W. F. 1966, *Astronomical Journal*, 71, 482
- van Belle, G. T., & von Braun, K. 2009, *The Astrophysical Journal*, 694, 1085
- West, A. A., Hawley, S. L., Bochanski, J. J., et al. 2008, *The Astronomical Journal*, 135, 785
- West, A. A., Morgan, D. P., Bochanski, J. J., et al. 2011, *The Astronomical Journal*, 141, 97
- Wilson, R. E. 1953, Washington, 0
- Wright, C. O., Egan, M. P., Kraemer, K. E., & Price, S. D. 2003, *The Astronomical Journal*, 125, 359
- Wright, E. L., Eisenhardt, P. R. M., Mainzer, A. K., et al. 2010, *The Astronomical Journal*, 140, 1868
- Zuckerman, B., Bessell, M. S., Song, I., & Kim, S. 2006, *The Astrophysical Journal*, 649, L115
- Zuckerman, B., & Song, I. 2004, *Annual Review of Astronomy & Astrophysics*, 42, 685